Diss. ETH Nr. 14608

Characterisation of Naturally Occurring Variants of the Enzyme, UDP-*N*-Acetylglucosamine Enolpyruvyltransferase and Analysis of Conformational Changes

a dissertation submitted to the
SWISS FEDERAL INSTITUTE OF TECHNOLOGY ZÜRICH

for the degree of
DOCTOR of NATURAL SCIENCES

presented by

Alison M. Thomas

B.Sc. (Hons) Medical Biochemistry
University of Glasgow, Scotland
born September 10, 1976
in Edinburgh, Scotland

accepted on the recommendation of
Prof. Dr. N. Amrhein, examiner
PD Dr. P. Macheroux, co-examiner
Prof. Dr. H. Hennecke, co-examiner

Zürich, 2002

Table of contents

Abbreviations **VII**

Summary **IX**

Zusammenfassung **XI**

1. Introduction **1**

1.1 The bacterial cell wall, peptidoglycan and its biosynthesis 1

1.2 UDP-*N*-acetylglucosamine enolpyruvyltransferase (MurA) 6

1.3 The structure of MurA 7

1.4 The reaction mechanism of MurA 9

1.5 Comparison of MurA and EPSPS 13

1.6 Objectives 14

1.6.1 Characterisation of the naturally occurring variants of MurA 14

1.6.2 *Enterobacter cloacae* MurA as a histidine-tagged protein 15

1.6.3 A study of the conformational changes of *Enterobacter cloacae* MurA 15

2. Characterisation of the naturally occurring variants of MurA **16**

2.1 Materials 16

2.1.1 Chemicals and enzymes 16

2.1.2 Bacterial strains 16

2.1.3 Vectors 17

2.2 Methods 17

2.2.1 Genomic DNA 17

2.2.2 Primers 18

2.2.3 PCR 19

2.2.4 Site-directed mutagenesis of *Mt*MurA 20

2.2.4.1 Primers 20

2.2.4.2 PCR 21

2.2.5 Restriction enzyme digestion 21

2.2.5.1 Digestion of PCR products with restriction enzymes 21

2.2.5.2 Digestion of plasmids with restriction enzymes 21

2.2.6 Ligation 22

2.2.7 Ligation of DNA into the PCR-Script Amp SK (+) vector 22

2.2.8 Production of *E. coli* DMSO competent cells 22

2.2.9 Transformation of *E. coli* DMSO competent cells 23

2.2.10 Minipreps of plasmid DNA 23

2.2.10.1 QIAprep spin miniprep kit 23

2.2.10.2 Adaptation of the "Holmes and Quigley" plasmid miniprep 24

2.2.10.3 Plasmid miniprep for sequencing 24

2.2.11 DNA sequencing 25

2.2.12 Sodium Dodecyl Sulphate (SDS)-Polyacrylamide gel electrophoresis 26

2.2.13 Small scale expression of the target protein 27

2.2.14 Large scale expression of the target protein using a 12 L fermentor 27

2.2.15 Determination of the solubility of the target proteins 28

2.2.16 Purification of *Mt*MurA and D117CMurA 28

2.2.17 Purification of *Mt*MurA-His under native conditions 29

2.2.18 Purification of *Mt*MurA-His under denaturing conditions 30

2.2.19 Purification of *Ct*MurA 30

2.2.20 Western blotting 30

2.2.21 Immunodetection 31

2.2.21.1 Immunodetection using the rabbit anti-MurA antibody 31

2.2.21.2 Immunodetection using an anti-His antibody 31

2.2.22 Antibody purification 32

2.2.23 N-terminal sequencing 32

2.2.24 Bradford reagent calibration 32

2.2.25 Preparation and calibration of Lanzetta reagent 32

2.2.26 *Mt*MurA and D117CMurA activity assays using Lanzetta reagent 33

2.2.26.1 Specific activity 33

2.2.26.2 pH dependence 33

2.2.26.3 K_M determination 34

2.2.27 Determination of the effect of fosfomycin on *Mt*MurA and D117CMurA 34

2.2.28 Trypsin digestion and MALDI-TOF MS analysis 35

2.3 MurA from *Mycobacterium tuberculosis* (*Mt*MurA) 36
2.3.1 Cloning of *MtmurA* into pKK233-2 36
2.3.2 Expression of *Mt*MurA 37
2.3.3 Cloning and expression of *Mt*MurA and D117CMurA in the pET21d (+) expression vector 38
2.3.4 Purification of *Mt*MurA and D117CMurA 40
2.3.5 Cloning and expression of *Mt*MurA-His and D117CMurA-His 41
2.3.6 Purification of *Mt*MurA-His 43
2.3.7 Activity of *Mt*MurA and D117CMurA 47
2.3.8 pH dependence of *Mt*MurA and D117CMurA 49
2.3.9 Effect of fosfomycin on *Mt*MurA and D117CMurA 50

2.4 MurA from *Chlamydia trachomatis* (*Ct*MurA) 53
2.4.1 Cloning of *CtmurA* into pKK233-2 53
2.4.2 Cloning of *CtmurA* into pET21d (+) 53
2.4.3 Expression of *Ct*MurA 54
2.4.4 Purification of *Ct*MurA 55

2.5 MurA from *Borrelia burgdorferi* (*Bb*MurA) 58
2.5.1 Cloning of *BbmurA* into pET21a (+) 58
2.5.2 Expression of *Bb*MurA 59

3. *Enterobacter cloacae* MurA as a histidine-tagged protein 62
3.1 Materials 62
3.1.1 Chemicals and enzymes 62
3.1.2 Bacterial strains 62
3.1.3 Vectors 62

3.2 Methods 62
3.2.1 Primers 62
3.2.2 PCR of the *En. cloacae* MurA gene 62
3.2.3 Digestion of DNA with restriction enzymes 63
3.2.4 Ligation 63

3.2.5 Transformation 63
3.2.6 Plasmid minipreps 63
3.2.7 Expression of the *Enc*MurA-His protein 63
3.2.8 Purification of *Enc*MurA-His 63
3.2.9 Western blotting and immunodetection using an anti-His antibody 64
3.2.10 Activity assays using *Enc*MurA-His 64

3.3 Results 65
3.3.1 Cloning of *EncmurA* gene into pET21d (+) 65
3.3.2 Expression of *Enc*MurA-His 65
3.3.3 Purification of *Enc*MurA-His 66
3.3.4 Determination of *Enc*MurA-His enzyme activity 68

4. A study of the conformational changes of *Enterobacter cloacae* MurA 70
4.1 Materials 70
4.1.1 Chemicals and enzymes 70
4.1.2 Bacterial strains 70
4.1.3 Vectors 70

4.2 Methods 70
4.2.1 Expression and purification of *En. cloacae* MurA and K22 mutants 70
4.2.2 MALDI-TOF analysis of wild type MurA and the K22 mutant proteins 70
4.2.3 Isothermal titration calorimetry (ITC) 71

4.3 Results 72
4.3.1 Purification of wild type and K22 mutant proteins 72
4.3.2 Tryptic digestion and MALDI-TOF analysis of wild type and K22 mutant proteins 72
4.3.3 Isothermal titration calorimetry of K22V MurA 76

5. Discussion 79
5.1 The naturally occurring variants of MurA 79
5.2 The conformational changes of MurA 89

5.3 Outlook 95

6. Bibliography 99

7. Publications 109

8. Acknowledgements 110

9. Curriculum vitae 111

Abbreviations

A	absorbance
Amp	ampicillin
ANS	1-anilino-1-naphthalene-8-sulphonic acid
BCIP	5-bromo-4-chloro-3-indolyl phosphate *p*-toluidine salt
bp	base pair
C_p	heat capacity
DEAE	diethylaminoethyl
DMSO	dimethylsulphoxide
DTT	1,4-dithio-DL-threitol
E. coli	*Escherichia coli*
EDTA	ethylenediaminotetraacetic acid
En. cloacae	*Enterobacter cloacae*
EPSPS	5-enolpyruvylshikimate-3-phosphate synthase
Fosfomycin (FF)	(1*R*, 2*S*)-1,2-epoxypropylphosphonic acid
ΔG	Gibbs free energy change
Glyphosate	*N*-(phosphonomethyl)-glycine
ΔH	enthalpy change
HEPES	4-(2-hydroxyethyl)piperazine-1-ethanesulphonic acid
IPTG	isopropyl-β-D-thiogalactopyranoside
ITC	isothermal titration calorimetry
k_{cat}	turnover number
K_D	dissociation constant
kDa	kilodaltons
K_i	inhibitor constant
K_M	Michaelis-Menten constant
LB	Luria-Bertani
MALDI-TOF	matrix-assisted layer desorption/ionization-time of flight
*m*DAP	*meso*-diaminopimelate
MES	2-morpholino-ethanesulphonic acid
MurA	UDP-*N*-acetylglucosamine enolpyruvyltransferase
NBT	nitrotetrazolium blue chloride
NCBI	National Centre for Biotechnology Information

Ni-NTA	nickel-nitrilotriacetic acid
OD	optical density
PAGE	polyacrylamide gel electrophoresis
PBP	penicillin binding protein
PCR	polymerase chain reaction
PEP	phosphoenolpyruvate
PVDF	polyvinyldifluoride
ΔS	entropy change
SDS	sodium dodecyl sulphate
TEAA	triethylammonium acetate
TFA	trifluoroacetic acid
Tm	melting temperature
Tris	tris-(hydroxymethyl)-aminomethane
Triton-X	octylphenol-polyethylenglycoether
TTBS	tris buffered saline + tween 20
U	unit
UDPNAG	UDP-*N*-acetylglucosamine
UDPNAG-EP	UDP-*N*-acetylenolpyruvylglucosamine
WT	wild type

Amino acids are abbreviated according to the one and three letter code.

Summary

The enzyme UDP-*N*-acetylglucosamine enolpyruvyltransferase (MurA) catalyses the first committed step in peptidoglycan biosynthesis. In this reaction, the enolpyruvyl moiety from phosphoenolpyruvate (PEP) is transferred to the 3' hydroxyl group of UDP-*N*-acetylglucosamine (UDPNAG) to form the product, UDP-*N*-acetylenolpyruvylglucosamine (UDPNAG-EP) with the concomitant release of inorganic phosphate.

As shown for MurA of *En. cloacae,* MurA can form two tetrahedral intermediates with the enolpyruvyl moiety of PEP, a covalently enzyme bound form and a non-covalent form with UDPNAG. Only the non-covalently bound form is required for completion of the reaction. The covalently bound intermediate is formed by the nucleophilic attack of the thiol group of the cysteine 115 residue on the C2 of PEP. The same cysteine residue also attacks the C2 of the antibiotic fosfomycin ((1*R*,2*S*)-1,2-epoxypropylphosphonic acid) to form a covalent adduct that results in the irreversible inhibition of MurA. Mutagenesis of this highly conserved Cys115 in *E. coli* MurA has demonstrated that replacement of the cysteine with an alanine or a serine residue renders the enzyme inactive, however the replacement of the cysteine with an aspartate, and to a lesser extent glutamate, retains some activity. In nature, some pathogenic organisms e.g. *Mycobacterium tuberculosis*, *Chlamydia trachomatis* and *Borrelia burgdorferi*, have exchanged this cysteine residue for an aspartate in MurA, rendering them fosfomycin resistant. The effect of this exchange on the catalytic properties of the enzyme was investigated in MurA from *Mycobacterium tuberculosis* (*Mt*MurA). Additionally, a *Mt*MurA aspartate to cysteine mutant (D117C) was characterised. Both proteins are enzymatically active, albeit with a large reduction in the catalytic efficiency compared to *En. cloacae* MurA. Moreover, the K_M values for both of the substrates were found to be the same for *Mt*MurA as for *En. cloacae* MurA, while those for D117CMurA were about 10-fold lower. *Mt*MurA is able to maintain the same K_M values as the cysteine-containing enzymes, probably as a result of favourable interactions occurring between neighbouring amino acid residues in the active site. However, the aspartate-containing enzymes appear to have sacrificed their catalytic efficiency in exchange for fosfomycin resistance. The pH of *Mt*MurA was also shifted to a slightly more acidic pH compared to the D117C mutant protein, representing the presence of the aspartate in the active site of this enzyme. The weak pH dependence of the aspartate-containing MurAs may reflect a difference in the rate-limiting step. The role of the cysteine as both a nucleophile and a general acid may be important in maintaining catalytic efficiency.

The structures of MurA in the absence and the presence of UDPNAG and fosfomycin have previously been solved. In the absence of substrates, the enzyme forms an open structure where the loop containing the reactive cysteine is solvent accessible. As a result of UDPNAG binding, a tighter more compact structure is observed with the loop forming a lid over the active site. Previous studies had implicated the residue, lysine 22, as part of the conformational switch mechanism. Analysis of lysine 22 mutant proteins have shown that fosfomcyin can only bind to the K22V mutant in the presence of UDPNAG. The measurement of the change in heat capacity in the K22V mutant using isothermal titration calorimetry, demonstrated that the conformational change occurs as in the wild type MurA. The presence of a positively charged side chain at this position is required for the binding of fosfomycin and probably PEP to the active site. However, the lack of activity of the K22V mutant suggests that it also has a role in the positioning of PEP in the correct steric conformation.

Zusammenfassung

Das Enzym UDP-*N*-acetylglucosamin enolpyruvyl Transferase (MurA) katalysiert den ersten Reaktionsschritt in der Biosynthese des Zellwandbestandteils Peptidoglykan (auch Murein genannt). Die Reaktion beinhaltet die Übertragung des Enolpyruvyl-Bausteins von Phosphoenolpyruvat (PEP) auf die 3'–Hydroxylgruppe von UDP-*N*-acetylglucosamin (UDPNAG), wobei UDP-*N*-acetylenolpyruvylglucosamin (UDPNAG-EP) und anorganisches Phosphat gebildet werden.

Mechanistische Untersuchungen erbrachten Hinweise für das Auftreten zweier unterschiedlicher Reaktionsintermediate: ein kovalent und ein nicht-kovalent gebundenes. Das kovalent-gebundene Intermediat entsteht beim nucleophilen Angriff der Thiolgruppe der Aminosäure Cystein 115 auf das C-2 Atom von PEP während das nicht-kovalente Intermediat durch den nucleophilen Angriff der 3'-Hydroxylgruppe von UDPNAG auf eben dieses Kohlenstoffatom des PEP gebildet wird. Dieses nicht-kovalent gebundene Intermediat befindet sich auf dem katalytischen Reaktionsweg zu den Produkten. MurA wird irreversibel durch das Antibiotikum Fosfomycin ((1*R*, 2*S*)-1,2-Epoxypropylphosphonsäure) gehemmt. Diese Hemmung kommt durch den nucleophilen Angriff der Thiolgruppe von Cystein 115 auf den Epoxid-Ring zustande. Durch Austausch dieses hochkonservierten Cysteins mittels ortsspezifischer Mutagenese konnte gezeigt werden, dass ein Serin bzw. Alanin in dieser Position zu einer vollständigen Inaktivierung des Enzyms führt. Andererseits führte ein Austausch mit den Aminosäuren Asparagin- oder Glutaminsäure zu einer Erhaltung der enzymatischen Aktivität. Interessanterweise kommt in einigen pathogenen Bakterien, wie z. B. *Mycobacterium tuberculosis*, *Chlamydia trachomatis* und *Borrelia burgdorferi*, anstelle des Cysteins eine Asparaginsäure vor. Dieser natürlich auftretende Aminosäureaustausch konserviert die Aktivität des Enzyms und bedingt gleichzeitig eine Resistenz gegenüber dem Antibiotikum Fosfomycin. In der vorliegenden Arbeit wurde die Fosfomycin-resistente MurA von *M. tuberculosis* heterolog in *Escherichia coli* exprimiert und aus Rohextrakten gereinigt. Dieses Wildtyp Protein wurde hinsichtlich seiner enzymatischen Eigenschaften charakterisiert. Anschliessend wurde die Asparaginsäure gegen Cystein ausgetauscht und das mutierte Protein hinsichtlich seiner katalytischen Eigenschaften mit dem zuvor charakterisierten Wildtyp Protein verglichen. Es zeigte sich, dass der Austausch der Asparaginsäure mit Cystein zu einer Hemmung durch Fosfomycin führt. Sowohl das Wildtyp Protein als auch die Mutante

(Asparaginsäure zu Cystein) zeigten enzymatische Aktivität, die allerdings im Vergleich zu MurA aus *Enterobacter cloacae* sehr gering ist. Andererseits zeigte sich, dass die Michaelis-Menten Parameter für beide Substrate im Falle der Wildtyp MurA aus *M. tuberculosis* vergleichbar sind mit denjenigen, die für das Enzym aus *En. cloacae* (besitzt ein Cystein in der korrespondierenden Position) bestimmt wurden. Die D117C Mutante zeigte demgegenüber eine ca. 10-fache Verringerung der K_M-Werte für beide Substrate. Das pH-Optimum von Wildtyp MurA ist im Vergleich zur Asparaginsäure zu Cystein-Mutante leicht zu einem niedrigeren pH-Wert verschoben. Diese Verschiebung kann durch den unterschiedlichen pK_a-Wert der Carboxylgruppe im Vergleich zur Thiolgruppe verstanden werden.

Die dreidimensionale Struktur von MurA (aus *E. coli* und *En. cloacae*) konnte sowohl in einer freien Form als auch im Komplex mit UDPNAG und Fosfomycin mittels Röntgenstrukturanalyse gelöst werden. In Abwesenheit von Liganden liegt das Protein in einer “offenen” Konformation vor und das oben erwähnte reaktive Cystein befindet sich in einer dem Lösungsmittel zugänglichen Schleife. In Anwesenheit von UDPNAG befindet sich das Protein in einer “geschlossenen” Konformation, in der sich diese Schleife über das Aktivzentrum legt und dieses damit für Lösungsmittel unzugänglich werden lässt. Frühere Untersuchungen ergaben Hinweise darauf, dass die Aminosäure Lysin 22 massgeblich an dieser Konformationsänderung beteiligt ist. Eine weiterführende Charakterisierung von Proteinen, die in Position 22 entweder ein Arginin, eine Glutaminsäure oder ein Valin trugen, haben diese Hypothese nicht bestätigen können. Mikrokalorimetrische und massenspektrometrische Untersuchungen zeigten jedoch, dass eine positiv geladene Seitenkette in Position 22 essentiell für die Bindung von Fosfomycin ist.

1. Introduction

1.1 The bacterial cell wall, peptidoglycan and its biosynthesis

Most bacteria contain a cell wall that is essential to provide shape, strength and rigidity to the cell (Bugg and Walsh 1992, Brock and Madigan 1997). It is also involved in maintaining the integrity of the cell by withstanding osmotic pressure (Nanninga 1998). Differences are present in the cell walls of Gram negative and Gram positive bacteria. In Gram negative bacteria, the cell wall is composed of multiple layers that include a thin layer of peptidoglycan and an outer membrane that is made up of lipopolysaccharides and porins (figure 1.1A) (Brock and Madigan 1997). On the other hand, Gram positive bacteria have a thicker cell wall that is composed of only one molecule, peptidoglycan (murein), although 10 to 25 layers of it may be present (figure 1.1B) (Brock and Madigan 1997).

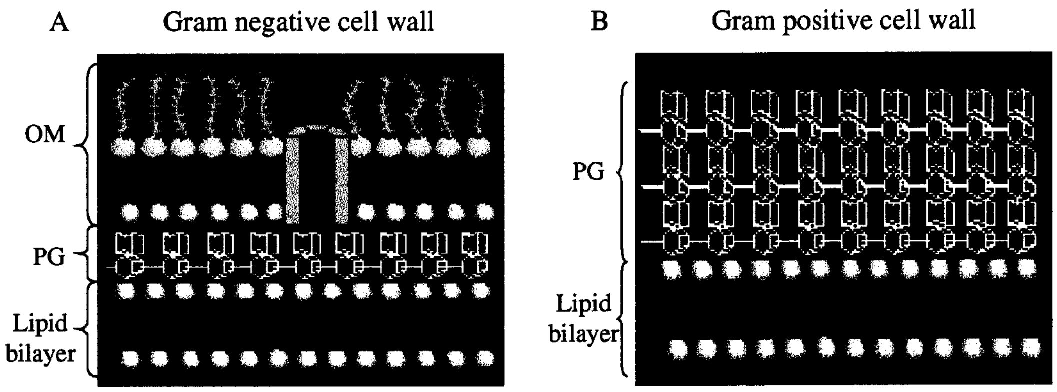

Figure 1.1: Architecture of the cell wall in Gram negative (A) and Gram positive bacteria (B). OM: outer membrane consisting of lipids, lipopolysaccharides and porins. PG: peptidoglycan. Adapted from http://www.uct.ac.za/depts/mmi/lsteyn/lecture.html.

In eubacteria, peptidoglycan is the macromolecule that provides the cell wall with its strength and rigidity (Nanninga 1998). It is a polysaccharide molecule composed of alternating sugar residues, *N*-acetylglucosamine (NAG) and *N*-acetylmuramic acid (NAM), joined by a β1,4-glycosidic bond (Brock and Madigan 1997, Nanninga 1998). Small chains of peptides are attached to the carboxyl group of the NAM residues and these chains are subsequently cross-linked in order to provide strength and rigidity to the structure (Brock and Madigan 1997). Peptidoglycan is synthesised by a series of enzymatic reactions that occur in the cytoplasm and in the periplasm (figure 1.2). Its synthesis is stringently controlled by processes occurring upstream of the precursor of peptidoglycan biosynthesis (Mengin-Lecreulx et al. 1989).

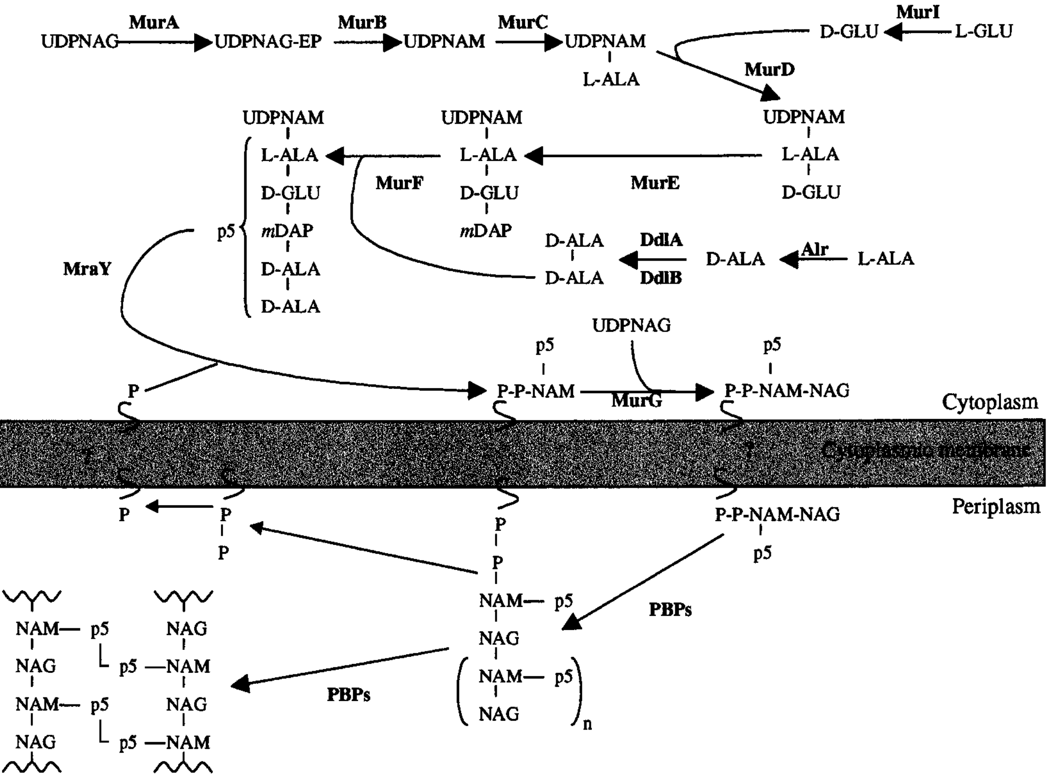
MurA
UDPNAG
UDPNAG-EP
MurB
UDPNAM
MurC
UDPNAM
L-ALA
D-GLU
MurI
L-GLU
MurD
UDPNAM
L-ALA
D-GLU
MurE
UDPNAM
L-ALA
D-GLU
mDAP
MurF
UDPNAM
L-ALA
D-GLU
mDAP
D-ALA
D-ALA
p5
D-ALA
D-ALA
DdlA
DdlB
D-ALA
Alr
L-ALA
MraY
P
UDPNAG
p5
P-P-NAM
MurG
p5
P-P-NAM-NAG
Cytoplasm
?
?
Cytoplasmic membrane
Periplasm
P
P
P
P
P
NAM— p5
NAG
NAM— p5
NAG
n
P-P-NAM-NAG
p5
PBPs
PBPs
NAM— p5
NAG
NAM— p5
NAG
NAG
p5 —NAM
NAG
p5 —NAM

Figure 1.2: The steps involved in peptidoglycan biosynthesis and the enzymes that catalyse them. UDP: uridine diphosphate. NAG: *N*-acetylglucosamine. NAG-EP: *N*-acetylenolpyruvylglucosamine. NAM: *N*-acetylmuramic acid. L-ALA: L-alanine. D-ALA: D-alanine. D-GLU: D-glutamate. *m*DAP: *meso*-diaminopimelic acid. P-P: undecaprenyl pyrophosphate carrier. ?: unidentified flippase. PBPs: Penicillin binding proteins. The enzymes catalysing the various stages are depicted in bold type above or below the arrows.

Firstly, UDP-*N*-acetylglucosamine (UDPNAG) is converted into UDP-*N*-acetylmuramic acid (UDPNAM) by the enzymes MurA and MurB. A pentapeptide chain is then added to the UDPNAM residue by the sequential addition of each amino acid by ATP-dependent amino acid specific ligases (figure 1.2) (Bugg and Walsh 1992, Ghuysen and Hackenbeck 1994). Amino acids of the D-configuration are commonly found in peptidoglycan because they provide resistance to external degradative enzymes (Bugg and Walsh 1992). The UDPNAM-pentapeptide is added to a membrane-bound lipid carrier, undecaprenyl pyrophosphate (a C_{55} lipid), to create lipid I (Bugg and Walsh 1992). The subsequent addition of UDPNAG by MurG, results in the formation of lipid II (Bugg and Walsh 1992). This lipid carrier renders the sugars sufficiently hydrophobic in order to allow transportation across the cytoplasmic membrane (Brock and Madigan 1997). A flippase enzyme may be responsible for this, but it has so far not been identified. In the periplasm, a bifunctional penicillin binding protein (PBP) has been identified that acts as a transglycosylase and a transpeptidase (Nanninga 1998). *N*-acetylglucosamine (NAG) and *N*-acetylmuramic acid (NAM) are linked by a β1,4-glycosidic bond in a reaction catalysed by the transglycosylase domain, the mechanism of which is as yet unknown (van Heijenoort 2001). The same penicillin binding protein also catalyses the transpeptidation reaction between the pentapeptide chains. In Gram negative bacteria, the chains are directly cross-linked by the penultimate D-ALA residue of one chain with the *m*DAP residue of the other chain (van Heijenoort 2001). In Gram positive bacteria, the *m*DAP residue is replaced by L-lysine and the cross-linked peptide chain may consist of a variety of amino acids including glycine, L-alanine, L-serine and D-asparagine. The length of the cross-link and the amino acids that are added to it varies between species (Bouhss et al. 2001, van Heijenoort 2001).

In the Gram positive organism *Mycobacterium tuberculosis*, the cell wall is composed of peptidoglycan covalently linked to mycolylarabinogalactan chains to provide a hydrophobic barrier that acts to enhance the impermeability of the cell wall (figure 1.3) (Chatterjee 1997, Dmitriev et al. 2000).

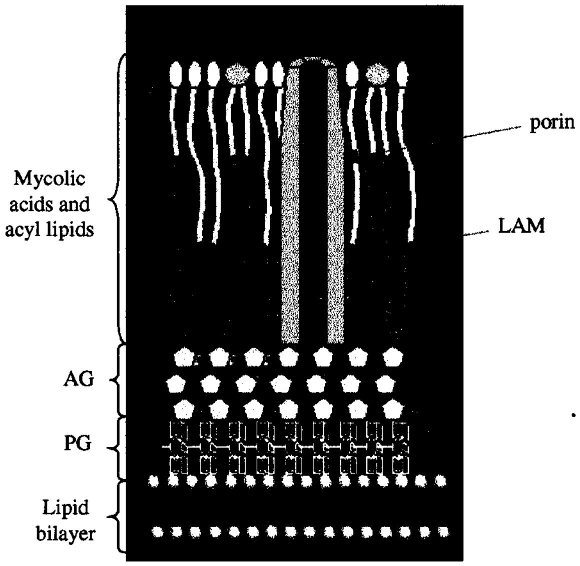

Figure 1.3: The architecture of the mycobacterial cell wall. PG: peptidoglycan. AG: arabinogalactan. AG is linked to mycolic acids. LAM: lipoarabinomannosides. Adapted from http://www.uct.ac.za/depts/mmi/lsteyn/lecture.html.

There are two main differences in the *M. tuberculosis* peptidoglycan structure as compared to other Gram positive bacteria (Chatterjee 1997). The first is that the muramic acid residues are *N*-acylated with glycolyic acid instead of the commonly found acetyl acid, which may be involved in protecting the organism from lysozyme degradation (Chatterjee 1997). It has been shown that the acetyl group of *N*-acetylmuramic acid is hydroxylated by an acetyl hydroxylase to give *N*-glycolylmuramic acid (Gateau et al. 1976, Essers and Schoop 1978). The second difference is that the cross-links include peptide bonds between *m*DAP and *m*DAP, in addition to those of *m*DAP and L-alanine as found in Gram negative bacteria (Chatterjee 1997).

Peptidoglycan is a dynamic structure that undergoes constant recycling. *E. coli*, for example, recycle six to eight percent of their peptidoglycan per generation, however the Gram positive bacteria recycle 25 to 50 % of their peptidoglycan per generation (Bugg and Walsh 1992). This rate of turnover has been correlated with the growth rate (Cheung et al. 1983). It is a very efficient recycling mechanism as the NAG-NAM-peptides are broken down into NAG-anhydroNAM and a tripeptide of L-ALA, D-GLU and *m*DAP. The tripeptide can be reincorporated into the NAM-pentapeptide in one step before incorporation into the wall (Bugg and Walsh 1992). The NAG-anhydroNAM units are degraded into their constituents by a recently identified pathway and can subsequently be reused in the synthesis of new peptidoglycan (Park 2001). Incorporation of the newly synthesised peptidoglycan has to occur without causing cell lysis, which suggests that newly synthesised peptidoglycan layers are added before hydrolases can remove the old layers (Holtje and Heidrich 2001).

Peptidoglycan is found in most eubacteria except for mycoplasma, which do not have cell walls (Brock and Madigan 1997). Archaebacteria do not contain peptidoglycan, instead the common types of cell wall that are found consist of a paracrystalline surface layer (S-layer) of hexagonal symmetry that is composed of polysaccharides, proteins or glycoproteins (Brock and Madigan 1997). Some Archae, e.g. methanogenic Archae, contain pseudopeptidoglycan that is composed of alternating repeats of *N*-acetylglucosamine and *N*-acetyltalosaminourionic acid that is connected by β1,3-glycosidic bonds (Brock and Madigan 1997). Incidentally, they are resistant to lysozyme that causes cell lysis by breaking the β1,4-glycosidic bonds between the NAG and NAM residues. Interestingly, the presence of peptidoglycan in one of the Gram negative bacteria, which was of interest to us during this study, is currently under debate. In *Chlamydia trachomatis*, a member of the Chlamydiae, the presence or absence of peptidoglycan has so far eluded scientists. Various studies using methods such as colourimetric analysis, radioactive labeling, immunoprecipitation, electron microscopy, amino acid analysis, gas chromatography and mass spectrometry, have given conflicting results as to the existence of peptidoglycan within these intracellular parasitic organisms (Barbour et al. 1982, Chopra et al. 1998). It has been proposed that instead of peptidoglycan they have an envelope layer, composed of cysteine-rich proteins that are extensively cross-linked via disulphide bonds (the P-layer) to provide a degree of strength and osmotic stability to the organism (Hatch 1996). However, their growth is inhibited by the group of β-lactam antibiotics that have been shown to inhibit the penicillin binding proteins (PBPs) involved in peptidoglycan biosynthesis (Barbour et al. 1982). Interestingly when the genome was sequenced in 1998, it transpired that all of the genes for the peptidoglycan pathway were present suggesting that these organisms do indeed synthesise peptidoglycan (Stephens et al. 1998). Predictive studies have suggested that the PBPs identified by sequencing show similarity to the Class 2 PBPs from *E. coli*, which are monofunctional enzymes only capable of catalysing transpeptidation reactions. Additionally, no genes encoding monofunctional transglycosylases have so far been identified in the genome. This suggests that the wall consists of cross-linked disaccharide peptides, i.e. it is glycanless, lipoproteins, lipopolysaccarides and the highly cross-linked cysteine rich proteins (Ghuysen and Goffin 1999, Storey and Chopra 2001). However, the debate is ongoing.

Peptidoglycan is an important target for antibiotics, especially as it is only found in eubacteria and not humans. Many antibiotics that are in current use have been shown to target enzymes in this pathway. For example, the β-lactam group of antibiotics inhibits the transpeptidation reaction by acylation of the enzyme's active site serine (Frere et al. 1999). Others include D-cycloserine, which inhibits the alanine racemase enzyme, Alr (figure 1.2) (Walsh 2000), fosfomycin that targets the MurA enzyme (see section 1.4 for further details) (Kahan et al. 1974) and vancomycin that binds the peptide, D-ALA-D-ALA preventing transglycosylation from occurring (Bugg and Walsh 1992). One of the major problems in the last few years has been the increasing resistance of many bacteria to these commonly used antibiotics. The resistance mechanisms may take the form of decreased uptake or increased excretion of the drug, overexpression of the target protein, mutations within the target protein or inactivation of the drug (Walsh 2000). For example, fosfomycin is inactivated by the addition of glutathione by a specific metalloglutathione transferase, FosA (figure 1.4) (Arca et al. 1988, 1990, Bernat et al. 1997).

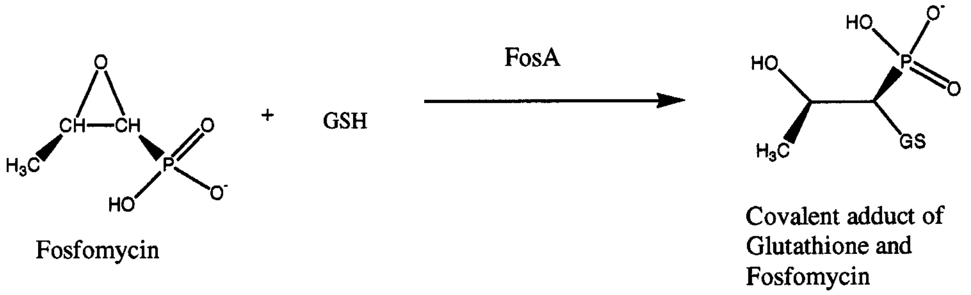

Figure 1.4: Inactivation of fosfomycin by the addition of glutathione, in a reaction catalysed by the manganese metalloglutathione transferase, FosA.

In the case of vancomycin, bacteria have developed a novel peptidoglycan structure by altering the pathway of peptidoglycan biosynthesis (Bugg and Walsh 1992, Walsh 2000).

1.2 UDP-*N*-acetylglucosamine enolpyruvyltransferase (MurA)

The enzyme UDP-*N*-acetylglucosamine enolpyruvyltransferase (MurA) (E.C.2.5.1.7) catalyses the first committed step in the biosynthesis of peptidoglycan (figure 1.2). The reaction involves the transfer of the enolpyruvyl moiety from phosphoenolpyruvate (PEP) to the 3'-hydroxyl group of UDP-*N*-acetylglucosamine (UDPNAG) to generate the product UDP-*N*-acetylenolpyruvylglucosamine (UDPNAG-EP) with the concomitant release of inorganic phosphate (figure 1.5, scheme A). The product, UDPNAG-EP, is subsequently reduced by the enzyme, MurB, to generate UDP-*N*-acetylmuramic acid (figure 1.2). MurA is irreversibly inhibited by the antibiotic fosfomycin that acts as a phosphoenolpyruvate analog (Kahan et al. 1974). Very recently, a lytic protein, A2, from the phage Qβ virion has also been shown to inhibit MurA (Bernhardt et al. 2001).

This type of enolpyruvyl transfer is known to be catalysed by only one other enzyme, i.e. 5-enolpyruvylshikimate-3-phosphate synthase (EPSPS) (E.C.2.5.1.19) (figure 1.5, scheme B) that is inhibited by the herbicide glyphosate (Steinrücken and Amrhein 1984). Recently, a putative enolpyruvyltransferase, NikO, was identified in the nikkomycin biosynthetic pathway of *Streptomyces tendae* by sequence homology but the reaction catalysed by this enzyme remains to be elucidated (Lauer et al. 2000).

MurA is present in all eubacteria except mycoplasma, as described above, and *Bacteriodes forsythus*, which appears to have replaced MurA with a *N*-acetylmuramic acid scavenging pathway (Wyss 1989). MurA is present as a single copy gene in Gram negative and most Gram positive bacteria. In some Gram positive bacteria that have a low G + C content, e.g. *Streptococcus pneumoniae*, *Bacillus subtilis*, there are 2 copies of the gene, the products of which both catalyse the transfer of the enolpyruvyl moiety of PEP (Du et al. 2000). These are thought to have arisen by gene duplication (Du et al. 2000). The MurA enzymes from *Enterobacter cloacae* (Wanke et al. 1992) and from *Escherichia coli* (Marquardt et al. 1992) have been expressed in large quantities and extensively characterised.

A: Reaction catalysed by MurA

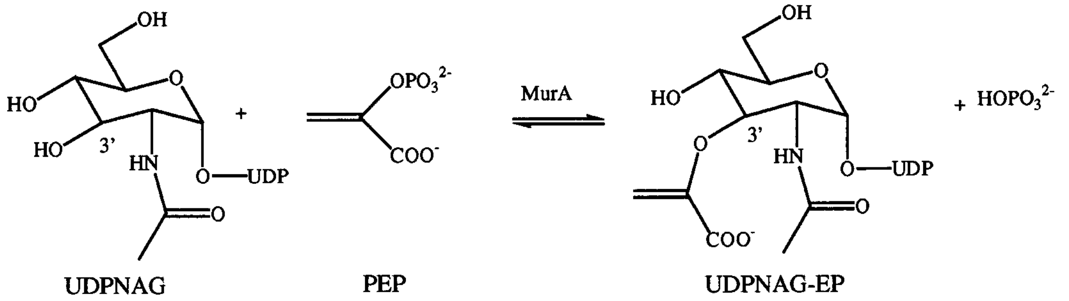

B: Reaction catalysed by EPSP Synthase

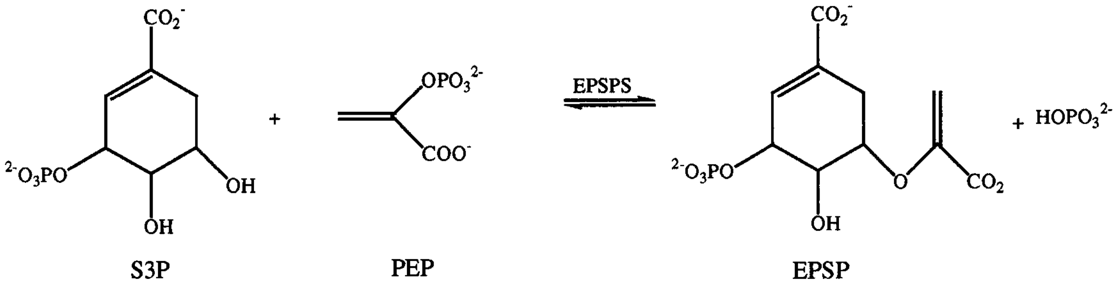

Figure 1.5: The reactions that are catalysed by the enzymes MurA (scheme A) and EPSP Synthase (scheme B). UDPNAG: UDP-*N*-acetylglucosamine, UDPNAG-EP: UDP-*N*-acetylenolpyruvylglucosamine, S3P: shikimate 3-phophate, EPSP: 5-enolpyruvylshikimate-3-phosphate, PEP: phosphoenolpyruvate, MurA: UDP-*N*-acetylglucosamine enolpyruvyltransferase, EPSPS: 5-enolpyruvylshikimate-3-phosphate synthase.

1.3 The structure of MurA

The MurA enzymes from *Enterobacter cloacae* and *E. coli* have been crystallised. The structures of wild type MurA and C115S mutant proteins are available in the unliganded form at 2.0 Å and 1.9 Å resolution, respectively (Schönbrunn et al. 1996, 2000a). The structure of wild type MurA is also available in the presence of UDPNAG and fosfomycin (1.8 Å resolution) (Skarzynski et al. 1996). The structure of a C115A mutant enzyme has also been elucidated in the presence of UDPNAG and the fluorinated analog of PEP (FPEP) at 2.8 Å resolution (Skarzynski et al. 1998).

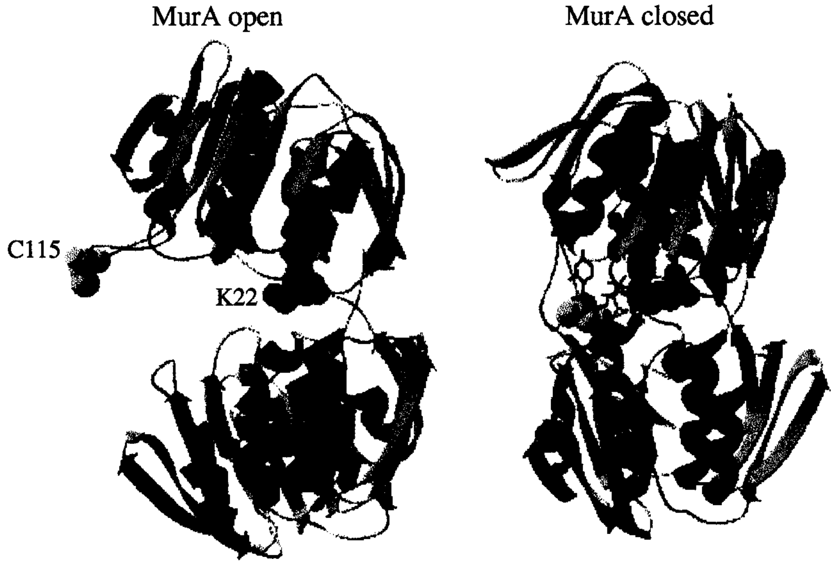

MurA open

MurA closed

Figure 1.6: The open (PDB coordinates 1NAW) and closed (PDB coordinates 1UAE) conformations of MurA. The C115 and the K22 residues are highlighted in yellow and blue respectively. The closed form is complexed with UDPNAG (purple) and fosfomycin (green). Alpha helices, beta-strands and loops are shown in red, blue and orange, respectively.

The elucidation of the structures indicated two possible conformations of the enzyme, an "open" and a "closed" form (figure 1.6) (Schönbrunn et al. 1996, Skarzynski et al. 1996). The overall structure of the enzyme consists of two globular domains that are connected by a rigid hinge domain (Schönbrunn et al. 1996, Skarzynski et al. 1996). Each domain consists of a specific fold that comprises six α-helices and three β-sheets (four-stranded), i.e. an inside out α/β barrel (Schönbrunn et al. 1996, Skarzynski et al. 1996). Additionally, in the open form there is a solvent accessible loop structure (residues 112 to 121) containing the cysteine residue (C115) (figure 1.6) (Schönbrunn et al. 1996). In the closed structure, this loop forms a lid over the active site and interacts with fosfomycin (figure 1.6) (Skarzynski et al. 1996). This loop has been shown at high salt concentrations to adopt a less solvent accessible conformation in the open form, which may function as a protective mechanism for the cysteine residue (Eschenburg and Schönbrunn 2000). The open form appears to be stabilised by the repulsive forces arising from the parallel arrangement of the residues Arg397 and Lys48 as well as an overall macrodipole effect (Schönbrunn et al. 1996, 1998). The phosphate group of UDPNAG has a negative charge and may be attracted to the resulting positive charge in the active site. On binding, this charge is neutralised allowing the reactive cysteine to move towards the active site for reaction with PEP or fosfomycin. Small angle X-ray scattering, fluorescence studies using the hydrophobic probe ANS (8-anilino-1-naphthalene sulphonate), isothermal titration calorimetry and tryptic digestion followed by MALDI-TOF mass spectrometry have shown that the conformational change occurs upon UDPNAG binding to the enzyme (Schönbrunn et al. 1998, Krekel et al. 1999, Samland et al. 2001b).

Other amino acid residues present in the cleft of the open conformation of MurA make connections that are subsequently broken in the closed conformation. These include Lys22 and Asp49, which are linked by a salt bridge in the open conformation (Schönbrunn et al. 1996). In the closed conformation, Asp49 forms a salt bridge with Arg397 while Lys22 interacts with the Asn23 side chain and the oxygen of the phosphonate group of fosfomycin (Skarzynski et al. 1996). Site-directed mutagenesis studies of Lys22 indicate that the binding of UDPNAG or PEP is not dependent on this residue (Samland et al. 1999). Isothermal titration calorimetry (ITC) experiments also indicated that the loss of the positively charged side chain in the Lys22 mutants affected fosfomycin binding (Samland et al. 1999). However, Arg120 and Arg397 also interact with the phosphonate group of fosfomycin by electrostatic interactions and hydrogen bonds (Skarzynski et al. 1996). Hence, the loss of Lys22 was not thought to be sufficient to affect fosfomycin binding, instead Lys22 was suggested to be involved in the conformational change (Samland et al. 1999). In the closed conformation, the uridine ring of UDPNAG is found between 2 hydrophobic surfaces created by Arg120 and Pro121 on one face and Leu124 on the other, whereas the sugar part of UDPNAG makes hydrogen bond contacts with Asn23 and Asp305 (Skarzynski et al. 1996). Mutagenesis studies confirmed that Asp305 is involved in the deprotonation of the 3'-hydroxyl group of UDPNAG in order to facilitate nucleophilic attack on PEP (Samland et al. 2001a). The involvement of Asn23 in the stabilisation of the transition state after deprotonation was also shown by mutagenesis studies (Samland et al. 2001a).

1.4 The reaction mechanism of MurA

For the reaction to occur, the C3 of PEP must be protonated and the 3'-hydroxyl group of UDPNAG deprotonated in order to facilitate the nucleophilic attack on the C2 of PEP. Phosphate and the product, UDPNAG-EP, are then released (figure 1.7). Two types of reaction intermediates have been identified in the reaction pathway. These are an enzyme-bound covalent intermediate with PEP, an *O*-phosphothioketal, (Cassidy and Kahan 1973, Zemell and Anwar 1975, Wanke and Amrhein 1993, Ramilo et al. 1994) and a non-covalently bound tetrahedral intermediate of UDPNAG and PEP (Marquardt et al. 1993). This suggests that there may be two intermediate forms involved in the reaction pathway, however it has been shown that only the non-covalent intermediate is required for completion of the reaction (figure 1.7). These two forms have been identified as being in rapid equilibrium with each other (figure 1.7) (Brown et al. 1994, Kim et al. 1995). The covalent intermediate is therefore an "off" pathway intermediate and is not involved directly in the reaction mechanism.

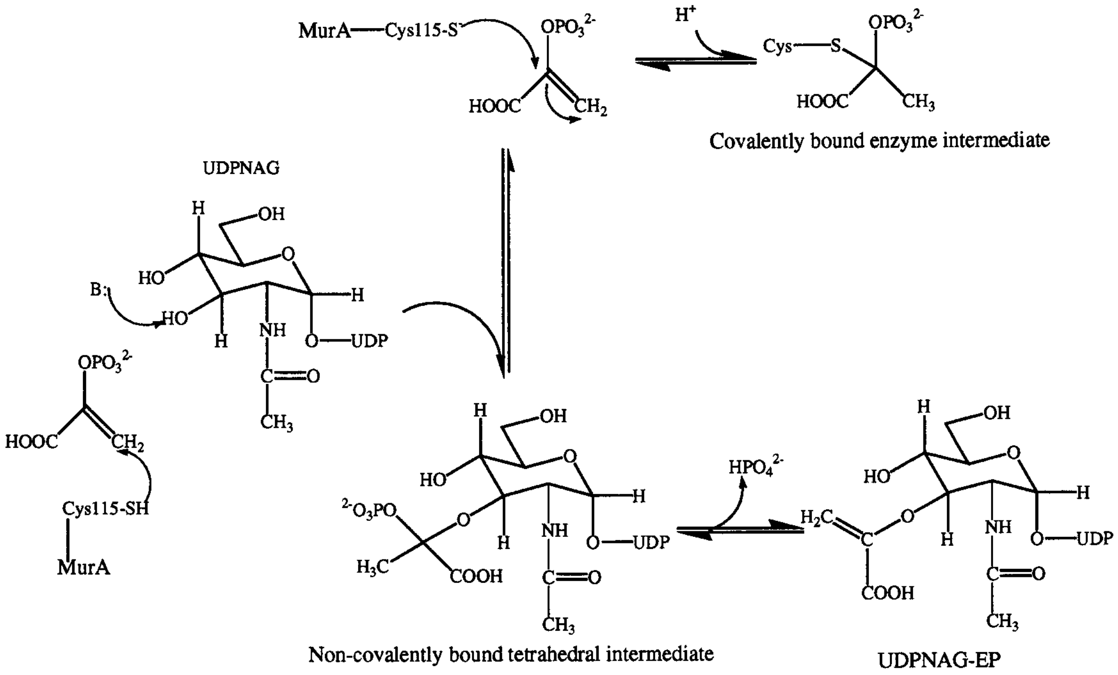
MurA—Cys115-S⁻
OPO₃²⁻
HOOC
CH₂
H⁺
Cys—S
OPO₃²⁻
HOOC
CH₃
Covalently bound enzyme intermediate
UDPNAG
H
OH
O
HO
B:
HO
H
NH
H
O—UDP
C=O
CH₃
OPO₃²⁻
HOOC
CH₂
Cys115-SH
MurA
²⁻O₃PO
H₃C
COOH
HPO₄²⁻
H₂C
C
COOH
Non-covalently bound tetrahedral intermediate
UDPNAG-EP

Figure 1.7: The proposed reaction mechanism indicating the formation of the covalent and non-covalent tetrahedral intermediates. They have been shown to be in equilibrium. Only the non-covalent intermediate is required for completion of the reaction.

The overall stereochemistry of the formation of the tetrahedral intermediate was determined to proceed as *anti/syn* or *syn/anti* addition-elimination steps (figure 1.8) (Lees and Walsh 1995). Kim et al. (1996b) observed the addition of the H^+ to the C3 of PEP from the si-face of PEP indicating that the addition across the double bond of PEP was in the *anti*-configuration. Analysis of the C115A mutant that was unable to form the covalent enzyme intermediate, indicated that the stereochemistry of elimination was in the *syn* configuration and that the absolute configuration of the C2 was in the 2-*S*-configuration (Skarzynski et al. 1998). Therefore, the reaction undergoes an *anti*/*syn* addition-elimination mechanism (figure 1.8).

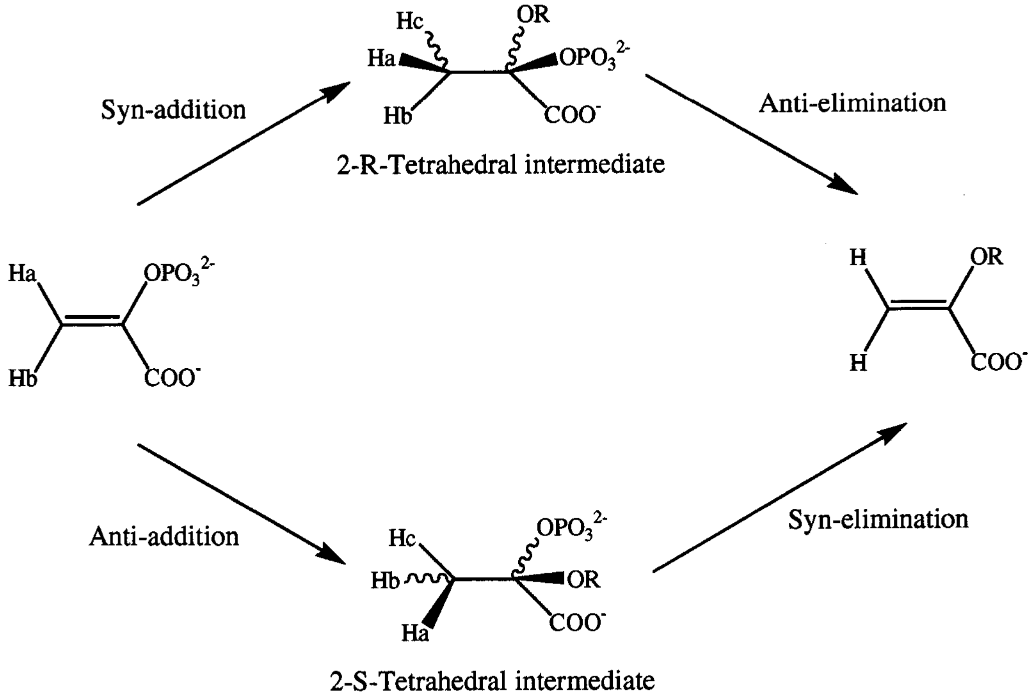
Syn-addition
Anti-elimination
Anti-addition
Syn-elimination
2-R-Tetrahedral intermediate
2-S-Tetrahedral intermediate
Ha
Hb
Hc
H
OR
OPO3 2-
COO-

Figure 1.8: The two stereochemical possibilities of MurA and the addition-elimination mechanisms. Redrawn from Kim et al. (1996b).

The covalent intermediate is formed by the nucleophilic attack of a cysteine residue on the C2 of PEP to form an *O*-phosphothioketal (figure 1.7). This cysteine residue was identified by protection studies and site-directed mutagenesis to be the cysteine 115 residue (Wanke and Amrhein 1993, Marquardt et al. 1994). The nucleophilic attack of Cys115 on the C2 of fosfomycin results in the opening of the highly reactive epoxide ring and the alkylation of the thiol group of C115 (figure 1.9) leading to the irreversible inhibition of the enzyme (Kahan et al. 1974).

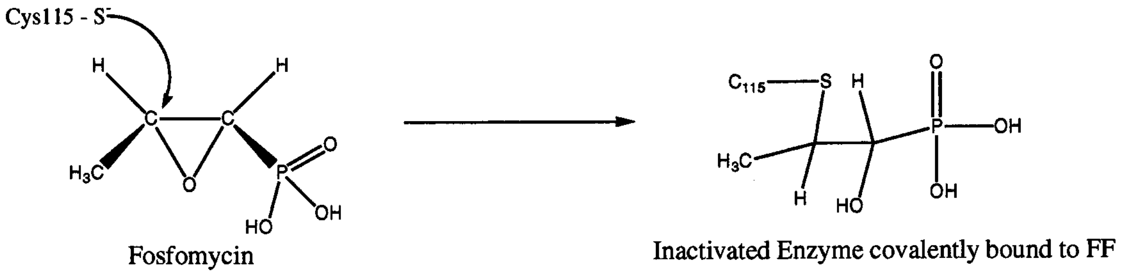

Figure 1.9: Inactivation of fosfomycin by nucleophilic attack on the C2 of the epoxide ring by C115.

Fosfomycin and PEP binding have been shown to be favoured in the presence of UDPNAG. This is due to the conformational change of the enzyme upon UDPNAG binding that allows the positioning of the loop for favourable interactions with fosfomycin or PEP (see section 1.3). This accelerating effect is not due to a change in reactivity of the thiol group of the Cys115 as the pKa value of this residue is unaffected by the binding of UDPNAG (Krekel et al. 2000). The covalent binding of fosfomycin is possible in the absence of UDPNAG as determined by tryptic digestion and MALDI-TOF mass spectrometry (Samland 2001). However, the affinity of fosfomycin in the absence of UDPNAG is much lower compared to the affinity observed in the presence of UDPNAG (1.1 mM compared to 25 nM respectively) (Samland 2001). The same effect was observed with PEP, a K_M of 7.5 μM was observed in the presence of UDPNAG whereas a K_D of 220 μM was observed in its absence (Samland 2001). Fosfomycin can also be bound in the absence of the cysteine. Studies with the Cys115 to serine mutant protein indicated that the K_D of fosfomycin binding is 1.4 mM and 4.6 mM in the absence and the presence of UDPNAG, respectively (Samland 2001). This indicates an initial binding of fosfomycin to the active site before it forms the covalent adduct with the cysteine residue (Marquardt et al. 1994). The purpose of the covalent enzyme-bound intermediate has not been identified although it has been suggested that it may afford protection from oxidation of the Cys115 residue in the absence of UDPNAG. This is supported by the observation that 80 % of MurA that is isolated from bacteria is isolated as the *O*-phosphothioketal form (Wanke and Amrhein 1993, Brown et al. 1994).

Site-directed mutagenesis studies of Cys115 have promoted the understanding of the role of this residue in catalysis. The Cys115 residue has been mutated to alanine (Skarzynski et al. 1998), serine (Wanke and Amrhein 1993), aspartate and glutamate

(Kim et al. 1996a). The C115A and C115S mutants are inactive (Wanke and Amrhein 1993). On the other hand, the C115D mutant, and to a lesser extent the C115E mutant, show activity albeit to a reduced level (Kim et al. 1996a). These studies indicate that the C115 residue must function other than as a nucleophile (Kim et al. 1996a). It was observed that the activity of the C115D was dependent on the pH. A higher activity was observed at pH 5.5 than at pH 8.0. In contrast, the activity of the wild-type enzyme was pH independent in this pH range. This indicated that the C115 residue functions as a general acid in the active site serving to protonate the C3 methylene group of PEP subsequent to the nucleophilic attack on the C2 of PEP. As the C115D mutant retains activity it indicates that the role of the C115 residue as a nucleophile is dispensible. Additionally, the presence of aspartate at this position conferred fosfomycin resistance (Kim et al. 1996a).

Interestingly, the C115D mutation has been found to occur in a number of MurA sequences from eubacteria, mainly pathogenic bacteria. For example it is found in Mycobacterium species (*Mycobacterium tuberculosis*, *Mycobacterium leprae*), Chlamydiae species (*Chlamydia trachomatis*, *Chlamydia pneumoniae*), *Borrelia burgdorferi* and *Treponema pallidum*. These organisms exhibit fosfomycin resistance due to the absence of the reactive thiolate of C115. They are the causative agents of many human diseases, e.g. *Mycobacterium tuberculosis* is the causative agent of tuberculosis, which causes over 3 million deaths per year and infects a third of the world's population (Dye et al. 1999). Therefore, it is imperative, especially with the advent of bacteria that are resistant to multiple drugs, to develop new antibiotics. The biochemical characterisation of MurA containing the natural mutation of a cysteine to aspartate from one of these organisms may lead to new approaches in the development of antibiotics.

1.5 Comparison of MurA with EPSPS

The presence of 5-enolpyruvylshikimate-3-phosphate synthase (EPSPS) but absence of MurA in archae suggests that the MurA's have evolved from EPSPS. The sequence identity of MurA and EPSPS is only about 20 %, however, they have in common the conserved residues that are thought to be involved in catalysis. The structures of EPSPS are available in the unliganded form (Stallings et al. 1991) and together with its substrate, shikimate 3-phosphate (S3P), and inhibitor, glyphosate, (Schönbrunn et al.

2001). The overall topology of the enzyme is similar to that of MurA, with the exception of the absence of the loop structure found in MurA. In EPSPS, this is replaced by a short sequence. Consequently, EPSPS is unable to form the covalent enzyme-bound intermediate. A non-covalent tetrahedral intermediate has been identified (Lewis et al. 1999) and the addition-elimination mechanism is proposed to occur via an *anti/syn* stereochemistry as in MurA (Skarzynski et al. 1998). Based on the similarity in structure with MurA, the enzyme is also thought to undergo a conformational change. Tryptic analysis of EPSPS confirmed that protection from digestion occurred in the presence of S3P and glyphosate (Krekel et al. 1999). It was also observed that EPSPS was more resistant to tryptic digestion in both conformations compared to MurA (Krekel et al. 1999). This may be due to the more open active site of MurA as the UDPNAG substrate is larger than S3P. The MurA and EPSPS enzymes therefore have a structural and mechanistic relationship as well as an evolutionary one.

1.6 Objectives

As described above, MurA has been extensively characterised with respect to its structure and reaction mechanism. However, the discovery of a naturally occurring MurA containing an aspartate residue instead of the reactive cysteine indicates that there is still much to be learnt with regard to the reaction mechanism and how the enzyme responds to environmental pressures. So far none of these naturally occurring variant MurA's have been characterised in biochemical detail and therefore it is not known if the presence of the aspartate residue confers the same properties on MurA as those observed with the C115D mutant described in section 1.4.

1.6.1 Characterisation of the naturally occurring variants of MurA

MurA's from *Mycobacterium tuberculosis*, *Chlamydia trachomatis* and *Borrelia burgdorferi* contain a naturally occurring aspartate residue in place of the cysteine residue as described previously. The aim of this work was to clone, express and purify MurA from these three organisms and characterise them biochemically with respect to their kinetic parameters, pH dependence and fosfomycin sensitivity.

1.6.2 *Enterobacter cloacae* MurA as a histidine-tagged protein

So far the *En. cloacae* MurA has been used in our laboratory only in the native form. To facilitate purification of this protein and allow comparison with the *Mt*MurA-His tagged protein, the aim of this work was to clone, express, purify and measure activity of the *En. cloacae* MurA in a histidine-tagged form.

1.6.3 A study of the conformational changes of MurA from *Enterobacter cloacae*

The aim of this work was to investigate the propensity of MurA from *Enterobacter cloacae* to undergo the conformational change. Previous studies indicated that the K22 residue may play a role in the conformational switch mechanism (Samland et al. 1999). Tryptic digestion and MALDI-TOF mass spectrometry together with isothermal titration calorimetry (ITC) were employed to investigate the role of this residue further, with particular attention to the K22V mutant.

2. Characterisation of the naturally occurring variants of UDP-*N*-acetylglucosamine enolpyruvyltransferase (MurA)

2.1 Materials

2.1.1 Chemicals and enzymes

UDP-*N*-acetylglucosamine and fosfomycin (disodium salt) were from Fluka, Buchs, Switzerland. Phosphoenolpyruvate (potassium salt) was from Sigma, Buchs, Switzerland. Tris was from BDH laboratory supplies, Poole, England. Unless otherwise indicated in the text, all other fine chemicals were of the highest possible grade from Fluka or Sigma.

All components for bacterial media were obtained from Difco, Basel, Switzerland.

All restriction enzymes and DNA modification enzymes were obtained from New England Biolabs (NEB), Frankfurt am Main, Germany or MBI Fermentas, Heidelberg, Germany. Except for calf intestinal alkaline phosphatase (CIAP) and Pwo DNA polymerase which were from Roche Molecular Biochemicals, Rotkreuz, Switzerland.

All primers that were used for DNA amplification and DNA sequencing were obtained from Microsynth, Balgach, Switzerland.

2.1.2 Bacterial strains

E. coli DH5α	*sup E44 Δlac U169 (φ80lac ZΔMI5) hsd R17 rec endAI gyrA96 thi-irelAI*
E. coli JM105	*sup E end A sbc B 15 hsd R4 rpsL thi Δ(lac-proAB) F'{tra D36 proAB*$^{+}$ *lacI*^{q} *lac ZΔMI5}*
E. coli BL21(DE3)	*hsd S gal (λcIts 857 ind 1 sam 7 nin 5 lac UV5-T7gene1)*
E. coli BL21 (DE3) RIL	*B F*$^{-}$ *omp T hsdS(*$r_B^{-} m_B^{-}$*) dcm*$^{+}$ *Tet*^{r} *galλ(DE3) endA Hte [argU ileY leuW Cam*^{r}*]*

E. coli DH5α is a bacterial strain commonly used in the initial cloning of target DNA and the maintenance of plasmids. *E. coli* JM105, *E. coli* BL21 (DE3) and *E. coli* BL21 (DE3) RIL bacterial strains on the other hand, are used for expression of the target proteins. *E. coli* BL21 (DE3) RIL competent cells (Stratagene) contain tRNA's carrying rare codons for the amino acids, arginine, isoleucine and leucine.

2.1.3 Vectors

The vector pKK233-2 (Pharmacia, Dübendorf, Switzerland) is 4593 bp in size and carries a trc promoter as well as an ampicillin resistance (Amp^r) gene. It is also IPTG inducible (Amann and Brosius 1985).

The vectors pET21d (+) and pET21a (+) (Novagen, Luzern, Switzerland) are 5440 and 5443 bp in size, respectively and have a T7 promoter. They have a multiple cloning site that contains NcoI or NdeI cleavage sites. They also confer ampicillin resistance and are IPTG inducible. These plasmids also allow the option of introducing either a N-terminal T7-tag or a C-terminal histidine-tag to the protein.

The PCR-Script Amp SK (+) vector (Stratagene) is used in order to facilitate cloning into other expression vectors. The vector carries the ampicillin resistance gene and a unique SrfI restriction site, which allows the blunt end ligation of a PCR product.

2.2 Methods

All cloning procedures were adapted from Sambrook et al. (1989) or Ausubel (1987).

2.2.1 Genomic DNA

Genomic DNA from *Mycobacterium tuberculosis* strain H37Rv was kindly provided by Dr G. Pfyffer of the National Centre for Mycobacteria, University of Zurich, Switzerland.

Genomic DNA of *Chlamydia trachomatis* serovar L2 was kindly provided by Dr U. Mamat, Department of Immunochemistry and Biochemical Microbiology, Research Centre Borstel, Germany.

A NaCl suspension containing cells of the non-virulent *Borrelia burgdorferi* strain OMZ 494-P were kindly provided by Dr. C. Wyss, Institute of Oral Microbiology and General Immunology, University of Zurich. The genomic DNA was isolated using the QIAamp Tissue Kit (Qiagen Ltd) according to the manufacturer's instructions. The genomic DNA was eluted in 400 µL of buffer AE and stored at -20 °C. The concentration and the purity of the genomic DNA were determined spectrophotomerically by measuring the A_{260} and the A_{260}/A_{280} respectively. The yield of genomic DNA was 152 ng/µL.

2.2.2 Primers

The following primers were designed for the cloning of the *murA* gene. The respective restriction sites are underlined and the start and stop codons, when present, are depicted in bold type.

Primers for the cloning of the *MtmurA* gene:

MtMurA 5' 5' GGCTCACATGCC**ATG**GCCGAGCGTTTCGTC 3'
Nco I

MtMurA 3' 5' GGCCCAAGCTT**CTA**ACAGCATACCCGTTCG 3'
Hind III

MtMurA-His3' 5' ATAAGAATGCGGCCGCACAGCATACCCGTTCGATC 3'
Not I

Primers for the cloning of the *CtmurA* gene:

CtMurA5' 5' GCATGCC**ATG***G*CTGGTATCAAGGTTTTTG 3'
NcoI

CtMurA3' 5' GCATGCCATGG**TTA**AACATACACAGATACTGAG 3'
NcoI

CtMurA3'-2 5' GCCCAAGCTTG**TTA**AACATACACAGATACTGAG 3'
HindIII

CtMurA3'-3 5' CGCGGATCCGC**TTA**AACATACACAGATACTGAG 3'
BamHI

To create a NcoI restriction site in primer CtMurA5', a C base was mutated to a G base. The mutated base is shown in italics. This resulted in an amino acid change from a proline to an alanine, however, none of the residues at the N-terminus of the protein are conserved and therefore, this change was not expected to affect the properties of the protein.

Primers for the cloning of the *BbmurA* gene:

BbMurA5' 5' CGGGAATTCCAT**ATG**CGATTTAATTTTATTAAG 3'
NdeI

BbMurA5'-2
5'GGGAATTCCAT**ATG**CGATTTAATTTTATTAAGTTTTTATATATAG 3'
NdeI

BbMurA3' 5' GCGCGGATCC**CTA**TTGACTTTTAACTTTCTTG 3'
BamHI

All of these primers are considerably long, between 32 to 46 bp, due to the low G+C content of the gene.

The primers were designed to ensure annealing of 18 to 20 bases to the *murA* gene sequence. The melting temperature, Tm, of the section of the primer that annealed to the gene sequence is calculated using the following formula:

Tm (°C) = (no. of A + T bases x 2) + (no. of G + C bases x 4)

This was then used to determine the annealing temperature to be used in the corresponding PCR, i.e. Tm minus 5°C.

2.2.3 PCR

The PCR was set up in thin-walled 0.5 mL tubes to contain the following: 50 to 150 pmol of each primer (both 5' and 3'), 0.2 mM of PCR nucleotide mix (Roche Molecular Biochemicals), 1 x reaction buffer, 1.5 to 2.5 mM of $MgSO_4$, 0.1 µg to 1.7 µg of genomic DNA or 5 to 25 µg of plasmid DNA, 2.5 to 5 U of Pwo DNA polymerase and sterile water to give a final volume of 50 µL. The control reactions did not contain Pwo DNA polymerase. Each reaction was overlaid with 2 drops of sterile mineral oil.

The PCR was carried out in a Perkin Elmer Cetus DNA Thermal Cycler. The reactions were placed into the Thermal Cycler (preheated to 95 °C) and the following cycles were carried out:

4 minutes at 95 °C

$$\left.\begin{array}{l}\text{45 seconds at 95 °C}\\ \text{60 seconds at 54 °C}\\ \text{2 minutes at 72 °C}\end{array}\right\}\text{ x 10 cycles}$$

$$\left.\begin{array}{l}\text{45 seconds at 95 °C}\\ \text{60 seconds at 54 °C}\\ \text{2 minutes at 72 °C + 20 second extension time per cycle}\end{array}\right\}\text{ x 20 cycles}$$

10 minutes at 72 °C

The above cycles specifically describe those used to produce the untagged *MtmurA* PCR product. An annealing temperature of 52 °C was used in the PCR to obtain *MtmurA-His* and *CtmurA*. As the overall G+C content of the *Borrelia burgdorferi* genome is very low, i.e. around 28 %, the annealing temperatures used were in the region of 39 °C, when the BbMurA5' primer was used, and 45 °C, when the BbMurA5'-2 primer was used.

The PCR products were analysed on a 1 % agarose gel (1 g agarose (Eurobio, Les Ulis Cedex, France) dissolved in 100 mL of 1 x Tris acetate EDTA (TAE) buffer and 0.5 µg/mL ethidium bromide added). Samples were loaded in 6 x blue/green loading dye (Promega). The relevant bands were detected and excised using a UV transilluminator. The PCR products were purified using the QIAquick Gel Extraction Kit (Qiagen Ltd, Basel, Switzerland) according to the manufacturer's instructions. The PCR product was eluted in either sterile water or EB buffer (10 mM Tris, pH 8.5) and stored at - 20 °C. The yield was ca. 0.2 µg/µL of DNA.

2.2.4 Site-directed mutagenesis of *Mt*MurA

2.2.4.1 Primers

Primers were designed to carry the mutation in the middle of the primer and to have ≥ 40 % G + C content. The mutation from a GAC codon coding for a cysteine *in M. tuberculosis* to the most commonly used cysteine codon in *E. coli*, TGC, involved the replacement of only 2 bases. The following primers were used and the cysteine codon is underlined:

MtD117C 5' 5' CGCTGCCGGGCGGTTGCGCGATCGGGTCGCG 3'
MtD117C 3' 5' CGCGACCCGATCGCGCAACCGCCCGGCAGCG 3'

The respective Tm of the primers was calculated as described in section 2.2.3.

Before the primers were used, they were first purified using Sep-Pak 3cc C18 cartridges, i.e. by reverse phase (Waters). The cartridges were pre-equilibrated with 2.5 mL 50 % (v/v) MeOH, 2.5 mL pure MeOH and 2.5 mL sterile water. The primers were resuspended in 500 µL of 50 mM triethylammonium acetate (TEAA) and then loaded onto the column. The cartridges were washed with 6 mL of sterile water and the primers eluted with 1 mL of 50 % (v/v) MeOH, 50 mM TEAA, pH 7.0. The primers were dried in the speed vac and resuspended in 100 µL 80 % (v/v) EtOH. Again they were dried down in the speed vac and finally resuspended in 500 µL of sterile water. The concentration of the primer was determined by measuring the A_{260} on a Uvikon 933 spectrophotometer (Kontron Instrument AG, Zurich, Switzerland).

2.2.4.2 PCR

For site-directed mutagenesis, the Quikchange^{TM} site-directed mutagenesis kit (Stratagene) was used according to the manufacturer's instructions.

The PCR was set up as recommended by the manufacturer using 5 to 50 ng of pET*MtMurA* as the template DNA and the primers described in section 2.2.4.1. The reaction was carried out in the pre-heated Perkin Elmer Cetus DNA Thermal Cycler as before, using the following cycles recommended by the manufacturer:

30 seconds at 95 °C

$$\left.\begin{array}{l}\text{30 seconds at } 95\,^\circ\text{C}\\ \text{1 minute at } 55\,^\circ\text{C}\\ \text{15 minutes at } 68\,^\circ\text{C}\end{array}\right\}\ \text{x } 16$$

The extension time was calculated on the basis of 2 minutes per kb length.

After the PCR was finished, the restriction enzyme DpnI was added in order to digest the parental supercoiled DNA. Subsequently, the DNA was transformed into the cells provided by the manufacturer.

2.2.5 Restriction enzyme digestion

2.2.5.1 Digestion of PCR products with restriction enzymes

The purified PCR products that were required to have cohesive "sticky" ends were digested with the appropriate restriction enzymes. The digestion reaction was set up in a total volume of 10 to 50 µL: 1 to 10 µg of the purified PCR product, 1 x the appropriate reaction buffer for the enzymes used, 1 x BSA, if required by the restriction enzymes, and 10 to 20 U of the appropriate restriction enzymes. The reactions were incubated at the required temperature for 12 to 16 hours. The digested PCR products were separated on a 1 % agarose gel and viewed under a UV transilluminator. The digested PCR products that were required for ligation were subsequently purified from the agarose gel as previously described in section 2.2.3.

2.2.5.2 Digestion of plasmids with restriction enzymes

The vectors were also digested with the appropriate restriction enzymes in a total volume of 10 to 50 µL with 5 to 50 µg of plasmid DNA, 1 x the appropriate reaction buffer, 1 x BSA, if required by the restriction enzymes, and 10 to 20 U of each of the restriction enzymes. The reactions were incubated for 3 to 4 hours at the required temperature and the products of the digests viewed on a 1 % agarose gel as described above.

For vectors that were required for ligation, dephosphorylation was also necessary. For this, 2 U of Calf Intestinal Alkaline Phosphatase (CIAP) was added and the reaction was incubated for a further 1 to 2 hours at 37 °C. The enzymes were then inactivated at 75 °C for 10 minutes before the digested vectors were purified using the QIAquick gel extraction kit as described previously.

2.2.6 Ligation

The relative concentrations of the purified PCR and the purified vector were first estimated on a 1 % agarose gel. Ligation reactions were set up to include 5 to 10 ng of the vector, 3 x concentration of insert compared to vector, 1 x T4 DNA Ligase buffer and 4 U of T4 DNA ligase in a total volume of 10 µL. The reactions were left for 16 to 20 hours at 16 °C.

2.2.7 Ligation of DNA into the PCR-Script Amp SK (+) vector

In order to facilitate cloning of the gene into the desired expression vectors, the PCR-Script Amp SK (+) vector was used. A higher vector to insert ratio (between 40:1 and 100:1) was required for ligation of the blunt ended PCR product into this vector, compared to ligations described in section 2.2.6. Ligation reactions were set up using 200 to 500 ng of PCR product and the products subsequently transformed into the supplied *E. coli* competent cells according to the manufacturer's instructions. Blue-white colour screening was used to identify transformants containing the inserted gene.

Inserts were excised from the PCR-Script vector using the appropriate restriction enzymes and then ligated into the pET21d (+) vector as described in section 2.2.6.

2.2.8 Production of *E. coli* DMSO competent cells

A 2 mL culture of medium A (10 g bactotryptone, 2.5 g yeast extract, 0.01 M NaCl, 0.005 M KCl, 0.01 M $MgCl_2$, 0.01 M $MgSO_4$) was inoculated with a single colony of the desired *E. coli* strain and incubated overnight at room temperature. An aliquot of the overnight culture was used to inoculate 250 mL medium A and grown at room temperature until the OD_{600} was 0.6. At this point, the culture was transferred to ice-cold centrifuge beakers, left for 10 minutes on ice and centrifuged for 10 minutes at 2500 *g* (4 °C). The pellet was resuspended in 80 mL ice-cold TB medium (10 mM PIPES, 55 mM $MnCl_2$, 15 mM $CaCl_2$, 250 mM KCl) and left for 10 minutes on ice before centrifuging as above. The pellet was resuspended in 20 mL TB medium and 1.4 mL DMSO was slowly added to the cells. They were left for 10 minutes on ice before they were distributed into aliquots of 400 µL and frozen in liquid nitrogen. Cells were stored at - 80 °C until use.

2.2.9 Transformation of *E. coli* DMSO competent cells

To 100 µL of the desired host cells, 5 µL of the ligation reaction or 1 to 5 µg of plasmid DNA was added. This was gently mixed and incubated for 30 minutes on ice, before heatshocking the cells for 90 seconds at 42 °C, then returning them to ice for 5 minutes. LB medium (800 µL) was added and the cells incubated at 37 °C for 1 hour with shaking. The cells were briefly centrifuged and the pellet resuspended in 100 µL of LB medium before plating onto LB agar plates containing the desired antibiotic. Plates were incubated for 16 hours at 37 °C and stored at 4 °C once colonies were visible.

2.2.10 Minipreps of plasmid DNA

For all minipreps, a 5 mL LB overnight culture containing 100 µg/mL of ampicillin was inoculated with a single colony and grown for 16 hours at 37 °C. Depending on the method to be used, between 1 and 5 mL of the overnight culture was centrifuged at 13,400 *g*.

2.2.10.1 QIAprep spin miniprep kit

Plasmid DNA that was required for salt sensitive applications such as digestion, ligation and transformation was purified using the QIAprep Spin Miniprep Kit (Qiagen Ltd.) according to the manufacturer's instructions. The plasmid was eluted in 50 µL of either sterile water or EB buffer (10 mM Tris, pH 8.5) and stored at -20 °C until required. The yield of plasmid DNA was ca. 0.15 µg/µL.

2.2.10.2 Adaptation of the "Holmes and Quigley" plasmid miniprep

This method was adapted from Holmes and Quigley (1981). The cell culture was centrifuged and the resulting pellet dried. This was resuspended in 300 µL STET buffer (0.1 M NaCl, 10 mM Tris, 1 mM EDTA, 5 % Triton X-100, pH 8.0) and 240 µg of lysozyme were added. The suspension was incubated for 2 minutes at 37 °C before immediately transferring the tubes to a boiling water bath for 1 minute. The sample was centrifuged for 10 minutes at 13,400 *g* and the resulting pellet removed with a sterile toothpick. NaOAc (0.3 M) and 50 % isopropanol were added and mixed. This was centrifuged for 5 minutes at 13,400 *g*, the supernatant discarded and the pellet washed with 250 µL of 70 % ice-cold EtOH. The pellet was dried in the speed vac before resuspension in 15 to 30 µL sterile water. If the plasmid was subsequently used for restriction enzyme digestion, 1 µL of 10 mg/mL RNase was added after the digestion was complete.

2.2.10.3 Plasmid miniprep for sequencing

This is the recommended protocol for DNA preparation for sequencing on the ABI 373 sequencer, Perkin Elmer (taken from ABI373 sequencer manual). A 3 mL overnight culture of Terrific Broth (12 g bactotryptone, 24 g yeast extract, 4 mL glycerol and add 0.17 M KH_2PO_4 and 0.72 M K_2HPO_4 after autoclaving) containing 100 µg/mL of ampicillin was inoculated with a single colony and grown overnight at 37 °C. The culture was centrifuged and the pellet dried. The pellet was resuspended in 200 µL Mini-prep buffer (25 mM Tris, pH 7.5, 50 mM Glucose, 10 mM EDTA) and 300 µL 0.2 N NaOH/1 % SDS for cell lysis (mixed by inversion) and the suspension left on ice for 5 minutes. Then 300 µL of 3 M KOAc was added for neutralisation and left on ice for a further 5 minutes. The cells were centrifuged at 13,400 *g* for 10 minutes and the supernatant transferred to a fresh tube to which 2 µL of 10 mg/mL RNase was added. This was incubated for 20 minutes at 37 °C followed by two chloroform extractions. A 0.1 volume of 3 M NaOAc and 0.6 volumes of room temperature isopropanol were added, left on ice for 5 minutes for a precipitate to form before centrifuging at room temperature for 10 minutes. The resulting pellet was washed with 500 µL 70 % EtOH and dried. It was then resuspended in 32 µL dH_2O, 8 µL 4 M NaCl and finally 40 µL 13 % PEG 8000, mixed and left on ice for 20 to 30 minutes. A clear pellet was obtained by centrifuging (13,400 *g*) for 15 minutes at 4 °C, washing with 500 µL of 70 % EtOH before drying in the speed vac. The pellet was resuspended in 30 µL of dH_2O and stored at - 20 °C until required.

2.2.11 DNA sequencing

In all constructs containing the pET21 vectors, the T7 sequencing primers were used to determine the sequence of the 5’ and the 3’ ends of the gene:

T7 promoter	5’ TAATACGACTCACTATAGGG 3’
T7 terminator	5’ GCTAGTTATTGCTCAGCGG 3’

The primers that were used for the sequencing of pET*MtmurA*, pET*MtMurA*-D117C and pET*MtMurA*-Histag are as follows:

Mtseqa5’	5’ CCTCGGTCTGTGTGCTG 3’
Mtseqb5’	5’ CGCAATGACCCGTGGTG 3’
Mtseqc5’	5’ GTTCGGACATCCGTGCC 3’
Mtseqa3’	5’ CCTCGAACACGTTCTCC 3’
Mtseqb3’	5’ CCAACTGAATCTCCGCAC 3’
Mtseqc3’	5’ CCAGACCACGCAGTACC 3’

The primers that were used for the sequencing of pET*CtmurA* are as follows:

Ctseqa5’	5’ CGTTGTTACGTCGTTGTC 3’
Ctseqb5’	5’ CTGCGGTAGTTTCTCAGG 3’
Ctseqc5’	5’ CTCATAGCGCAGTCATTC 3’
Ctseqa3’	5’ CGACACGACTTAGCACTC 3’
Ctseqb3’	5’ CGAAAGAAGCAGCCTCG 3’
Ctseqc3’	5’ CGTAACAACGCTCCTAAC 3’

The primers that were used for the sequencing of pET*BbmurA* are as follows:

Bbseqa5	5’ CCTAATATTAATGATGTAAAAGTTG 3’
Bbseqb5	5’ CGCTGCTTGTGAGCCAC 3’
Bbseqc5	5’ GCAACGCAAGTAGAAGGC 3’
Bbseqa3	5’ CTACGCGGTGTGGATCAC 3’
Bbseqb3	5’ CCTGTTAATGCAGCAAGGC 3’
Bbseqc3	5’ CTCCTCCTGGAAGCGCC 3’

Recombinant plasmids were sequenced either by Microsynth, Balgach, Switzerland, or on an ABI 373 sequencer, Perkin Elmer, using the dye terminator method described by Sanger et al. (1977).

Firstly, in a total volume of 10 µL, 0.25 to 0.5 µg of plasmid DNA, 1.6 pmol of the sequencing primer and 4µL of the reaction mix (Perkin Elmer) were added. To overlay the reaction and prevent evaporation, 1 drop of sterile mineral oil was used. The reactions were placed in the pre-heated Perkin Elmer Cetus DNA Thermal Cycler and denatured for 3 minutes at 95 °C. The following reaction cycles were repeated 25 times: 30 seconds at 95°C, 15 seconds at 50 °C and 4 minutes at 60 °C. The PCR mix was removed from the tube and added to 10 µL of water, 0.1 volumes of 3 M NaOAc and 50 µL of EtOH. This was left for 15 minutes on ice, centrifuged for 10 minutes at 4 °C, washed with 250 µL of 70 % EtOH and dried.

To prepare the sequencing gel, the gel plates were first washed on both sides, with Alconox (2 x), dH_2O (2 x) and isopropanol (2 x). Plates were clamped together once they were free of all dust particles. To form the gel, 600 µL of 10 % APS was added to 75 mL Ultra-pure Sequagel (National Diagnostics) and the gel poured without the formation of air bubbles. After 2 hours, the gel was placed into the ABI 373 sequencer. Samples were resuspended in 3 or 4 µL of sequencing loading dye (4 parts formamide, 1 part 25 mM EDTA, pH 8.0 with 50 mg/mL blue dextran) depending on the comb size, vortexed, denatured at 95 °C for 2 minutes and immediately cooled on ice. The samples were loaded into the wells and the gel left to run for 17 hours. The computer program 373 sequencer was used to interpret the data, which was then compared to the sequence available in the databases.

Sequences obtained from Microsynth were read using the program Chromas (http://bioinfo.weizmann.ac.il/pub/software/chromas/) and the data obtained again compared to the sequence available in the databases.

2.2.12 Sodium Dodecyl Sulphate (SDS)-Polyacrylamide gel electrophoresis (PAGE)

This was carried out as described by Laemmli (1970) and used the Mini-Protean II System from BioRad (BioRad, CA, USA). A 10 % separating gel was prepared (0.375 M Tris/HCl (pH 8.8), 10 % acrylamide/bis (Carl Roth GmBH, Karlsruhe, Germany), 0.1 % SDS, 0.05 % APS, 0.05 % TEMED (Servar, Heidelberg, Germany)) and poured into the casting plates. Once set, the 4 % stacking gel (0.125 M Tris/HCl (pH 6.8), 4 % acrylamide/bis, 0.1 % SDS, 0.05 % APS, 0.1 % TEMED) was poured and the comb placed into the gel. The electrophoresis tank was filled with 1 x SDS Running buffer (0.25 M Tris, 1.92 M glycine, 1 % (w/v) SDS). The samples were resuspended in 2 x SDS loading buffer (0.06 M Tris/HCl (pH 6.8), 2 % SDS, 10 % glycerol, 0.02 % Bromophenol Blue, 5 % β-mercaptoethanol (added directly before use)) and denatured for 3 to 5 minutes at 95 °C, depending on the sample volume. A 120 V current was applied for 90 minutes and the gels were run until the solvent front had moved to the bottom. Gels were stained in Coomassie Blue (0.1 % (w/v) Coomassie Brilliant Blue R250 in 40 % isopropanol, 10 % acetic acid and filtered) for 20 minutes and destained with 20 % acetic acid.

2.2.13 Small scale expression of the target protein

A 5 mL 2 x YT Amp culture was inoculated with a single colony of the desired clone and incubated for 16 hours at 37 °C. A 50 mL 2 x YT Amp culture was then inoculated with 500 μL of the starting culture, i.e. 1 % of the final volume, and grown at 37 °C until the culture had reached an OD_{600} of 0.6 to 0.8. At this point, IPTG was added and growth continued at the optimum temperature that was necessary for expression of the target protein. After 4 to 5 hours of further growth, the cells were centrifuged at 17,000 *g* for 30 minutes at 4 °C. The pellet was stored at -20 °C until required. At various time points, 1 mL samples of the culture were removed and the cells centrifuged, resuspended in 2 x SDS loading buffer and subjected to 10 % SDS-PAGE gel to determine whether or not expression of the target protein had occurred. For the expression of the *Mt*MurA-Histag and the *Ct*MurA, the above method was used but on a larger scale, i.e. a 1 L culture.

2.2.14 Large scale expression of the target protein using a 12 L fermentor

This was carried out only for the *Mt*MurA and the D117CMurA proteins. A starting culture of 5 mL 2 x YT Amp was inoculated with a single colony from the desired clone and was grown at 37 °C for 10 hours. A 250 mL 2 x YT Amp culture was inoculated with 2.5 mL of the starting culture and grown for 16 hours at 37 °C. Twelve L of 2 x YT was sterilised in the fermentor (Bioengineering, type L1523). Ampicillin, to a final concentration of 100 µg/mL, and the bacterial culture were added to the fermentor. The cells were grown at optimum conditions (30 °C, 500 rpm, 500 L/hour of air) until the OD_{600} was 0.6 to 0.8. At this point IPTG was added to a final concentration of 0.1 mM. Growth was continued for 4 hours at 30 °C after which the bacteria were harvested by continuous flow centrifugation (Haereus flow-through centrifuge 17RS). Cell paste was removed from the rotor and frozen at -80 °C in aliquots of 20 g until required. The typical yield was 100 to 120 g of wet cell paste per 12 L. A small sample of the cells was lysed and the proteins subjected to 10 % SDS-PAGE to determine whether expression had occurred.

2.2.15 Determination of the solubility of the target proteins

An aliquot of 1 g of cells was resuspended in extraction buffer (details in section 2.2.15), 1 mg of lysozyme added and left for 30 minutes at 4 °C. Cells were sonicated for 3 x 60 seconds with one minute in between each pulse to allow the cells to recover. The suspension was centrifuged at 17,000 *g* for 20 minutes (4 °C) and the supernatant removed. The pellet was resuspended in 2 mL extraction buffer. Samples from both the supernatant and the pellet were subjected to 10 % SDS-PAGE to determine whether or not the target protein was present in the membrane or in the cytoplasmic fraction.

2.2.16 Purification of *Mt*MurA and D117CMurA

All purification steps were carried out at 4 °C. A 20 g aliquot of cells was resuspended in 100 mL extraction buffer (50 mM Tris/HCl, 2 mM DTT, 1 mM EDTA, 0.1 M NaCl, 0.1 % Triton X-100, pH 8.0). Lysozyme (1 mg/g cells) was added and cells were left for 30 minutes, stirring, at 4 °C. The suspension was sonicated for 60 seconds for 4 times with a 1 minute interval in between each pulse. The resulting mixture was centrifuged at 17,000 *g* for 30 minutes. The supernatant was removed and re-centrifuged at 44,000 *g* for 30 minutes. It was then slowly bound to 200 mL of Hydroxyapatite Biogel HTP (BioRad), which had been pre-equilibrated with buffer A (10 mM NaPO4, 2 mM DTT, 1 mM EDTA, pH 6.8). The material was subsequently washed, under batch conditions, with 10 bed volumes of buffer B (50 mM NaPO4, 2 mM DTT, 1 mM EDTA, pH 6.8) and the *Mt*MurA proteins were eluted with 4 bed volumes of buffer C (100 mM NaPO4, 2 mM DTT, 1 mM EDTA, pH 6.8). The resulting fractions were pooled and were brought to 60 % ammonium sulphate saturation. The precipitated proteins, containing *Mt*MurA, were collected by centrifugation at 44,000 *g* for 30 minutes and the pellet resuspended in 5 mL of buffer D (50 mM Tris, 2 mM DTT, 1 mM EDTA, pH 7.8) also containing 0.15 M KCl. The proteins were subsequently loaded onto a pre-equilibrated Gel filtration, G-75 Sephadex, column (100 x 2.5 cm) (Pharmacia) and eluted using a flow rate of 0.15 mL/min. The fractions containing the *Mt*MurA protein (50 to 60 mL) were pooled and concentrated three-fold in an ultrafiltration Amicon cell using a membrane with a retention limit of 30 kDa (Amicon). Concentrated *Mt*MurA was subjected to anion exchange chromatography using DEAE-Sephacel (Pharmacia), which was equilibrated with Buffer D, pH 7.8 (19.5 x 2.5 cm). Prior to DEAE-Sephacel chromatography, D117CMurA was incubated with 1 mM UDPNAG for 45 minutes at 37 °C in order to remove any of the *O*-phosphothioketal that may have been present. The *Mt*MurA protein was eluted using a linear gradient of 0 to 0.5 M KCl and a flow rate of 0.5 mL/min. The fractions containing *Mt*MurA were pooled, desalted and concentrated, ca. 10 fold, in the Amicon cell as before. Further concentration of the protein was achieved using centricons (Millipore) with a molecular weight cut off point of 30 kDa, until the concentration of the protein was about 10 mg/mL. The protein was frozen in liquid nitrogen and stored at - 80 °C. The yield was 10 to 15 mg protein from 20 g cell paste. The protein concentration was determined using Bradford reagent (see section 2.2.24 for calibration details).

2.2.17 Purification of *Mt*MurA-His under native conditions

All purification steps were carried out at 4 °C. The cells (4g from a 1 L culture) were resuspended in 2 mL lysis buffer (50 mM Tris or 50 mM NaH_2PO_4, 300 mM NaCl, 1 mM imidazole, 10 % glycerol, pH 8.0). Lysozyme to a final concentration of 1 mg/mL was added and the mixture was incubated for 20 minutes on ice. Cells were sonicated 3 times for a period of 30 seconds each time. The cells were centrifuged at 10,000 *g* for 20 minutes. The resulting supernatant was loaded onto 0.5 mL of Ni-NTA agarose (Qiagen Ltd.) either by gently mixing or by gravity flow. To elute the protein, the material was washed with the same buffer as the lysis buffer but with increasing concentrations of imidazole. The material was washed with about 10 bed volumes for each imidazole concentration. Samples were taken at different concentrations and subjected to 10 % SDS-PAGE to determine in which fraction the *Mt*MurA-His protein was eluted.

2.2.18 Purification of *Mt*MurA-His under denaturing conditions

In 3 mL of lysis buffer (100 mM NaH2PO4, 10 mM Tris, 8 M urea, pH 8.0), 1.2 g cells were resuspended and stirred until the mixture became transparent. Cells were centrifuged at room temperature for 30 minutes at 10,000 *g*. The resulting supernatant was loaded onto 0.5 mL of Ni-NTA agarose, which had been equilibrated with 5 bed volumes of lysis buffer. The column was washed with 16 bed volumes of wash buffer (same as lysis buffer except pH 6.9) before the protein was eluted, first with 4 bed volumes of elution buffer 1 (same as lysis buffer except pH 5.3) then another 4 bed volumes of elution buffer 2 (same as above except pH 4.5). SDS-PAGE was used to identify the fractions containing *Mt*MurA-His.

2.2.19 Purification of *Ct*MurA

All steps were carried out at 4 °C. Purification was attempted using ca. 6 g of cells (obtained from 2 L of cell culture). The cells were lysed as described in section 2.2.16 and the resulting supernatant was subjected to dialysis against buffer A (50 mM Tris, 2 mM DTT, 1 mM EDTA, pH 7.8). The dialysed sample was subjected to anion exchange chromatography using DEAE-Sephacel (33 x 2.5 cm) that had been pre-equilibrated with buffer A. The sample was loaded onto the column and eluted with an increasing linear gradient of KCl, from 0 to 0.4 M. The flow rate used was 0.5 mg/mL and fractions of 7 mL were collected. Analysis of the elution profile was carried out using SDS-PAGE. Fractions that were thought to contain *Ct*MurA were pooled and concentrated ca. 20 fold using an Amicon ultrafiltration cell equipped with a YM-30 membrane.

2.2.20 Western blotting

Between 2 and 10 μg of protein was first subjected to 10 % SDS-PAGE. One of the gels was stained with Coomassie Blue stain and the other used for Western blotting. The Whatman paper, sponges and nitrocellulose membrane (Schleider and Schüll) were soaked in the transfer buffer (0.025 M Tris, 0.19 M glycine, 20 % MeOH). The blot was prepared in the following order: 1 x sponge, 2 x Whatman paper, SDS-PAGE gel, nitrocellulose, 2 x Whatman paper and 1 x sponge, placed in the electrophoresis apparatus and the tank filled with transfer buffer. It was run for 1 hour at 100 V, 250 mA at 4 °C with stirring.

2.2.21 Immunodetection

The nitrocellulose membrane was removed from the blotting apparatus, described in section 2.2.20, and immersed into Ponceau Red stain until the protein bands became visible. The positions of the SDS-PAGE markers were indicated using a waterproof pen and the membrane destained using TTBS (20 mM Tris, 500 mM NaCl, 0.05 % Tween 20, pH 7.5).

2.2.21.1 Immunodetection using the rabbit anti-MurA antibody

The membrane was incubated for 1 hour in TTBS and 5 % blocking grade blocker non-fat dry milk (BioRad). Subsequently, it was incubated for 1 hour or overnight with the rabbit anti-MurA antibody (Krekel 1998), either as a purified solution or a 1:1000 dilution of the crude antibody, in the blocking buffer used above. The nitrocellulose membrane was washed 4 times with TTBS for a period of 5 minutes each time before incubation with the goat anti-rabbit secondary antibody coupled to the enzyme, alkaline phosphatase (BioRad) for 1 hour in TTBS plus 5 % blocking grade blocker non-fat dry milk (1:3000 dilution). The membrane was washed twice with TTBS (5 minutes) and twice with alkaline phophatase buffer (100 mM Tris, 100 mM NaCl, 5 mM $MgCl_2 \bullet 6H_2O$, pH 9.5) for 5 minutes. The membrane was incubated with the detection solution (66 µL NBT, 33 µL BCIP in 10 mL of alkaline phosphatase buffer) until the bands became visible, at which point the reaction was stopped with water.

2.2.21.2 Immunodetection using an anti-His antibody

Immunodetection using the murine anti-His (Qiagen Ltd.), which recognises six histidine residues, was carried out according to the manufacturer's instructions. The subsequent chemiluminescence detection reaction and exposure to X-ray film were performed according to the manufacturer's instructions.

2.2.22 Antibody purification

Twenty to fifty µg of protein was subjected to SDS-PAGE and subsequently transferred to a nitrocellulose membrane, as described in section 2.2.20. The membrane was incubated for 1 hour with blocking buffer (section 2.2.21.1) and 1 mL of the crude extract of the antibody solution. The membrane was subsequently washed 4 times (5 minutes each time) with TTBS. To elute the antibody, 1 mL of 0.2 M glycine (pH 2.5) was added and the membrane washed for 10 minutes. The antibody containing solution was removed and the pH increased to pH 8.0 using Tris buffer.

2.2.23 N-terminal sequencing

Samples containing between 5 to 10 µg of the desired protein were subjected to 10 % SDS-PAGE. The proteins were then transferred to a pre-equilibrated polyvinyldifluoride (PVDF) membrane (Millipore) as described in section 2.2.20. The proteins were detected by staining with Ponceau Red and the desired protein bands were subsequently excised. The samples were sent to Dr. R. Brunisholz, Institute for Molecular Biology and Biophysics, ETH Hönggerberg, for automated Edman sequencing using an Applied Biosystems 477A sequencer.

2.2.24 Bradford reagent calibration

Before use, the Coomassie Protein Assay Reagent (Socochim, Lausanne, Switzerland) was calibrated using a series of dilutions from 0 to 20 µg of BSA in a total volume of 100 µL. To this, 900 µL of the Coomassie Protein Assay Reagent was added. After 5 minutes, the OD_{595} was measured. The average value from 3 measurements was calculated and plotted against the BSA concentration (µg) in Sigma plot 2000. From this calibration curve, the slope of the best-fit line was calculated and used in subsequent calculations of protein concentration.

2.2.25 Preparation and calibration of Lanzetta reagent

The Lanzetta reagent was adapted from Lanzetta et al. (1979). Firstly, 5.25 g of ammoniumheptamolybdate was dissolved in 41 mL of HCl (37 %) and 84 mL dH_2O added. This solution was added to 169 mg Malachite green dissolved in 375 mL dH_2O and stirred for 16 hours until the solution became yellow. The solution was filtered through a 0.2 μm membrane filter and stabilised by the addition of 10 mL 2 % Tergitol NPX. The solution was stored in a dark plastic container at 4 °C.

To calibrate the reagent, a dilution series from 0 to 20 nmol was set up using Na_3PO_4 in a total volume of 100 μL. To this, 800 μL of the Lanzetta reagent was added and after 5 minutes 100 μL of a 34 % Na_3citrate solution was added to quench the release of phosphate. After a period of 30 to 60 minutes, the OD_{660} was measured. The average of 3 measurements was plotted against the phosphate concentration and the slope of the best-fit line determined.

2.2.26 *Mt*MurA and D117CMurA activity assays using Lanzetta reagent

All activity assays were performed at 25 °C in test buffer (50 mM Tris, 1 mM DTT, pH 7.5) unless otherwise described in the text.

2.2.26.1 Specific activity

To measure specific activity, 10 μM *Mt*MurA or D117CMurA was incubated with 1 mM UDPNAG for 5 minutes before an equimolar amount of PEP was added to start the reaction. Twenty μL samples were taken at the following time points over a 7 hour period: 0', 2', 5', 10', 20', 30', 45', 60', 90', 120', 180', 240', 300', 360' and 420'. Test buffer was used to increase the volume to 100 μL before 800 μL of the Lanzetta reagent was added. After 5 minutes, 100 μL of 34 % Na_3citrate was added to stop any further release of phosphate. After a further 30 to 60 minutes, the OD_{660} was measured and the values plotted against time (min) in Sigma plot 2000. k_{cat} (min^{-1}) was calculated using linear regression and the average activity was based on at least three measurements.

2.2.26.2 pH dependence

The pH dependence of the *Mt*MurA and the D117CMurA enzymes were determined using 10 μM enzyme and 1 mM UDPNAG, which were incubated together for 5 minutes before the addition of 1 mM PEP to start the reaction. The buffers used were 50 mM MES, pH 5.0 to pH 7.0 or 50 mM Tris, pH 7.0 to 9.0. All buffers contained 1 mM DTT. Samples of 20 μL were taken at various time points over a period of 7 hours as described in section 2.2.26.1. Finally, the average k_{cat} (min^{-1}) of two measurements was plotted against pH and a normal log function (equation: y = ae(-0.5 (ln(x/xo)/b)^2)) was used to fit the curve.

2.2.26.3 K_M determination

To determine the K_M value for PEP, 1 µM *Mt*MurA or D117CMurA was incubated with 10 mM UDPNAG for 5 minutes before 0.5, 1, 2, 4, 10, 20 or 50 µM of PEP was added to start the reaction. Samples (100 µL) were taken over a period of 180 minutes (0', 2', 5', 10', 20', 30', 45', 60', 90', 120', 180') and 800 µL of the Lanzetta reagent added. After 5 minutes, 100 µL of Na_3citrate was added and after a further 30 to 60 minutes, the OD_{660} was measured and the values plotted against time (min) as described in section 2.2.26.1. The average activity (nmol Pi/min) was determined based on at least 3 measurements and the values plotted against the concentration of PEP (µM). The curve was fitted in Sigma plot 2000 using a hyperbolic function (equation: y = ax/(b+x)) to obtain the K_M value of PEP.

The K_M values of UDPNAG for both enzymes was determined in the same way except that 1 mM PEP was used and the concentration of UDPNAG was varied from 0 to 500 µM.

2.2.27 Determination of the effect of fosfomycin on *Mt*MurA and D117CMurA

To determine the effect of fosfomycin on *Mt*MurA, 10 µM enzyme was incubated with 10 mM UDPNAG for 5 minutes in the absence or presence of either 0.1, 1 or 10 mM fosfomycin. Different concentrations of PEP were then added to start the reaction (10 µM, 100 µM, 1 mM, 10 mM, 50 mM). Samples (20 µL) were taken over a period of 7 hours as described in section 2.2.26.1. After 5 minutes, 100 µL of 34 % Na_3citrate was added and after a further 30 to 60 minutes the samples were measured at OD_{660}. These values were plotted in Sigma plot 2000 against time (min) and the activities calculated as described in section 2.2.26.1. The K_i was subsequently determined according to Dixon (1952) by plotting the slope of these lines against the concentration of fosfomycin.

To determine the effect of fosfomycin on D117CMurA, 10 µM enzyme was incubated with 1 mM UDPNAG and 1 mM fosfomycin or 10 mM UDPNAG and 10 mM fosfomycin for 5 minutes at 25 °C before an equimolar amount of PEP was added to start the reaction. Samples were taken as described above. The OD_{660} values obtained were plotted against time (min).

2.2.28 Trypsin digestion and MALDI-TOF MS analysis

The in-gel tryptic digest was adapted from Rosenfeld et al. (1992). All solutions were freshly prepared. Between 100 to 150 µg of the desired proteins were subjected to SDS-PAGE. The resulting SDS-PAGE gel was rinsed with dH_2O, the relevant bands excised using a clean scalpel and chopped into 1 mm by 1 mm cubes, which were placed into 1.5 mL Eppendorf tubes. The gel pieces were washed with dH_2O for 5 minutes, before acetonitrile (4 times the volume of gel pieces) was added and they were incubated for 10 to 15 minutes at room temperature. The liquid was removed and the gel pieces dried in the speed vac. They were then incubated at 56 °C in 10 mM DTT/0.1 M NH_4HCO_3 for 30 minutes to reduce the protein. Acetonitrile was again added as above to shrink the gel pieces. This solution was replaced by 55 mM iodoacetamide/0.1 M NH_4HCO_3 and incubated in the dark for 20 minutes at room temperature. The gel pieces were subsequently washed with 0.1 M NH_4HCO_3 for 15 minutes before acetonitrile was once again added. The next stage was to rehydrate the gel pieces in 0.1 M NH_4HCO_3, after 15 minutes an equal volume of acetonitrile was added and the mixture vortexed for a further 20 minutes. This was followed by shrinkage of the gel pieces with acetonitrile as above. The gel was once more rehydrated in digest buffer (50 mM NH_4HCO_3, 5 mM $CaCl_2$, 12.5 ng/µL Trypsin from bovine pancreas as before) and incubated at 4 °C for 45 minutes. An excess of the digest buffer, without trypsin, was added in order to keep the gel particles wet during cleavage and the digestion incubated at 37 °C for 16 hours or longer. The resulting supernatant was analysed.

For the MALDI-TOF mass spectrometry, 1 µL of the resulting supernatant was spotted onto the gold plate together with 1 µL of saturated dihydroxybenzoate (DHB) in 0.1 % TFA: acetone (2:1 (v/v)). Once the crystals had formed, they were washed twice with ice-cold dH_2O and dried. MALDI-TOF MS spectra of the peptide fragments were recorded with a Voyager Elite Mass Spectrometer using the reflectron mode for increased accuracy. The programs, PAWS or MS-FIT from Protein Prospector (http://prospector.ucsf.edu/ucsfhtml3.4/msfit.htm) were used to interpret the data.

2.3 MurA from *Mycobacterium tuberculosis* (*Mt*MurA)

2.3.1 Cloning of *MtmurA* into pKK233-2

The genomic DNA from the *M. tuberculosis* strain H37Rv was initially used to amplify the *MtmurA* gene using the primers MtMurA5' and MtMurA3'. These contained NcoI and HindIII restriction sites, respectively. The result of the PCR is shown in figure 2.3.1.

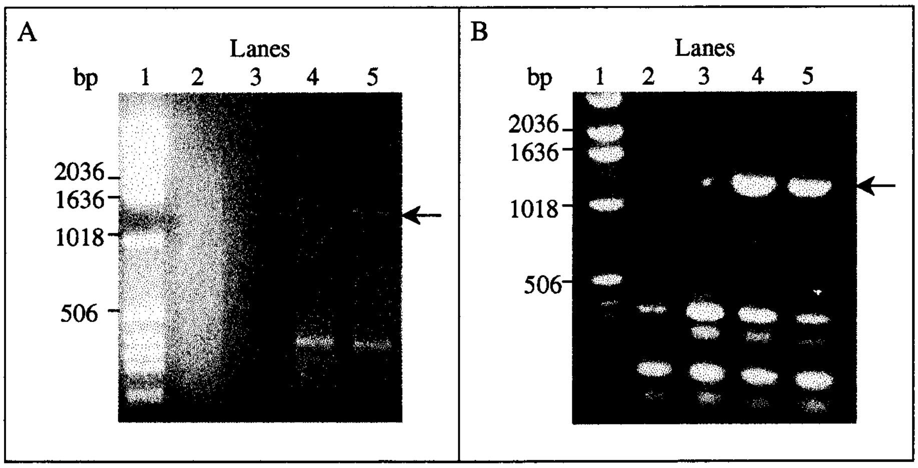

Figure 2.3.1: Agarose gels (1 %) showing the results of the PCR. Panel A shows the result of the PCR using genomic DNA as a template. Lane 1: 1 kb ladder (Gibco), lane 2: no Pwo DNA polymerase, lane 3: no genomic DNA, lanes 4 and 5: 100 ng genomic DNA and 2.0 mM $MgSO_4$. A 15 µL aliquot of the PCR was loaded into lanes 2 to 4. The annealing temperature was 54 °C. Panel B shows the PCR production using the PCR product in panel A, lane 4 as the template. Lane 1: 1 kb ladder as before, lanes 2 to 4: 1 µg of the previous PCR product and 1.5, 2.0 and 2.5 mM $MgSO_4$ respectively, lane 5: 1 µg of the previous PCR product and the $MgSO_4$ containing (2.0 mM) buffer supplied with the Pwo DNA polymerase. A 5 µL aliquot of the PCR was loaded into lanes 2 to 5. The annealing temperature was 52 °C. *MtmurA* is indicated in both panels by an arrow.

As can be seen in lanes 4 and 5 of panel A, a band of ca. 1300 bp was produced, although very faint. Additionally, there is an obvious smearing of the genomic DNA in lanes 2, 4 and 5 (Panel A). This was thought to be due to the degradation of the DNA, perhaps explaining the reduced amount of PCR product observed. PCR using the genomic DNA under the same conditions no longer produced a product indicating that the DNA was severely degraded. The bands in panel A, lanes 4 and 5, were excised and purified as described in section 2.2.3, and used as templates in another PCR (figure 2.3.1, panel B). Non-specific products of the PCR were obtained as a result of the lower annealing temperature used (52 °C). However, a large band of around 1300 bp (lanes 4 and 5) that was assumed to be *MtmurA* was produced and this was subsequently excised and inserted into the pKK233-2 expression vector using the restriction sites, NcoI and HindIII. This gave the construct, pKK*MtmurA*. DNA sequencing confirmed the presence of a 1257 bp insertion in the pKK233-2 plasmid and identified it as *MtmurA*.

2.3.2 Expression of *Mt*MurA

*Mt*MurA, from pKK*MtmurA*, was expressed in *E. coli* JM105 cells, as they are the most suitable host cells for the pKK233-3 plasmid. The results of the expression are shown in figure 2.3.2.

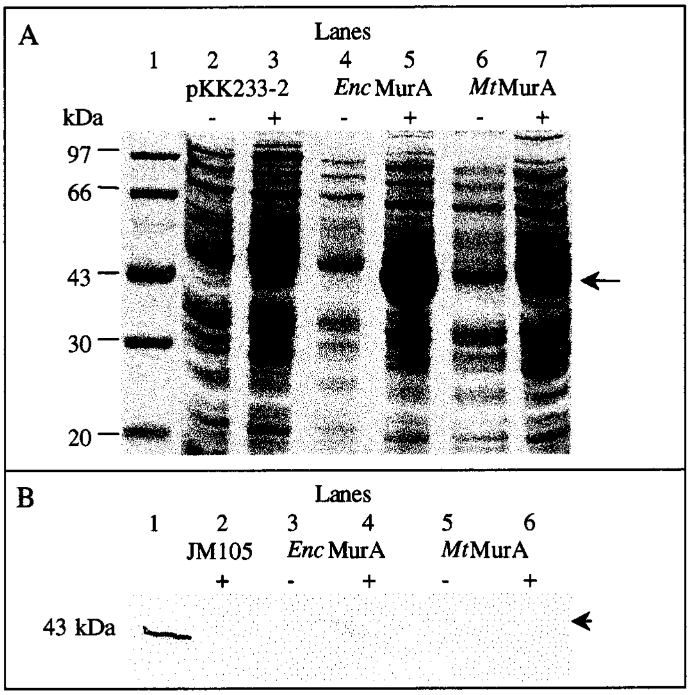

Figure 2.3.2: Expression and immunodetection of *Mt*MurA. Panel A: expression of *Mt*MurA at 37 °C as analysed by 10 % SDS-PAGE. Lane 1: Low molecular mass (LMW) markers (Pharmacia), lanes 2 and 3: uninduced (-) and induced (+) cells containing pKK233-2 respectively, lanes 4 and 5: uninduced and induced samples of pKK*EncmurA* expression respectively, lanes 6 and 7: uninduced and induced samples of pKK*MtmurA* respectively. Panel B: immunodetection of *Mt*MurA with anti-MurA antibody raised against *Enc*MurA. Lane 1: 43 kDa marker band as before, lane 2: induced (+) JM105 cells that have no plasmid, lanes 3 and 4: uninduced (-) and induced samples respectively from cells containing pKK*EncmurA*, lanes 5 and 6: uninduced and induced cells respectively containing pKK*MtmurA*. In both panels the arrow indicates the *Enc*MurA.

There is no obvious expression band at 44 kDa visible in the induced *Mt*MurA sample (panel A, lane 7). The protein expression in this lane is comparable to that of lane 3, containing only the pKK233-2 vector. However, the expression of *Enc*MurA (lane 5) indicates that the conditions chosen were suitable for expression. The expression in figure 2.3.2, panel A, was carried out using 0.1 mM IPTG for induction, higher concentrations of IPTG were also used, however, no expression was detectable under these conditions. A range of temperatures were investigated, as were different induction times. At no point was expression of *Mt*MurA visible. The presence of the plasmid was established by miniprep analysis, indicating that the plasmid had not been lost. Therefore, there are two possibilities to explain the lack of expression of the protein, (i) there is a mutation present in the gene sequence or (ii) there is only a low level of expression occurring and due to the "leakiness" of the trc promoter, expression is undetectable. The sequence of pKK*MtmurA* was obtained and no insertions, deletions or frameshift mutations were identified, indicating that the protein was not expressed as a truncated product. To determine whether there was a low level of expression occurring, immunodetection using the anti-MurA antibody was carried out (figure 2.3.2, panel B). The antibody only recognised the *Enc*MurA expressed in the induced cells (lane 3). The *Enc*MurA was also present in the uninduced cell samples (lane 4) indicating the "leakiness" of the trc promoter. No band was visible in the uninduced or the induced *Mt*MurA samples (lanes 5 and 6) suggesting that there was no expression of the protein in this vector. Alternatively, as the antibody was raised against the *Enc*MurA, it may not recognise the *Mt*MurA. It was decided that it would be more efficient to express the *Mt*MurA enzyme in a different expression system, such as the pET system.

2.3.3 Cloning and expression of *Mt*MurA and D117CMurA in the pET21d (+) expression vector

The *MtmurA* gene was excised from pKK*MtmurA* and cloned into the pET21d (+) expression vector. This resulted in the construct, pET*MtmurA*. DNA sequencing confirmed the identity of the inserted gene to be *MtmurA*. This was transformed into *E. coli* BL21 (DE3) cells and subsequently expressed. The expression was determined to be optimal at 30 °C as this temperature resulted in a higher proportion of the protein present in the soluble form. The expression is shown in figure 2.3.3. The expression of *Mt*MurA using the pET system resulted in a high yield of protein in comparison to that of the pKK233-2 expression system (figure 2.3.2) demonstrating that this is a much more suitable expression system.

In order to determine the effects of the replacement of the naturally occurring aspartate residue with a cysteine residue at position 117 in *Mt*MurA, site-directed mutagenesis was carried out as described in section 2.2.4. This resulted in the creation of the construct, pET*D117CmurA*. DNA sequencing confirmed the presence of the D117C mutation.

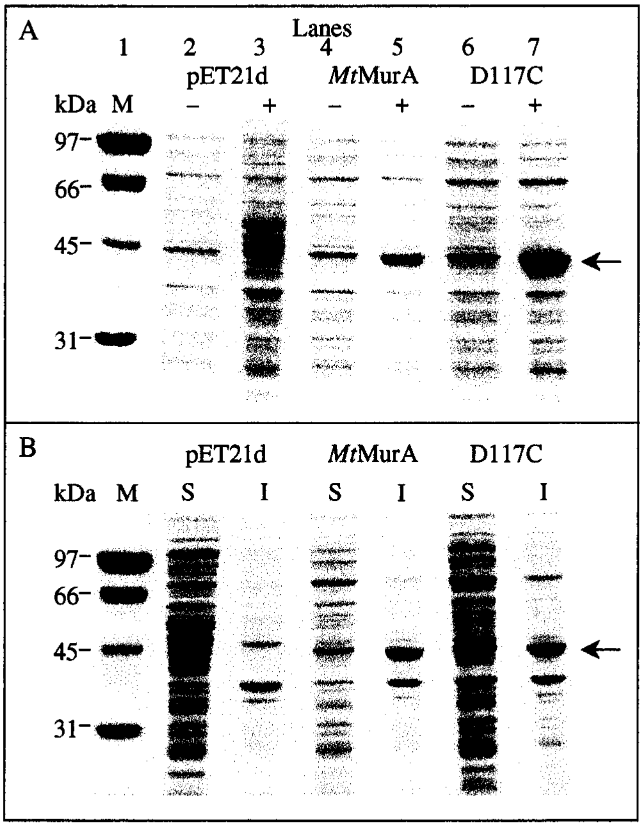

Figure 2.3.3: Expression and solubility of *Mt*MurA and D117CMurA as analysed by 10 % SDS-PAGE. Panel A: expression of *Mt*MurA and D117CMurA at 30 °C. Lane 1: BioRad low molecular mass (LMW) markers, lanes 2 and 3: uninduced (-) and induced (+) pET21d, lanes 4 and 5: uninduced and induced *Mt*MurA, lanes 6 and 7: uninduced and induced D117CMurA. Panel B: solubility of *Mt*MurA and D117CMurA. Lane 1: BioRad markers as before, lanes 2 and 3: soluble (S) cytoplasmic and insoluble (I) membrane fractions of pET21d, lanes 4 and 5: soluble and insoluble fractions of *Mt*MurA, lanes 6 and 7: soluble and insoluble fractions of D117CMurA. In both panels, arrows indicate the MurA enzymes.

In panel A, lanes 5 and 7 show the expression of a band at about 44 kDa, the expected size of *Mt*MurA, and this band is not observed in the induced pET21d sample (lane 3). These were assumed to be the *Mt*MurA and the D117CMurA proteins. The expression of both *Mt*MurA and D117CMurA is very similar in terms of amount and solubility. The expressed protein constitutes about 80 % of the total protein (lanes 5 and 7). On lysing the cells, both the *Mt*MurA and the D117CMurA proteins were found to be present in the insoluble membrane fraction (panel B, lanes 5 and 7). Around 90 to 95 % of the protein appeared to be insoluble, whereas only 5 to 10 % remained in the soluble fraction (lanes 4 and 6). The proteins were expressed in a 12 L fermentor in order to facilitate the isolation of the proteins in sufficiently high quantities.

2.3.4 Purification of *Mt*MurA and D117CMurA

The soluble proteins were purified using hydroxyapatite chromatography, ammonium sulphate precipitation, gel filtration (G-75) and anion exchange chromatography on DEAE-Sephacel (figure 2.3.4A).

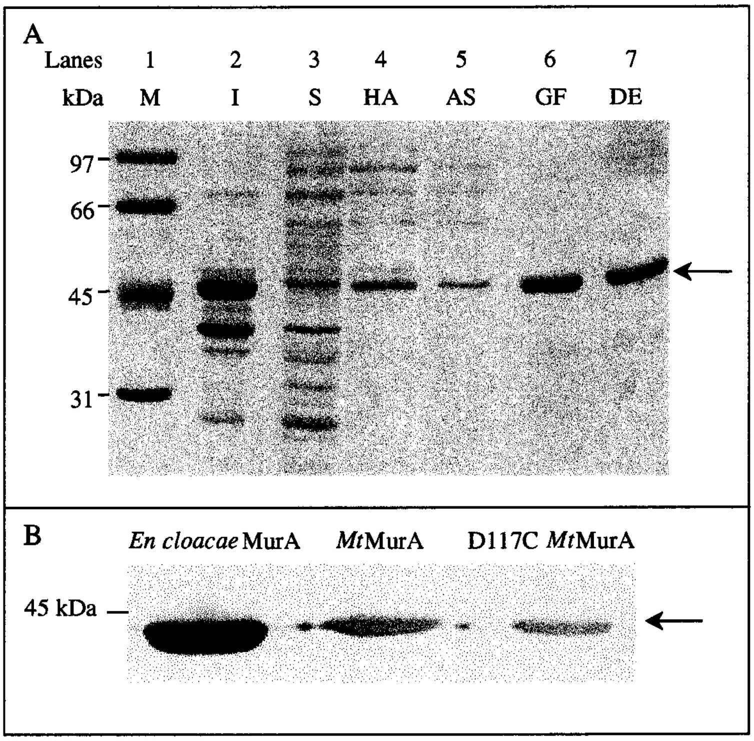

Figure 2.3.4: Purification and immunodetection of *Mt*MurA and D117CMurA. Panel A: purification of *Mt*MurA. Lane 1: BioRad low molecular mass marker as before, lanes 2 and 3: insoluble (I) and soluble (S) fractions respectively, lane 4: pooled *Mt*MurA after hydroxyapatite (HA) chromatography, lane 5: pooled *Mt*MurA after 60 % ammonium sulphate (AS) precipitation, lane 6: pooled *Mt*MurA after gel filtration (GF) chromatography, lane 7: pooled *Mt*MurA after DEAE-Sephacel (DE) chromatography. Lanes 4 to 7 were loaded with 2 µg of total protein. Panel B: immunodetection of *Enc*MurA, *Mt*MurA and D117CMurA using the anti-MurA antibody. The position of the 45 kDa marker (BioRad) is indicated. In both panels, arrows indicate the MurA enzymes.

The yield obtained from 20 g of cell paste was 10 to 15 mg for both *Mt*MurA and D117CMurA. Both were estimated to have between 95 to 98 % purity. Both N-terminal sequencing (table 2.3.1) and immunodetection with the *En. cloacae* anti-MurA antibody (figure 2.3.4, panel B) confirmed the identity of the two proteins. The N-terminal sequences were the same as the expected *Mt*MurA sequence from the database, except for the presence of leucine instead of glycine at position 10 of the sequence (underlined residue in table 2.3.1). This difference was not observed in the DNA sequence and may be an artifact of the N-terminal sequencing process. To ensure that the obtained protein was not the endogenous MurA from the *E. coli* expression strain, the N-terminal sequences were also compared to the sequence of *E. coli* MurA (table 2.3.1). The obtained *Mt*MurA sequence and that of *E. coli* MurA are extremely different indicating that any activity observed is not due to the presence of the endogenous *E. coli* MurA.

Table 2.3.1: Expected and observed N-terminal sequences of purified *Mt*MurA and histidine-tagged *Mt*MurA

	N-terminal Sequence[a]
*Mt*MurA Expected	MAERFVVTGGNRLSGE
*Mt*MurA Observed[b]	-AERFVVTGLNRLSGE
*Mt*MurA-His Observed	-AERFVVTGGN
E. coli MurA[c]	MDKFRVQGPTKLQGEV

[a] any changes from the expected sequences are underlined. Missing amino acids are indicated by a dash.

[b] data for D117CMurA not shown.

[c] the first 16 amino acids of *E. coli* MurA are shown for comparison.

2.3.5 Cloning and expression of *Mt*MurA-His and D117CMurA-His

Due to the extensive purification procedure required for the *Mt*MurA and the D117CMurA, an affinity chromatography approach was also utilised, i.e. expression of the proteins with a C-terminal six histidine-tag followed by chromatography on Ni-NTA agarose. It was hoped that the presence of the histidine-tag would also increase the solubility of the *Mt*MurA proteins and subsequently the yield of pure protein, as well as make the purification easier. To create the C-terminal six histidine-tag, the stop codon needed to be removed from the gene. PCR was used to amplify the *MtmurA* and *D117CmurA* genes using the primers MtMurA5' and MtMurA-His3', containing NcoI and XhoI restrictions sites respectively (figure 2.3.5).

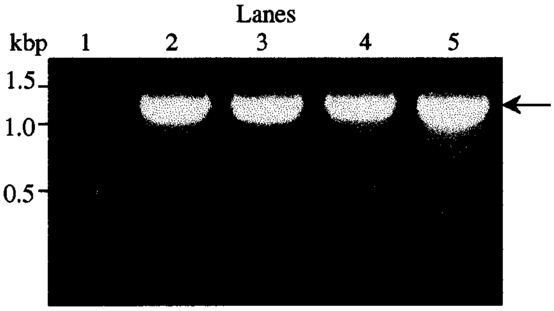

Figure 2.3.5: Agarose gel (1 %) showing results of PCR. Lane 1: 100 bp DNA ladder (Promega), lanes 2 and 3: 0.75 µg pET*MtmurA*, 2.0 and 2.5 mM $MgSO_4$ respectively, lanes 4 and 5: 0.75 µg pET*D117CmurA*, 2.0 and 2.5 mM $MgSO_4$ respectively. A 5 µL aliquot of each PCR was loaded into each lane. An annealing temperature of 52 °C was used. An arrow indicates the PCR products.

The PCR products (ca. 1300 bp) were cloned into pET21d (+) as before, to give the constructs, pET*MtmurA-his* and pET*D117CmurA-his*. The presence of the His-tag in the correct reading frame was confirmed by DNA sequencing. The proteins were expressed in the same way as the untagged proteins, i.e. at 30 °C and with 0.1 mM IPTG (figure 2.3.6, panel A). There are bands that are present in the induced samples at around 44 kDa that are not present in the uninduced samples (compare lanes 3 and 5 with lanes 2 and 4 in panel A). The expression of both proteins constitutes 80 % of the total expressed protein. Again, on lysing the cells the majority, about 85 % to 90 %, of the protein remained in the insoluble membrane fraction (figure 2.3.6, panel B, lanes 3 and 5). In panel B, lanes 2 and 4 demonstrate that 10 to 15 % of the protein may be in the soluble cytoplasmic fraction. This is similar to the solubility observed for the untagged *Mt*MurA and D117CMurA proteins. Therefore, the solubility of the *Mt*MurA and the D117CMurA proteins was not increased by the addition of a histidine-tag to the C-terminal end of the protein.

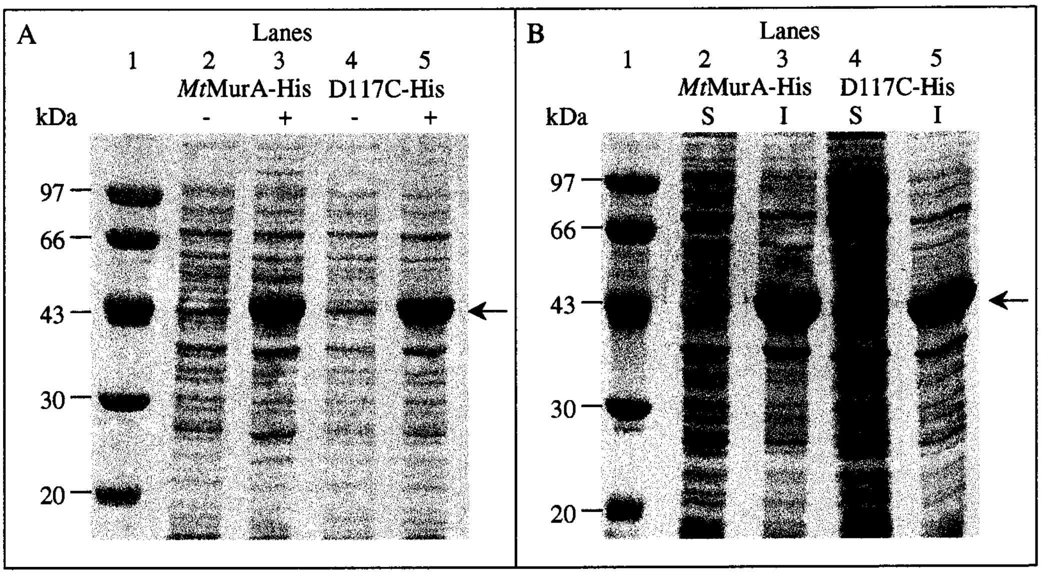

Figure 2.3.6: Expression and solubility of *Mt*MurA-His and D117CMurA-His at 30 °C, Panel A: Expression as analysed by 10 % SDS-PAGE. Lane 1: LMW markers (Pharmacia) as before, lanes 2 and 3: uninduced (-) and induced (+) samples of *Mt*MurA-His, lanes 4 and 5: uninduced and induced samples of D117CMurA-His. Panel B: Solubility as analysed by 10 % SDS-PAGE. Lane 1: LMW marker (Pharmacia) as before, lanes 2 and 3: soluble (S) cytoplasmic and insoluble (I) membrane fractions of *Mt*MurA, respectively, lanes 4 and 5: soluble and insoluble fractions of D117CMurA-His, respectively. Arrows indicate MurA in both panels.

2.3.6 Purification of *Mt*MurA-His

Purification was initially only attempted using the *Mt*MurA-His protein, until a suitable protocol had been established that could subsequently be applied to D117CMurA-His. The soluble cytoplasmic fraction from two litres of cell culture was subjected to metal affinity chromatography using Ni-NTA agarose. The protein was eluted using an increasing concentration of imidazole (figure 2.3.7), which competes with the histidine-tag for nickel (Ni) binding sites, resulting in the elution of the histidine-tagged protein.

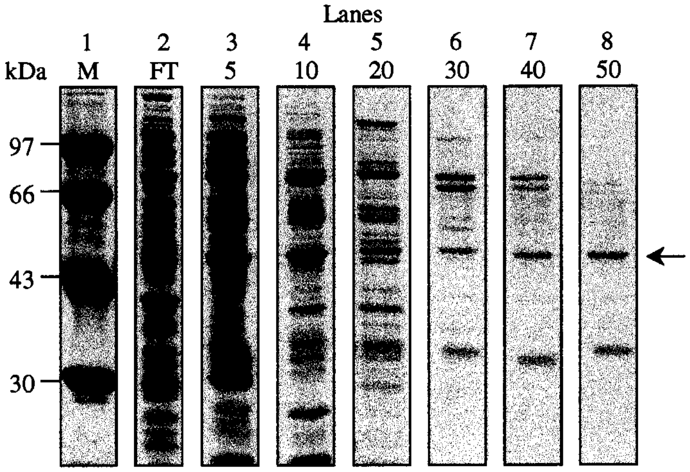

Figure 2.3.7: Purification of *Mt*MurA-His under native conditions as analysed by 10 % SDS-PAGE. Lane 1: LMW marker (Pharmacia) as before, lane 2: flowthrough (FT) containing 1 mM imidazole in the buffer, lane 3: the proteins that were eluted with 5 mM imidazole, lanes 4 to 8: proteins eluted consecutively using 10, 20, 30, 40 and 50 mM imidazole respectively. The concentrations (mM) of imidazole used are indicated above the lanes. A 100 µL aliquot from each fraction was precipitated using the MeOH/CCl_4 method and subjected to SDS-PAGE. The band thought to be *Mt*MurA-His is represented by the arrow.

Figure 2.3.7 shows the protein eluted using concentrations of imidazole from five to fifty mM. Up to 200 mM imidazole was used for the elution, however all of the protein appeared to have been eluted between the imidazole concentrations of five and fifty mM. This was confirmed by immunodetection using the anti-MurA antibody (figure 2.3.8).

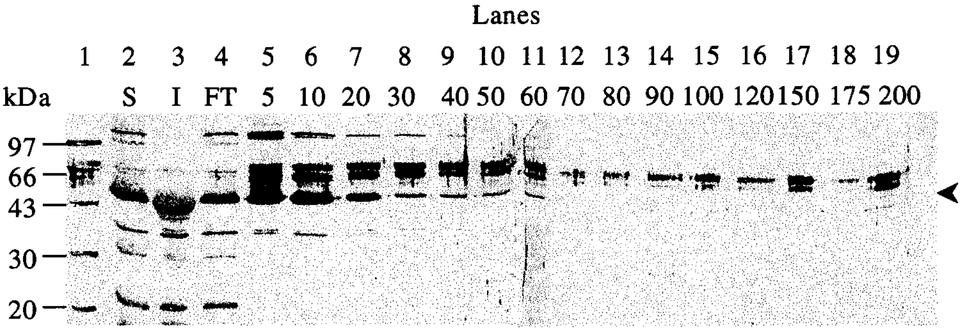

Figure 2.3.8: Immunodetection of *Mt*MurA-His eluted with increasing concentrations of imidazole. Lane 1: LMW marker as before, lane 2: soluble fraction (S) from cell lysis, lane 3: insoluble fraction (I) from cell lysis, lane 4: flowthrough (FT), lanes 5 to 19: stepwise increase in the concentration of imidazole from 5 to 200 mM. The concentrations (mM) of imidazole used are indicated above the lanes. The band thought to be *Mt*MurA-His is indicated by an arrow.

The *Mt*MurA-His protein did not bind tightly, if at all, to the Ni-NTA agarose as shown by the elution of the protein with 5 mM imidazole and the presence of the protein in the flowthrough (figure 2.3.8, lane 4). All of the *Mt*MurA-His present was eluted by 60 mM imidazole as the antibody did not recognise a band in the samples containing concentrations of imidazole greater than 60 mM (figure 2.3.8). In fact, most of the protein was eluted from the material at 20 mM imidazole. The *Mt*MurA-His protein, therefore, does not bind specifically to the Ni-NTA agarose and can not be purified successfully using this method. These results suggest that the histidine-tag has become inaccessible, perhaps it had been buried in the protein structure or produced the misfolding of the protein itself. Another possibility is that it had been cleaved by proteases present in the supernatant.

If *Mt*MurA-His can be purified using denaturing conditions this would suggest that the histidine-tag is still intact and that it has become inaccessible in the native protein. Firstly, the soluble fraction was denatured by the addition of urea and subjected to Ni-NTA agarose (figure 2.3.9A). Additionally, the cells were broken and resuspended in a buffer containing 8 M urea, before the extracted proteins were subjected to Ni-NTA agarose (figure 2.3.9B). In both cases, the *Mt*MurA-His protein was eluted by decreasing the pH of the buffers which alters the charge of the histidine and subsequently releases it from the Ni. The *Mt*MurA-His from the soluble fraction and the whole cells was eluted using pH 5.3 and 4.5 (figure 2.3.9). Some protein from the soluble fraction was released in the wash buffer, pH 6.9 (panel A, lane 3), and the remainder of the protein was eluted with pH 5.3 and 4.5 (panel A, lanes 4 and 5). There is an obvious difference in the amount of *Mt*MurA-His eluted at the different pHs between the soluble and the whole cell fraction. This is due to the small amount of protein present in the soluble fraction i.e. only 5 % of the total expressed protein. The *Mt*MurA-His from the whole cells binds very tightly to the Ni-NTA agarose and is eluted with pHs 5.3 and pH 4.5. Therefore, the histidine-tag can only tightly bind to the Ni-NTA agarose under denaturing conditions, suggesting that in the native form the histidine-tag is inaccessible.

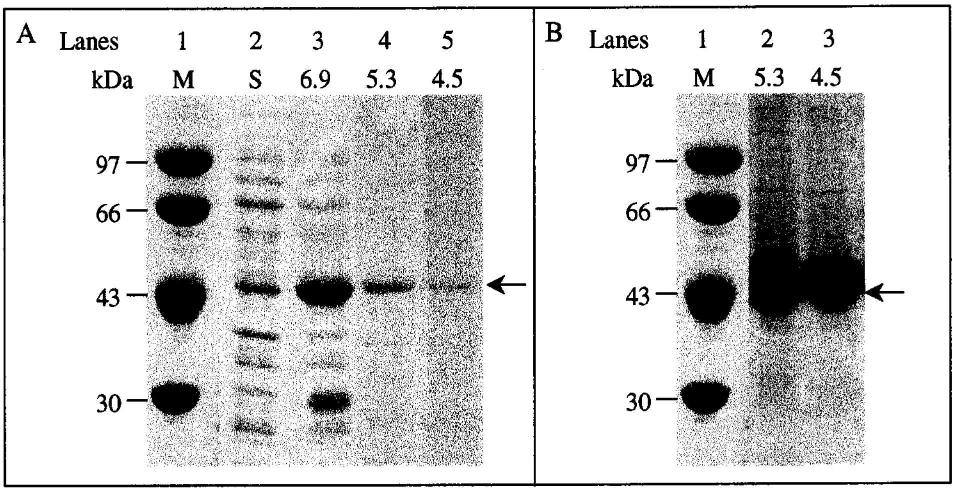

Figure 2.3.9: Elution of *Mt*MurA-His under denaturing conditions as analysed by 10 % SDS-PAGE. Panel A: Elution of soluble *Mt*MurA-His. Lane 1: LMW marker as before, lane 2: soluble (S) fraction denatured with urea and loaded onto the column, lane 3: proteins eluted using pH 6.9, lane 4: proteins eluted with pH 5.3, lane 5: proteins eluted with pH 4.5. Panel B: Elution of total *Mt*MurA-His present in the cells. Lane 1: LMW marker as before, lane 2: proteins eluted with pH 5.3, lane 3: proteins eluted with pH 4.5. Arrows indicate *Mt*MurA-His in both panels.

Immunodetection with the anti-MurA antibody (data not shown) and N-terminal sequencing (Table 2.3.1) confirmed the identity of the purified proteins. Additionally, immunodetection using an antibody directed against the six histidine residues that make up the tag, confirmed the presence of the intact histidine-tag (figure 2.3.10).

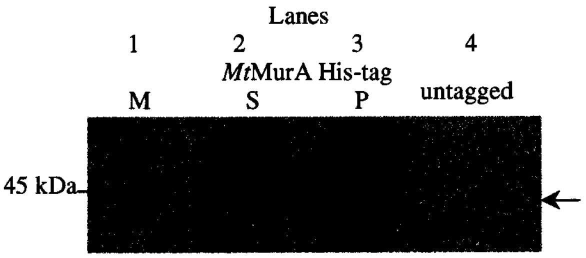

Figure 2.3.10: Immunodetection using the murine anti-His antibody. Lane 1: 45 kDa marker band (BioRad), lane 2: soluble (S) fractions of *Mt*MurA-His, lane 3: insoluble (I) fraction of *Mt*MurA-His, lane 4: 2 μg of *Mt*MurA. The arrow indicates *Mt*MurA.

The anti-His antibody recognises a band in the soluble and insoluble fractions (lanes 2 and 3) but there is no recognition of the *Mt*MurA (lane 4). This is expected as the antibody only recognises the six histidines that are present in the tagged proteins. This indicates again that the histidine-tag had not been degraded by proteases as the antibody only recognises a tag with a minimum of five histidine residues. This is further evidence that the histidine-tag is no longer accessible for binding to Ni-NTA agarose in the native state.

The question remains whether this inaccessibility of the histidine-tag is observed with other MurA enzymes, i.e. from *E. coli* or *En. cloacae*, or if this is only true of *Mt*MurA (see chapter 3). As *Mt*MurA-His could not be purified, all of the following activity studies were carried out using the native *Mt*MurA and D117CMurA enzymes.

2.3.7 Activity of *Mt*MurA and D117CMurA

The specific activities and K_M values of UDPNAG and PEP for *Mt*MurA and D117CMurA were determined as described in section 2.2.26. The results are shown in comparison with the previously published values for *E. coli* and *En. cloacae* MurA in table 2.3.2.

Table 2.3.2: Comparison of the kinetic parameters between *En. cloacae* MurA, *E.coli* MurA, *Mt*MurA and D117CMurA

	Specific activity (nmol/min/mg)	k_{cat} (min^{-1})	K_M (UDPNAG) (μM)	K_M (PEP) (μM)	k_{cat}/K_M (UDPNAG) ($M^{-1}\ min^{-1}$)	k_{cat}/K_M (PEP) ($M^{-1}\ min^{-1}$)
E. coli MurA[a]	-	285	2500	1000	1.1×10^5	2.8×10^5
E. coli MurA[b]	-	228	15	0.4[c]	1.5×10^7	5.7×10^8
E. coli C115D[d]	-	660	21	22	3.1×10^7	3.0×10^7
En. cloacae MurA	1300[e]*	60[f]*	70[g]	7.5[g]	8.6×10^5	8×10^6
*Mt*MurA	0.059*	0.0026*	40	4.5	6.5×10^1	5.8×10^2
D117C MurA	0.326*	0.014*	5.7	0.4	2.5×10^3	3.5×10^4

*values obtained using 1 mM substrate concentrations, [a]data from Marquardt et al. (1992), [b]data from Kim et al. (1996a), [c]data from Kim et al. (1996a), but quoted as unpublished results, [d]data from Kim et al. (1996a), taken from optimal pH of 6.0, [e]data from Samland et al. (1999), [f]data from Krekel. (1998), [g]data from Samland. (2001).

The activity of *Mt*MurA was shown to be 2 x 10^4-fold lower than that of *Enc*MurA (table 2.3.2). However the D117CMurA exhibited only 4 x 10^3-fold lower activity than *Enc*MurA. Hence, the D117CMurA exhibits a five-fold increase in activity compared to *Mt*MurA. It was also determined that the addition of a monovalent (NaCl or KCl) or a divalent ($MgSO_4$) ion in the range of 10 to 50 mM had little effect on the activities of the enzymes. If anything, the presence of the divalent ion caused some inhibition of the enzymes.

Although there is a large difference in the catalytic activities of the enzymes, the K_M values of UDPNAG and PEP determined for *Mt*MurA are the same as those previously determined for the *Enc*MurA (table 2.3.2, figure 2.3.12A and figure 2.3.13A).

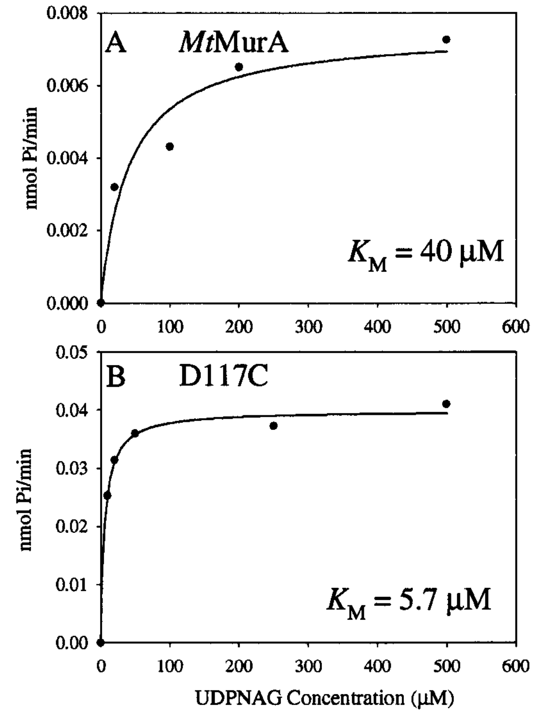

Figure 2.3.12: Determination of K_M (UDPNAG). The calculated nmol Pi/min was plotted against the UDPNAG concentration (μM) and a hyperbole equation used to determine the K_M value. Panel A: *Mt*MurA. Panel B: D117CMurA

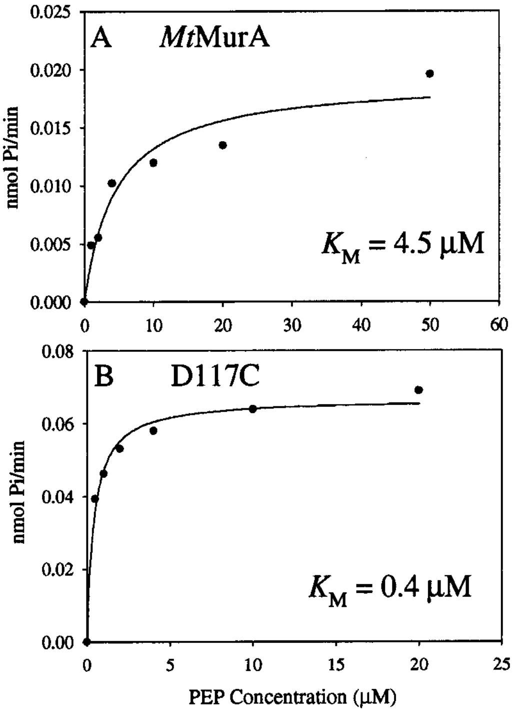

Figure 2.3.13: Determination of K_M (PEP). The calculated nmol Pi/min was plotted against the PEP concentration (μM) and a hyperbole equation used to determine the K_M value. Panel A: *Mt*MurA. Panel B: D117CMurA

The K_M values for UDPNAG and PEP for D117CMurA, on the other hand, are 7- and 11-fold lower than those of *Mt*MurA, respectively (table 2.3.2, figure 2.3.12B and figure 2.3.13B). This suggests that in the presence of a cysteine residue instead of an aspartate residue, the enzyme can bind UDPNAG and PEP more tightly than the *Mt*MurA and *Enc*MurA.

The catalytic efficiencies of *Mt*MurA and D117CMurA, as determined by k_{cat}/K_M, are considerably lower than that of the *Enc*MurA (table 2.3.2). The large difference in specific activity that was observed between *Mt*MurA and *Enc*MurA gives rise to a much lower catalytic efficiency of *Mt*MurA. *Enc*MurA exhibits 1.32 x 10^4- and 1.38 x 10^4-fold higher catalytic efficiencies for UDPNAG and PEP, respectively, compared to *Mt*MurA. The catalytic properties of the D117CMurA are significantly different which lead to a 38- and 60-fold higher catalytic efficiency of D117CMurA compared to *Mt*MurA with respect to UDPNAG and PEP.

2.3.8 pH dependence of *Mt*MurA and D117CMurA

This was investigated primarily as a result of the study by Kim et al. (1996a) of an *E. coli* C115D mutant protein. This mutant protein showed a pH profile that was different from that of the wild type protein, in that the activity of the C115D mutant was higher at pH 5.5 and linearly decreased over the pH range from pH 5.5 to 9.0. In contrast, the activity of the *E. coli* wild type enzyme was steady over the same pH range. Additionally, the activity of the *E. coli* C115D mutant exceeded that of the wild type about three-fold at pH 5.5.

The activities of *Mt*MurA and D117CMurA were investigated over the pH range of 5.0 to 9.0 as described in section 2.2.26.2. Activity of these enzymes was observed over a broader pH range than that of the *E. coli* C115D mutant, as shown in figure 2.3.14. The *Mt*MurA exhibits broad maximal activity in the pH range 5.5 to 9.5 (figure 2.3.14, panel A) which contrasts with the results obtained by Kim et al. (1996a) for the *E. coli* C115D mutant. The D117CMurA exhibits maximal activity in the pH range 7.0 to 9.0 (figure 2.3.14, panel B), indicating that the presence of the cysteine results in a shift in activity to a slightly more alkaline pH. Additionally, the activity of the D117CMurA remains higher than the wild type at all pH values measured, again contrasting the results of Kim et al. (1996a) where the *E. coli* C115D mutant had higher activity than the C115 containing wild type.

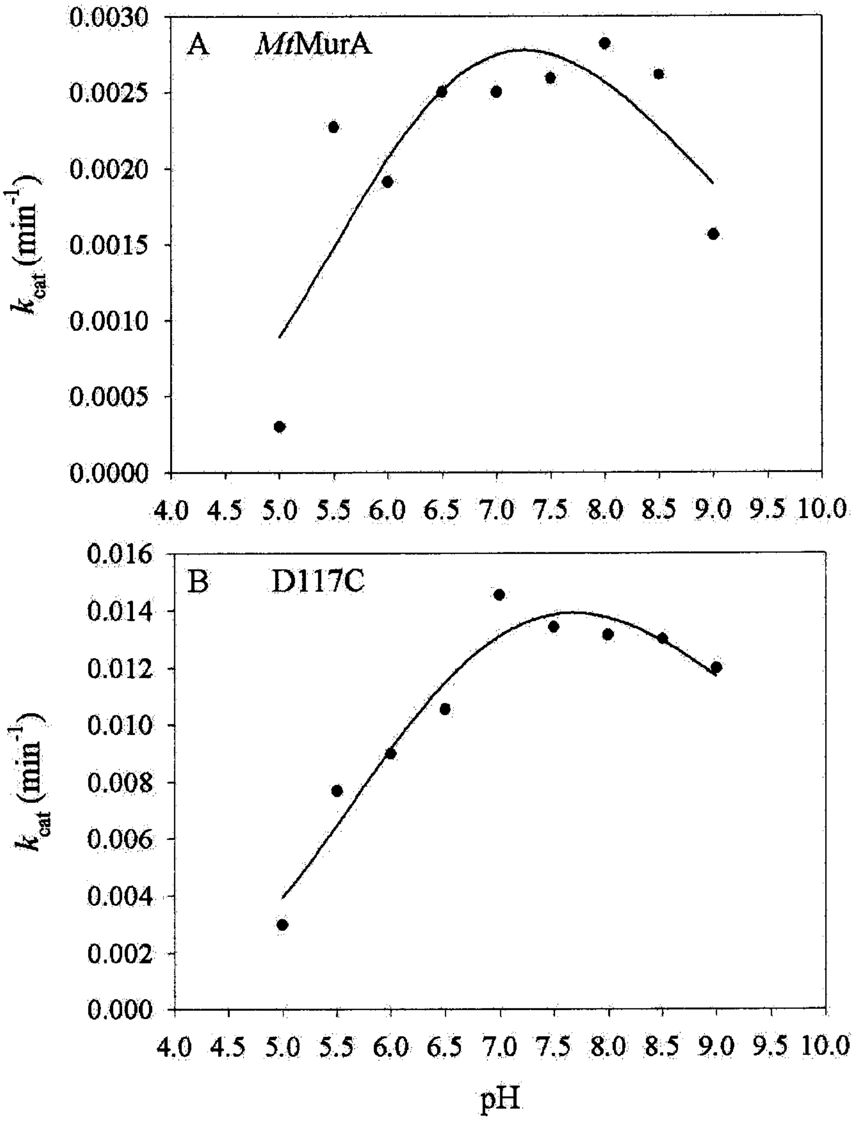

Figure 2.3.14: Effect of pH on the activities of *Mt*MurA and D117CMurA. The k_{cat} (min^{-1}) was plotted against pH and the values fitted using the normal log equation. The values are averages of at least two experiments. Panel A: pH profile of *Mt*MurA. Panel B: pH profile of D117CMurA.

2.3.9 Effect of fosfomycin on *Mt*MurA and D117CMurA

Fosfomycin is an irreversible inhibitor of MurA's that contain Cys115 (Wanke and Amrhein 1993). As the cysteine is no longer present in *Mt*MurA, what effect does fosfomycin have on the enzyme? It has been shown by De Smet et al. (1999) that fosfomycin does not inhibit the *Mt*MurA enzyme, however, no detailed biochemical study was carried out to determine whether fosfomycin is binding non-covalently to the enzyme as has been suggested by studies of other Cys115 mutants (Samland 2001). Here the binding of fosfomycin was investigated at different PEP and different fosfomycin concentrations with the aim of establishing whether the inhibition is competitive or noncompetitive.

The activity of *Mt*MurA was affected by the presence of fosfomycin even at low fosfomycin concentrations, however, as the concentration of PEP increased, the enzyme activity also increased. This suggests that fosfomycin is a competitive inhibitor of *Mt*MurA as its inhibitory effect can be overcome by increasing the concentration of PEP. This was confirmed when the K_i of fosfomycin was calculated by plotting the data according to Dixon (1952), where the 1/activity value is plotted at each PEP concentration against the fosfomycin concentration (figure 2.3.15).

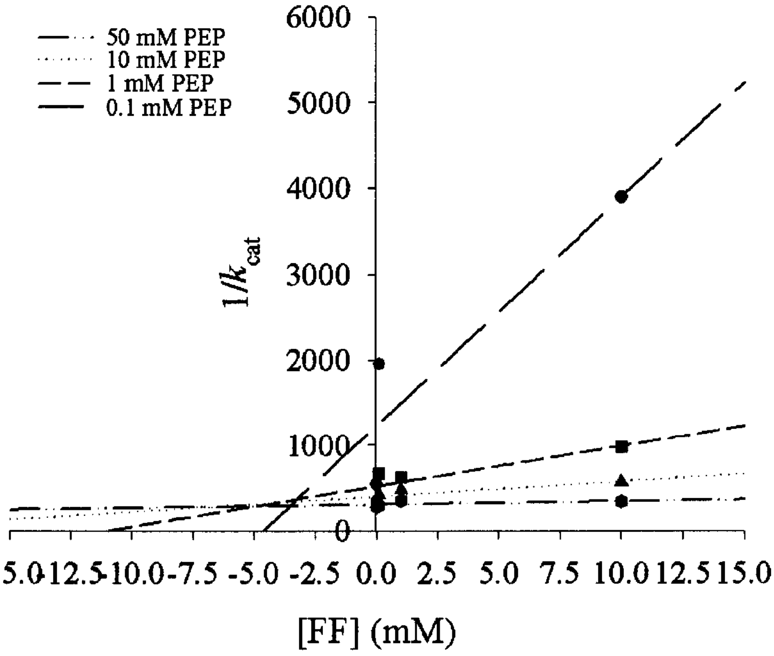

Figure 2.3.15: Dixon plot of fosfomycin inhibition of *Mt*MurA. The $1/k_{cat}$ (min^{-1}) value was plotted against the fosfomycin concentration (mM) for each PEP concentration that was measured. The point at which the lines intersect is the K_i value. Long dashes: 0.1 mM PEP, medium dashes: 1 mM PEP, dotted line: 10 mM PEP, dashes and dots: 50 mM PEP.

From the Dixon plot, the K_i was calculated to be 3.5 to 5.0 mM. As the lines also intersect above the X-axis this indicates that the inhibition is competitive. The K_i of fosfomycin towards the *E. coli* MurA was determined to be 8.6 µM and the K_i of the *E. coli* C115D mutant was 1 to 2 mM (Kim et al. 1996a). This indicates that the binding of fosfomycin to *Mt*MurA is greatly decreased, as the cysteine residue is not available for the formation of the covalent adduct.

Fosfomycin binding to the cysteine residue present in D117CMurA results in the irreversible inhibition of the enzyme (figure 2.3.16). As the enzyme remains inhibited even in the presence of higher amounts of PEP, this indicates that fosfomycin has probably formed the covalent adduct with D117C.

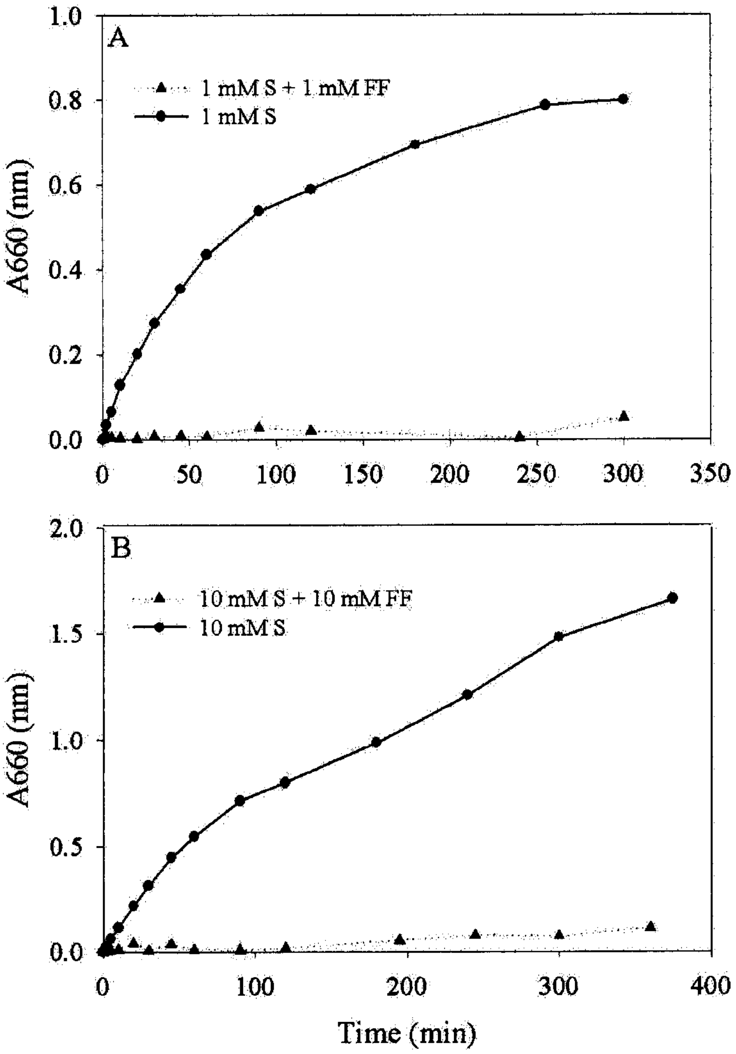

Figure 2.3.16: Inhibition of D117CMurA in the presence of fosfomycin (FF). The measured A660 was plotted against time (min). • represents UDPNAG and PEP (S) alone. ▲ represents UDPNAG and PEP (S) together with fosfomycin (FF). Panel A: 1 mM UDPNAG and 1 mM PEP in the presence and absence of 1 mM FF. Panel B: 10 mM UDPNAG and 10 mM PEP in the presence and absence of FF.

These results indicate that the presence of the aspartate within the MurA enzyme at this crucial position results in fosfomycin resistance. Some inhibition occurs, but this is overcome by increasing the PEP concentration indicating that fosfomycin is a competitive inhibitor with respect to PEP.

2.4 MurA from *Chlamydia trachomatis* (*Ct*MurA)

2.4.1 Cloning of *CtmurA* into pKK233-2

The *CtmurA* gene was amplified using PCR from the genomic DNA and the primers, CtMurA5' and CtMurA3'. A PCR product (ca. 1350 bp) was obtained with 2.5 mM $MgSO_4$ and 0.34 and 1.7 µg of genomic DNA only (figure 2.4.1, lanes 5 and 7).

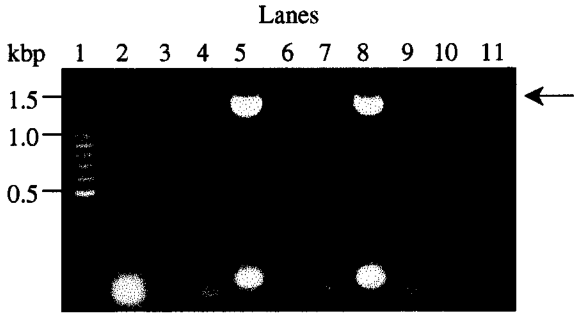

Figure 2.4.1: Agarose gel (1 %) showing the *CtmurA* PCR products. Lane 1: 100 bp DNA ladder (Promega), lane 2: no Pwo DNA polymerase, lanes 3 to 5: 1.7 µg of genomic DNA and $MgSO_4$ concentrations of 1.5, 2.0 and 2.5 mM respectively, lanes 6 to 8: 0.34 µg of genomic DNA and $MgSO_4$ concentrations of 1.5, 2.0 and 2.5 mM respectively, lanes 9 and 10: 3.4 µg of genomic DNA and $MgSO_4$ concentrations of 2.0 and 2.5 mM respectively, lane 11: 5.1 µg of genomic DNA and 2.0 mM $MgSO_4$. An aliquot of 5 µL was loaded in each lane. Annealing temperature was 53 °C.

The PCR products obtained were used for cloning the *CtmurA* into the pKK233-2 vector. However, this vector only contains 3 restriction sites that could be used for cloning, NcoI, HindIII and PstI. As the *CtmurA* has NcoI restriction sites at both the 5' and the 3' ends, there was a 50 % chance that the gene would be inserted into the vector in the opposite orientation. All of the recombinant plasmids that contained the *CtmurA* gene had inserted the gene in the wrong orientation as determined by restriction enzyme analysis. The inability to clone the *CtmurA* gene into the pKK233-2 vector in the correct orientation required for expression necessitated the use of an expression vector with greater variation in the multiple cloning site, i.e. the pET expression system.

2.4.2 Cloning of *CtmurA* into pET21d (+)

The *CtmurA* gene (expected size of 1335 bp) was amplified from the pKK*CtmurA* using PCR. Two strategies were undertaken in order to clone the gene into the pET21d (+) vector, i.e. (i) the initial cloning of the blunt-ended PCR product into the PCR-Script vector (Stratagene), before cloning it into the desired expression vector (see section 2.2.7), and (ii) the direct ligation of the digested PCR product into the pET21d (+) vector. Both of these strategies were successful and resulted in the cloning of pET*CtmurA*. The identity of the recombinant plasmids was confirmed by the sequencing of the gene as described in section 2.2.11.

2.4.3 Expression of *Ct*MurA

*Ct*MurA was expressed in *E. coli* BL21 (DE3) cells at 25, 30 and 37 °C using an IPTG concentration of 0.3 mM. Expression of a band of 48 kDa was observed at 30 and 37 °C (figure 2.4.2A) that was not observed in the uninduced cells after a 4 hour period (figure 2.4.2, lane 3). There was little observable difference in the expression levels at these temperatures (compare lanes 5 and 7) whereas at 25 °C, very little expression was observed (lane 9).

The solubility of *Ct*MurA was determined at all three temperatures (figure 2.4.2B). A comparison between lanes 4 and 5 and 6 and 7, indicates that the protein is 90 to 95 % insoluble and only 5 to 10 % of *Ct*MurA remains in the soluble cytoplasmic fraction. The lower expression level at 25 °C can clearly be seen in lanes 8 and 9, where the *Ct*MurA band is considerably reduced in comparison to the other temperatures. There appears to be very little difference in the solubility of *Ct*MurA between 30 and 37 °C, although there does appear to be slightly more *Ct*MurA present in the soluble fraction at 30 °C (lane 6) than at 37 °C (lane 4). Therefore, a temperature of 30 °C was subsequently used for expression.

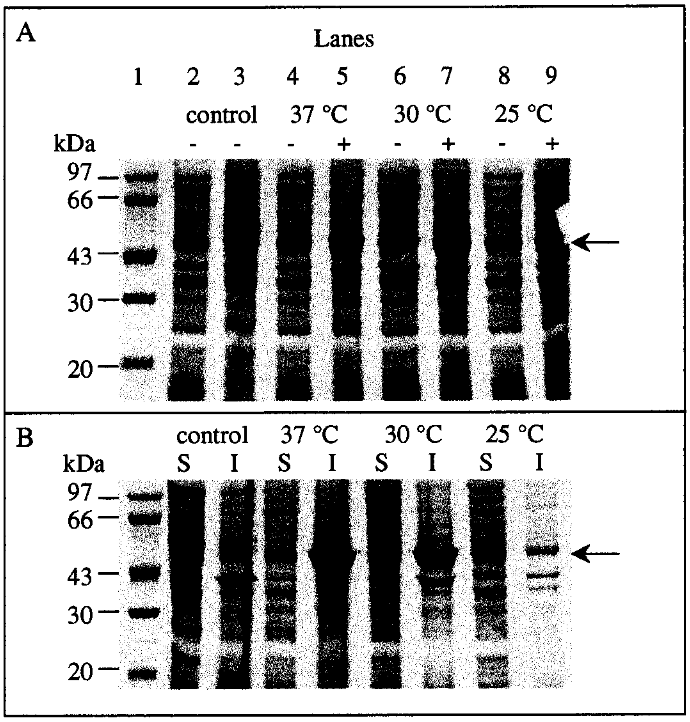

Figure 2.4.2: Expression and solubility of *Ct*MurA at different temperatures as analysed by 10 % SDS-PAGE. Panel A: expression of *Ct*MurA. Lane 1: Low molecular mass (LMW) markers (Pharmacia), lanes 2 and 3: uninduced (-) cells at 0 and 4 hours respectively, lanes 4 and 5: uninduced and induced (+) cells grown at 37 °C, lanes 6 and 7: uninduced and induced cells grown at 30 °C, lanes 8 and 9: uninduced and induced cells grown at 25 °C. The cells were induced with 0.3 mM IPTG. Panel B: solubility of *Ct*MurA. Lane 1: LMW marker as before, lanes 2 and 3: soluble (S) cytoplasmic and insoluble (I) membrane fraction of the uninduced cells after 4 hours, lanes 4 and 5: soluble and insoluble fractions of cells grown at 37 °C, lanes 6 and 7: soluble and insoluble fractions of cells grown at 30 °C, lanes 8 and 9: soluble and insoluble fractions of cells grown at 25 °C. In all lanes, 10 to 20 μg of protein was loaded.

2.4.4 Purification of *Ct*MurA

*Ct*MurA was partially purified using anion exchange chromatography. The supernatant from two litres of cell culture was loaded onto DEAE-Sephacel as described in section 2.2.19. The *Ct*MurA appeared to be eluted between 60 to 85 % of the linear KCl gradient that was applied to the material. However, the presence of two bands in these fractions, both of which correspond to ca. 45 to 48 kDa, made identification of the fractions containing *Ct*MurA difficult.

Western blotting using the crude rabbit anti-MurA antibody did not specifically identify one of these two bands as *Ct*MurA. The fractions that were thought to contain *Ct*MurA were pooled and concentrated. Both bands are clearly visible in figure 2.4.3.

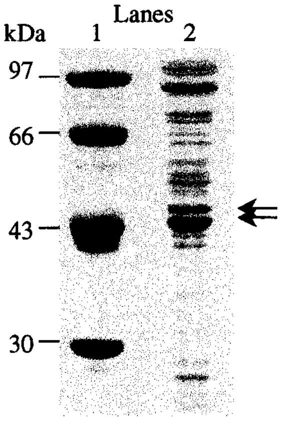

Figure 2.4.3: Concentrated sample containing two possible candidates for *Ct*MurA. Lane 1: LMW markers as before, lane 2: 4 μg of the concentrated fractions. The arrows indicate the two possible candidates for *Ct*MurA.

To confirm the identity of these two bands, N-terminal sequencing was attempted. Unfortunately, the N-terminuses of both of the proteins appeared to be blocked and no sequence could be obtained. This may have been due to artificial blocking by the electrograph or the solvents used. For example, this may be caused by the presence of peroxides or aldehydes in the MeOH used in the transfer buffer.

As N-terminal sequencing of the bands was not possible, in-gel tryptic digestion and MALDI-TOF mass spectrometry were used. Both bands (marked by arrows in figure 2.4.3) were subjected to this method. The resulting spectra are shown in figure 2.4.4, panels A and B, which correspond to the lower and the upper bands respectively.

The analysis of the peptides found in panel A, indicated that none of the peptides belonged to any *C. trachomatis* proteins. Instead they were identified as a variety of *E. coli* proteins. The highest scoring match was the *E. coli* modified methylase Eco47II (Acc # 1709155) which had 5 out of 26 peptides. Of the 26 peptides identified in panel B, eight of them were found to match peptides in the *in silico* tryptic digest of *Ct*MurA. However, the coverage of the *Ct*MurA was only 17 %. The remaining 18 peptides were identified as peptides from other *E. coli* proteins, for example, *E. coli* aldehyde dehydrogenase-like protein YNE1 (Acc # 3915524) matched five of these peptides. Therefore, although the majority of protein in the upper band can be indentified as *Ct*MurA there are also other proteins from *E. coli* present. During the further purification of *Ct*MurA this method can be used for identifying the protein at each stage.

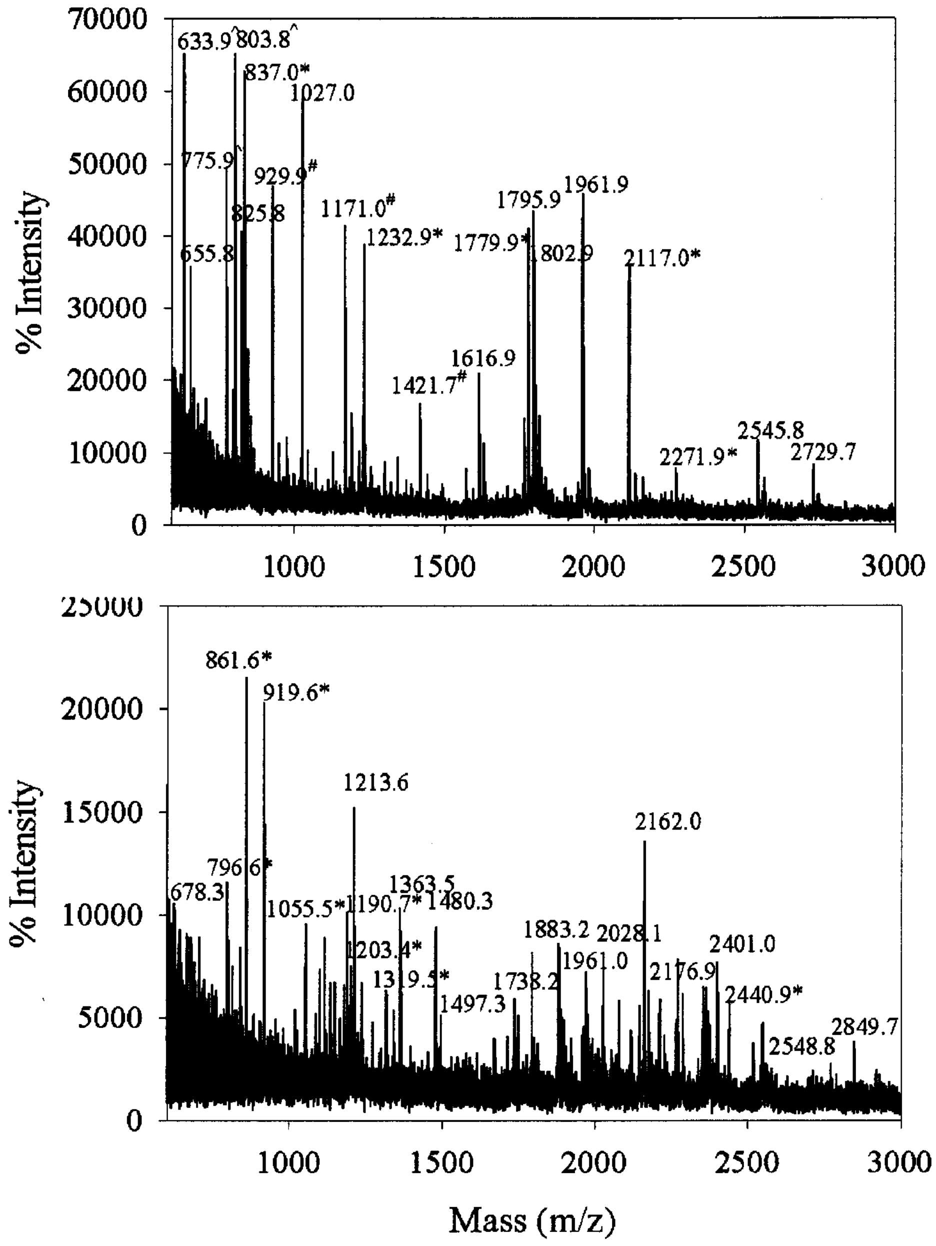

Figure 2.4.4: MALDI-TOF spectra of the upper and lower bands in figure 2.4.3. The % intensity is plotted against the mass (m/z). Panel A represents the lower band, 26 peptides were identified. * indicates *E. coli* modified methylase Eco47II, # indicates *E. coli* KLAA/TELA protein, ^ indicates *E. coli* WbnE protein. Panel B represents the upper band, 26 peptides were identified. * indicates *Ct*MurA peptides.

2.5 MurA from *Borrelia burgdorferi* (*Bb*MurA)

2.5.1 Cloning of *BbmurA* into pET21a (+)

The *BbmurA* gene was amplified by PCR from the genomic DNA, strain OMZ 494-P, using the primers BbMurA5' and BbMurA 3' and an annealing temperature of 39 °C. A PCR product of ca. 1400 bp was obtained under all of the reaction conditions used (figure 2.5.1). This amplified gene was cloned into the pET21a (+) vector using the restriction sites, NdeI and BamHI. Sequencing of this recombinant plasmid identified the presence of a ten bp insertion at the beginning of the gene (1329 bp), that resulted in a frameshift mutation and subsequently the protein would have been expressed in a truncated form.

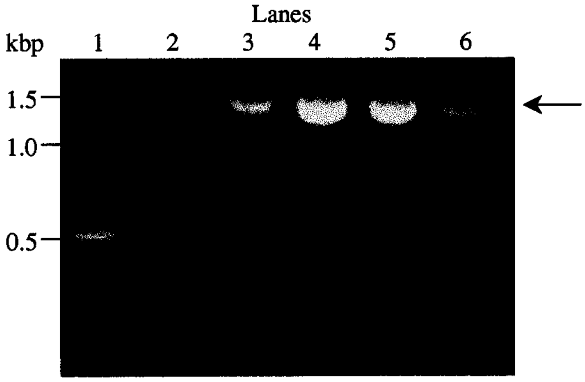

Figure 2.5.1: Agarose gels (1 %) showing the products of the PCR. Lane 1: 100 bp DNA ladder (Promega), lane 2: no Pwo DNA polymerase, lane 3: 2.0 mM $MgSO_4$ and 300 ng genomic DNA, lane 4: 2.5 mM $MgSO_4$ and 300 ng genomic DNA, lanes 5 and 6: 750 ng genomic DNA and 2.0 and 2.5 mM $MgSO_4$ respectively. Annealing temperature was 39 °C. Five µL of each reaction was loaded in each lane. The annealing temperature used was 45 °C.

A new primer was designed for the 5' end of the gene (BbMurA5'-2) that encompassed an extra 13 bases of the gene in order to prevent the same insertion occurring again. The *BbmurA* gene was then amplified as above except that, as the 5' primer was longer, an annealing temperature of 45 °C was used. A PCR product was again produced under all of the reaction conditions used. However, the amount of PCR product produced was significantly reduced in comparison to the amount of product present in figure 2.5.1 (data not shown). The amplified gene was cloned into the pET21a (+) vector to give pET*BbmurA*, in the same way as before. The inserted gene was sequenced as described in section 2.2.11. The sequence obtained indicated that there was an insertion of nine bp at position 32 of the gene (figure 2.5.2A). This insertion does not create a frameshift mutation but translates into the amino acids, isoleucine, valine and cysteine (figure 2.5.2B).

```
A: PETBbMurA: tgcgatttaattttattaagttttatatatagtatgtataggagggtgg 51
              |||||||||||||||||||||||||||||         ||||||| |||
   BbMurA:    tgcgatttaattttattaagttttatata---------taggaggatgg 12564

   PETBbMurA: gttatgtatagttatattgtagaaggtggt 81
               ||||| ||||||||||||||||||| ||
   BbMurA:    attatgcatagttatattgtagaaggcggc 12594


B:    pETBbMurA   MRFNFIKFLYIVCIGGWVMYSYIVEGG 27
                  MFRNFIKFLY   IGGW+M+SYIVEGG
      BbMurA      MRFNFIKFLY---IGGWIMHSYIVEGG 24
```

Figure 2.5.2: DNA and protein alignment of the mutated region of the *BbmurA* gene Panel A: alignment of the pET*BbmurA* gene and the *BbmurA* gene in Genbank. Panel B: alignment of the corresponding amino acid sequences (Acc no NP_212606).

An alignment of MurA sequences indicates that this insertion of three amino acids occurs in a non-conserved region of the protein and should not affect the activity of the enzyme. The presence of this extra nine bp may additionally explain the reduced amount of PCR product obtained as the extended primer, BbEPT5'-2, would not have been able to anneal tightly to the DNA due to the lack of these extra nine bases. Other base mutations occur throughout the gene but most of these appear to occur in the third base position, the so-called "wobble" position, and do not affect the conserved amino acid residues of MurA. Both the presence of the insertion, and the other base mutations, are most likely related to differences between the gene sequences of the *Borrelia* strains.

2.5.2 Expression of *Bb*MurA

The expression of *Bb*MurA was first attempted in *E. coli* BL21 (DE3) cells at 37 °C using various IPTG concentrations (0.3 to 1 mM). Two different clones were analysed for expression, *Bb*MurA-1 and *Bb*MurA-2. No expression of the 48 kDa protein was observed under any of the conditions tested (figure 2.5.3A).

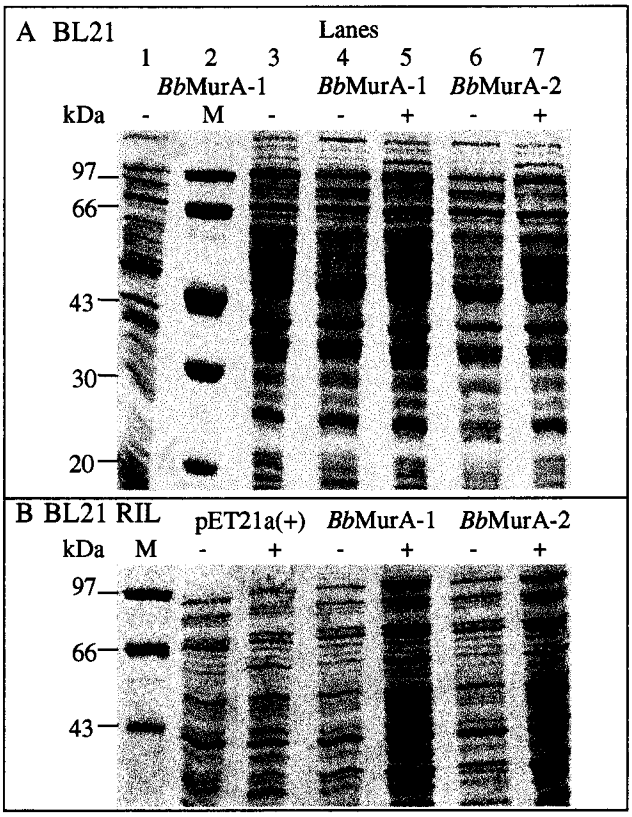

Figure 2.5.3: Expression of *Bb*MurA analysed by 10 % SDS-PAGE. Panel A: expression of *Bb*MurA at 37 °C in *E. coli* BL21 (DE3) cells. Lanes 1 and 3: uninduced (-) cells after 0 and 4 hours respectively, lane 2: low molecular mass (LMW) marker (Pharmacia), the corresponding molecular masses are shown on the left hand side of the gel, lanes 4 and 5: uninduced (-) and induced (+) samples of *Bb*MurA-1, lanes 6 and 7: uninduced (-) and induced (+) samples of *Bb*MurA-2. Induction with 0.3 mM IPTG. Panel B: expression of *Bb*MurA at 37 °C in *E. coli* BL21 (DE3) RIL cells. Lane 1: LMW markers as before, lanes 2 and 3: uninduced (-) and induced (+) pET21a, lanes 4 and 5: uninduced and induced samples of *Bb*MurA-1, lanes 6 and 7: uninduced and induced samples of *Bb*MurA-2. Induction was with 5 mM IPTG.

A band of around 50 kDa was present in the cells containing pET*BbmurA* (panel A, lanes 5 and 7), however, this band was also present in the uninduced cells after the same time period (lane 3) and also in the pET21a (+) containing cells (data not shown). Therefore, the expression of *Bb*MurA does not appear to be possible in *E. coli* BL21 (DE3) cells.

A comparison of the codon usage between *E. coli* MurA, *Mt*MurA and *Bb*MurA indicated that the use of the rare codons for Arg, Ile and Leu is increased in *Bb*MurA compared to *E. coli* MurA and *Mt*MurA (Table 2.5.1). This suggests that the lack of expression in *E. coli* BL21 (DE3) cells may be due to the lack of the required tRNA's for these rare codons.

	Arginine codons		Isoleucine codon	Leucine codon
	AGA	AGG	AUA	CUA
*Bb*MurA	8	6	12	3
E. coli MurA	-	-	-	4
*Mt*MurA	-	1	1	1

Table 2.5.1: Comparison of the codon usage between *Bb*MurA, *E. coli* MurA and *Mt*MurA with respect to the rare codons encoded for by *E. coli* BL21 RIL cells.

The expression of *Bb*MurA was then attempted in *E. coli* BL21 (DE3) RIL cells that contain additional plasmids encoding these rare tRNAs. The expression was attempted at 25, 30 and 37 °C with an IPTG concentration ranging from 0.3 to 5 mM. However, no expression of the 48 kDa band was detectable in either of the clones investigated (figure 2.5.3B). The expression profiles of the clones appear to be the same as that of pET21a (+) (compare lanes 5 and 7 with lane 3). Therefore, no expression of the *Bb*MurA occurred even in the presence of the extra codons provided by the *E.coli* cells. A western blot of these samples using the crude rabbit anti-MurA antibody only detected the endogenous *E. coli* MurA (data not shown). The presence of the recombinant plasmids within the cells was confirmed using plasmid miniprep analysis.
Therefore, it does not appear to be possible to express *Bb*MurA in either the *E. coli* BL21 (DE3) cells or the *E. coli* BL21 (DE3) RIL cells. The *BbmurA* gene sequence showed that no frameshift mutations, insertions or deletions had occurred that could have resulted in expression of a truncated protein. It is unlikely that *Bb*MurA is toxic to the cells as growth continues after induction. At the moment, we have no explanations for the lack of expression of *Bb*MurA under the conditions tested. Perhaps another expression system should be tested in order to obtain *Bb*MurA.

3. *Enterobacter cloacae* MurA as a histidine-tagged protein

3.1 Materials

3.1.1 Chemicals and enzymes

Refer to section 2.1.1 for further details.

3.1.2 Bacterial strains

E. coli DH5α and *E. coli* BL21 (DE3) competent cells were used. For details see section 2.1.2.

3.1.3 Vectors

The vector, pET21d (+) was used in the cloning of *Enc*MurA-His. For details see section 2.1.3.

3.2 Methods

3.2.1 Primers

The following primers were designed in order to clone the *EncmurA* gene containing a C-terminal six histidine-tag:

EncMurA 5' 5' CATGCC**ATG**GATAAATTTCGTGTACAGG 3'
NcoI

EncMurA 3' 5' CCGCTCGAGCTCGCCCTTCACACGCTCG 3'
XhoI

The appropriate restriction sites are underlined and the start codon in EncMurA5' is depicted in bold type. The EncMurA3' primer lacks a stop codon to facilitate the cloning of the C-terminal histidine-tag. The Tm value for each primer was calculated as described in section 2.2.2.

3.2.2 PCR of the *En. cloacae murA* gene

The PCR was set up as described in section 2.2.3, except that 20 to 50 μg of template DNA was added. In this case, the template was the plasmid pKK233-2 containing *En. cloacae murA* (pKK*EncmurA*) (Wanke et al. 1992).

The same PCR cycles were used as in section 2.2.3, except that the annealing temperature used in all cycles was 52 °C.

The PCR products were detected and purified as described in section 2.2.3.

3.2.3 Digestion of DNA with restriction enzymes

Both the plasmid, pET21d (+), and the purified PCR products were digested as previously described in section 2.2.5.

3.2.4 Ligation

The ligations were set up as described in section 2.2.6.

3.2.5 Transformation

All transformations were carried out as described in section 2.2.9.

3.2.6 Plasmid minipreps

All plasmid minipreps, including the plasmids that were to be used for DNA sequencing, were carried out using the QIAprep spin miniprep kit (Qiagen Ltd) as described in section 2.2.10.1.

3.2.7 Expression of the *Enc*MurA-His protein

Expression of the *Enc*MurA-His protein was carried out in *E. coli* BL21 (DE3) competent cells. Two overnight cultures of 5 mL 2 x YT medium containing 100 µg/mL of ampicillin were used to inoculate two 500 mL cultures of 2 x YTAmp, which were then grown at 37 °C. Once the OD_{600} of the cells was 0.8, IPTG to a final concentration of 0.1 mM was added. After a period of 4 hours at 37 °C, the cells were harvested by centrifugation (as described in 2.2.13) and stored at -20 °C. The extent of expression was analysed by 10 % SDS-PAGE (see section 2.2.12).

3.2.8 Purification of *Enc*MurA-His

All purification steps were carried out at 4 °C. The cell pellet was resuspended in 14 mL of lysis buffer (50 mM Tris, 300 mM NaCl, 10 mM imidazole, 0.1 mM DTT, pH 8.0). To this, 1 mg/mL of lysozyme was added and the solution incubated for 30 minutes. The mixture was sonicated 3 times, for a period of 60 seconds each time. The lysate was centrifuged for 30 minutes at 10,000 *g* and the supernatant removed. The pellet was resuspended in lysis buffer and samples of both the membrane and cytoplasmic fractions were subjected to 10 % SDS-PAGE to determine the solubility of the target protein.

A total of 4 mL of Ni-NTA agarose (Qiagen Ltd) was equilibrated with 5 bed volumes of lysis buffer. The resulting supernatant was slowly loaded onto the material using gravity flow. The column was washed with a further 5 bed volumes of lysis buffer to remove non-binding proteins. Wash buffer containing 20 mM imidazole was used to wash the column (2.5 bed volumes). A further 5 bed volumes of elution buffer containing 100 mM imidazole was used to elute the remaining proteins. The fractions which contained pure *Enc*MurA-His, as judged by SDS-PAGE, were pooled (30 mL) and subjected to dialysis in buffer A (50 mM Tris, 2 mM DTT, 1 mM EDTA, pH 7.0). The protein was subsequently concentrated to approximately 10 mg/mL using centripreps (Millipore) with a 30 kDa cut off limit. Protein concentration was determined using Bradford reagent (see section 2.2.24).

3.2.9 Western blotting and immunodetection using an anti-His antibody

At least 0.1 to 0.5 μg of protein was subjected to SDS-PAGE and subsequently transferred to a nitrocellulose membrane as was previously described in section 2.2.20. The membrane was stained with Ponceau Red and the position of the marker bands highlighted, before destaining.

Immunodetection using the murine anti-His antibody and the chemiluminescent detection system was carried out as described in section 2.2.21.2.

3.2.10 Activity assays using *Enc*MurA-His

Activity was measured using the Lanzetta colourimetric assay (section 2.2.25). In a total volume of 100 μL, 1 μM of either *Enc*MurA-His or *Enc*MurA (Wanke et al. 1992) was incubated with 1 mM of UDPNAG and 1 mM of PEP in test buffer (50 mM Tris, 1 mM DTT, pH 7.4) at 25 °C. Samples of 5 μL were taken at various intervals over a period of 20 minutes. Test buffer was added to increase the sample volume to 100 μL and 800 μL of Lanzetta reagent was added. After 5 minutes, 100 μL of Na_3citrate was added and 30 to 60 minutes later the OD_{660} was measured. These values were plotted versus time (seconds) and the activity (k_{cat} (s^{-1})) calculated via linear regression.

3.3 Results

3.3.1 Cloning of *EncmurA* gene into pET21d (+)

The *murA* gene (1260 bp) from the pKK*EncmurA* (Wanke et al. 1992) vector was amplified using PCR (figure 3.1) in order to obtain a gene that had a NcoI restriction site at the start codon and at the 3' end, no stop codon and a XhoI restriction site.

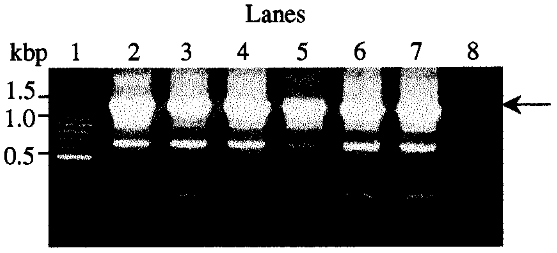

Figure 3.1: A 1 % agarose gel depicting the *EncmurA* PCR product (ca. 1300 bp) that was amplified from pKK*EncmurA*. Lane 1: 100 bp DNA ladder (Promega), lanes 2 to 4: 0.3 µg of template DNA and 1.5, 2.0 and 2.5 mM $MgSO_4$ respectively, lanes 5 to 7: 0.75 µg of template DNA and 1.5, 2.0 and 2.5 mM $MgSO_4$ respectively, lane 8: no Pwo DNA polymerase. A 15 µL aliquot of the PCR was loaded onto the gel. The annealing temperature was 52 °C.

A PCR product of ca. 1300 bp was produced under all of the conditions used, although a number of non-specific bands were also produced. The gene was cloned into the pET21d (+) vector to give pET*EncmurA-his* as described in sections 3.2.3 to 3.2.6, and the identity of the insertion was confirmed by internal digestion of the gene with restriction enzymes.

3.3.2 Expression of *Enc*MurA-His

The *Enc*MurA-His protein was expressed in *E. coli* BL21 (DE3) cells as shown in figure 3.2. In comparison to expression of the pET21d (+) vector alone in BL21 (DE3) cells, a band is clearly visible at around 44 kDa in the cells containing pET*EncmurA-his* after a period of 4 hours (Figure 3.2A, lane 5). This was assumed to be the *Enc*MurA-His protein.

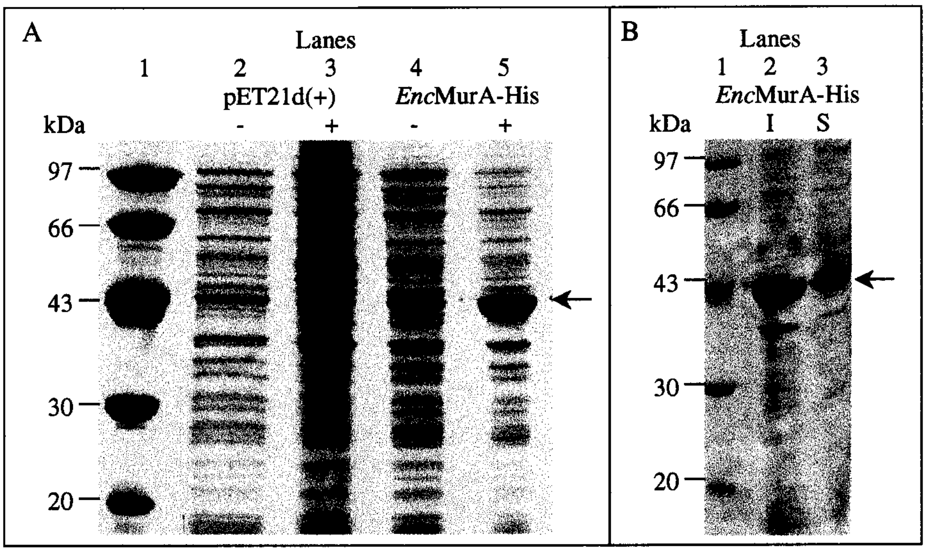

Figure 3.2: Expression and solubility of *Enc*MurA-His protein as analysed by 10 % SDS-PAGE. Panel A: Expression of *Enc*MurA-His at 37 °C. Lane 1: LMW marker (Pharmacia), lanes 2 and 3: uninduced (-) and induced (+) pET21d, lanes 4 and 5: uninduced and induced *Enc*MurA-His. The total amount of protein loaded in each lane was 10 to 20 µg. The arrow indicates *Enc*MurA-His. Panel B: Solubility of *Enc*MurA-His. Lane 1: LMW markers as before, lane2: insoluble (I) membrane fraction, lane 3: soluble (S) cytoplasmic fraction. The total amount of protein loaded in lanes 2 and 3 was 10 to 20 µg. The arrow indicates *Enc*MurA-His as before.

The cells were lysed as described in section 3.2.8 and five µL of both the soluble cytoplasmic and the insoluble membrane fraction were subjected to SDS-PAGE. The *Enc*MurA-His demonstrated 40 % solubility (figure 3.2B, lane 3) compared to 60 % of the protein that remained insoluble (figure 3.2B, lane 2). The solubility of the *Enc*MurA-His protein is comparable to that of the untagged *Enc*MurA protein (Wanke et al. 1992).

3.3.3 Purification of *Enc*MurA-His

The supernatant obtained after lysis of two litres of cell culture (figure 5.2B, lane 3) was subjected to Ni-NTA agarose as described in section 3.2.8. *Enc*MurA-His was eluted in the wash stages (20 mM imidazole) and with the higher concentrations of imidazole used (up to 100 mM imidazole) (Figure 3.3A). This suggests that *Enc*MurA-His was only weakly binding to the Ni-NTA agarose. After concentration of *Enc*MurA-His, the protein appeared to be at least 98 % pure (figure 3.3B). A yield of 83 mg per litre of cell culture was obtained.

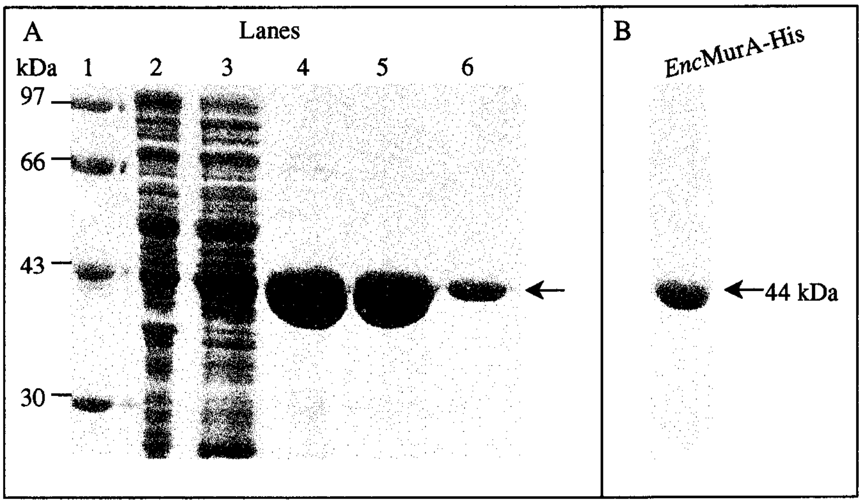

Figure 3.3: Purification of *Enc*MurA-His on Ni-NTA agarose as demonstrated by 10 % SDS-PAGE. Panel A. Lane 1: LMW marker as before, lanes 2 and 3: flowthrough, lanes 4 and 5: wash fractions containing 20 mM imidazole, lane 6: protein eluted by 100 mM imidazole. The arrow indicates the protein. The amount of protein is 2 to 20 µg. Panel B shows the 2 µg of the purified *Enc*Mur-His (indicated by the arrow) after concentration and dialysis.

The identity of the protein was confirmed by N-terminal sequencing. A sequence of the amino acids, MDKFRVQGPT, was obtained and determined to be the same as the sequence present in the NCBI database.

Western blotting using a murine anti-His antibody confirmed the presence of the histidine-tag (Figure 3.4).

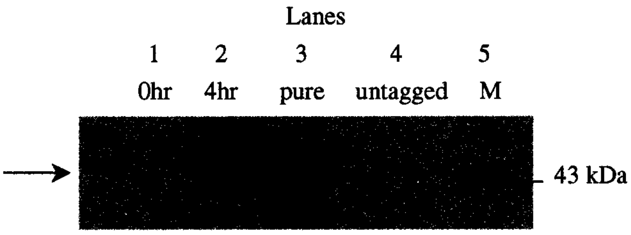

Figure 3.4: Western blotting of *Enc*Mur-His with the murine anti-His antibody. Lane 1: 0 hour (uninduced) sample, lane 2: sample 4 hours after induction, lane 3: 0.2 µg of the purified *Enc*Mur-His, lane 4: 0.2 µg of the purified untagged *Enc*MurA, lane 5: 43 kDa marker band from the LMW markers as before. The arrow indicates *Enc*MurA-His.

The murine anti-His antibody only recognised a band in the sample taken four hours after induction (figure 3.4, lane 2) and the purified *Enc*MurA-His (Figure 3.4, lane 3). No band was detected in the untagged *Enc*MurA sample (figure 3.4, lane 4) as expected. This demonstrates that the protein purified contains the histidine-tag. As the binding of the protein to the Ni-NTA agarose was still relatively weak, i.e the majority of the protein was eluted with 20 mM imidazole, in comparison with the recommended concentrations (100 to 250 mM) in the manufacturer's instructions, perhaps the histidine-tag was not completely available to the material. This partly supports the results obtained from the *Mt*MurA-His enzyme, in that the histidine-tag in this protein appeared to be folded in such a way that the tag was prevented from binding to the material (see section 2.3.6). Alternatively, there may have been too much *Enc*MurA-His loaded onto the column and there was a subsequent lack of binding sites for the histidine-tag. No further investigation into this factor was carried out as it was determined not to be necessary for the purpose of this study.

3.3.4 Determination of *Enc*MurA-His enzyme activity

The colourimetric Lanzetta assay was used as described in section 3.2.10, to determine the activity of the *Enc*MurA-His in comparison with the untagged *Enc*MurA enzyme. The assay was carried out using 1 μM of either of the enzymes and 1 mM of UDPNAG and 1 mM of PEP as described in section 3.2.10. The levels of enzyme activity as determined by the measurement of A_{660} over time demonstrate a difference (ca. 20 %) in the final absorbance obtained between the untagged and the tagged enzyme (Figure 3.5).

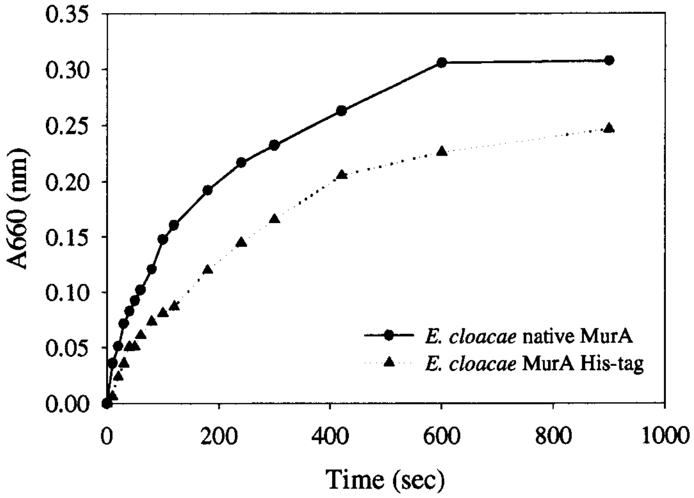

Figure 3.5: Line graph demonstrating the activity of *Enc*Mur-His compared to *Enc*MurA. The measured A_{660} was plotted against Time (sec). ● indicates untagged *Enc*MurA. ▲ indicates *Enc*MurA-His. The initial slope was used for linear regression.

The k_{cat} (s^{-1}) of the untagged *Enc*MurA was determined to be 1 s^{-1} whereas the k_{cat} of *Enc*MurA-His was 0.6 s^{-1}. This means that the *Enc*MurA-His has only 60 % of the activity of the untagged protein. Therefore, the presence of the His-tag appears to have a slight effect on the activity of the *Enc*MurA enzyme.

4. A study of the conformational changes of *Enterobacter cloacae* MurA

4.1 Materials

4.1.1 Chemicals and enzymes

All chemicals and enzymes were as described in section 2.1.1.

4.1.2 Bacterial strains

E. coli DH5α and *E. coli* JM105 competent cells were used. For further details see section 2.1.2.

4.1.3 Vectors

The vector pKK233-2 was used in the original cloning of the *murA* gene (Wanke et al. 1992). Further information on the plasmid can be found in section 2.1.3.

4.2 Methods

4.2.1 Expression and purification of *En.cloacae* MurA and K22 mutants

Wild type MurA from *Enterobacter cloacae* and MurA containing the K22V, K22R or K22E mutation were expressed and purified as described previously (Wanke et al. 1992, Samland et al. 1999). The protein concentration was determined using an extinction coefficient of 24 020 M^{-1} cm^{-1} at 280 nm.

4.2.2 MALDI-TOF analysis of wild type MurA and the K22 mutant proteins

The wild type, K22V, K22R and K22E MurA's (100 μM of each) were incubated for 50 minutes at 25 °C in 50 mM Tris pH 7.4 under each of the following conditions: (i) no substrates, (ii) 10 mM fosfomycin alone, (iii) 10 mM fosfomycin and 1 mM UDPNAG and (iv) 1 mM fosfomycin and 10 mM UDPNAG. Trypsin (0.5 mg/mL) was added to the reactions, followed by incubation at 25 °C for 16 hours. Removal of excess substrates was achieved by desalting the reactions using pre-equilibrated Sep-Pak C18 columns (Waters) as previously described (Samland et al. 2001a). MALDI-TOF spectra were recorded with a Voyager Elite mass spectrometer using the reflectron mode for increased mass accuracy and interpretation of the spectra was based on the analysis reported by Krekel et al. (1999).

4.2.3 Isothermal titration calorimetry (ITC)

All measurements were carried out in 50 mM HEPES/NaOH pH 7.4, containing 2 mM DTT and 0.5 mM EDTA using a MCS-isothermal titration microcalorimeter from Microcal Inc. Sample preparation and titrations were performed as described previously (Samland et al. 1999). K22V MurA (200 to 220 μM) was titrated with 5 mM UDPNAG at the following temperatures: 10, 15, 20, 25 and 30 °C. Dissociation constants, heats of binding and the stoichiometries were determined by fitting the binding isotherm according to the binding equations within Origin, version 2.9, Microcal Inc.

4.3 Results

4.3.1 Purification of wild type and K22 mutant proteins

The expression and purification of the wild type and the K22 mutant MurA proteins were the same as previously described (Wanke et al. 1992, Samland et al. 1999). The stages of purification of the K22V mutant protein are shown in figure 4.1.

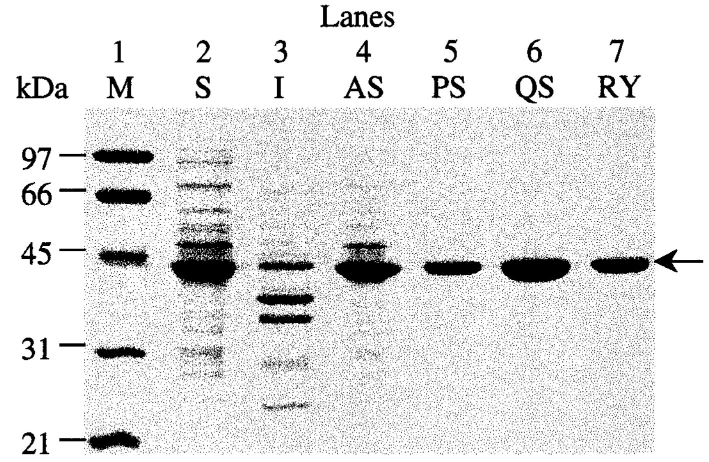

Figure 4.1: Purification of K22VMurA. Lane 1: BioRad low molecular mass markers (M) (masses indicated in kDa), lane 2: soluble cytoplasmic fraction (S) used for purification, lane 3: insoluble membrane fraction (I), lane 4: protein sample after 50 % ammonium sulphate saturation, lane 5: pooled sample after Phenyl Sepharose (PS) chromatography, lane 6: pooled sample after Q-Sepharose (QS) chromatography, lane 7: pooled K22V after Reactive Yellow (RY) chromatography. In lanes 4 to 7, 2 μg of protein was loaded. The arrow indicates the K22V protein (44 kDa).

After four purification steps the protein was deemed to be of ca. 98 to 99 % purity (figure 4.1, lane 7). The yield of protein obtained from 20 g of cell paste was 160 mg of protein. This was a vastly reduced amount compared to the amount of protein obtained from the wild type cells as only 40 % of the K22V mutant protein appeared to bind to the reactive yellow material (Samland et al. 1999).

4.3.2 Tryptic digestion and MALDI-TOF analysis of wild type and K22 mutant proteins

In order to determine whether fosfomycin can form the covalent adduct in the K22 mutant proteins, the wild type, K22R, K22V and K22E MurA proteins were subjected to a tryptic digest and the resulting peptides analysed by MALDI-TOF mass spectrometry (see section 4.2.2). Prior to the addition of trypsin, the enzymes were incubated with the following: (i) no UDPNAG or fosfomycin, (ii) 10 mM fosfomycin, (iii) 1 mM UDPNAG and 10 mM fosfomycin and (iv) 10 mM UDPNAG and 1 mM fosfomycin. The results for wild type MurA and K22V are shown in figure 4.2. In the absence of UDPNAG or fosfomycin, the wild type MurA and K22V both show a peak at 1616 m/z (panels A and B), that is attributed to the peptide fragment 104 to 120 and includes the C115 residue that is involved in fosfomycin binding. In the presence of only 10 mM fosfomycin, a peak of 1754 m/z is formed in the wild type sample (panel C) as a result of fosfomycin covalently binding to the cysteine residue. The mass difference between the peaks 1616 m/z and 1754 m/z is 138 mass units and corresponds to the molecular mass of fosfomycin. In this case, the 1616 m/z peak is no longer visible. However, the K22V protein in the presence of 10 mM fosfomycin does not appear to form the covalent adduct as the 1616 m/z peak is the only peak that is observed (panel D). The presence of 10 mM fosfomycin together with 1 mM UDPNAG in the wild type results in the formation of this adduct as shown in panel E by the presence of the 1754 m/z peak. The same is true for wild type MurA in the presence of 1 mM fosfomycin and 10 mM UDPNAG as shown in panel G. Interestingly, the K22V protein under these conditions also shows the formation of the fosfomycin adduct, as shown in panels F and H by the presence of the 1754 m/z peak. This suggests that the formation of the fosfomycin adduct is only possible when UDPNAG is present and therefore the conformational change has occurred. Previous analysis of the K22V MurA using isothermal titration calorimetry (ITC), indicated that the protein was not able to bind fosfomycin due to the absence of the conformational change in this mutant (Samland et al. 1999). These results are contradictory but may reflect the differences within the methods, i.e. the use of ITC is dependent on the release of heat by the binding, whereas the use of MALDI-TOF mass spectrometry reflects the events that occur within the proteins.

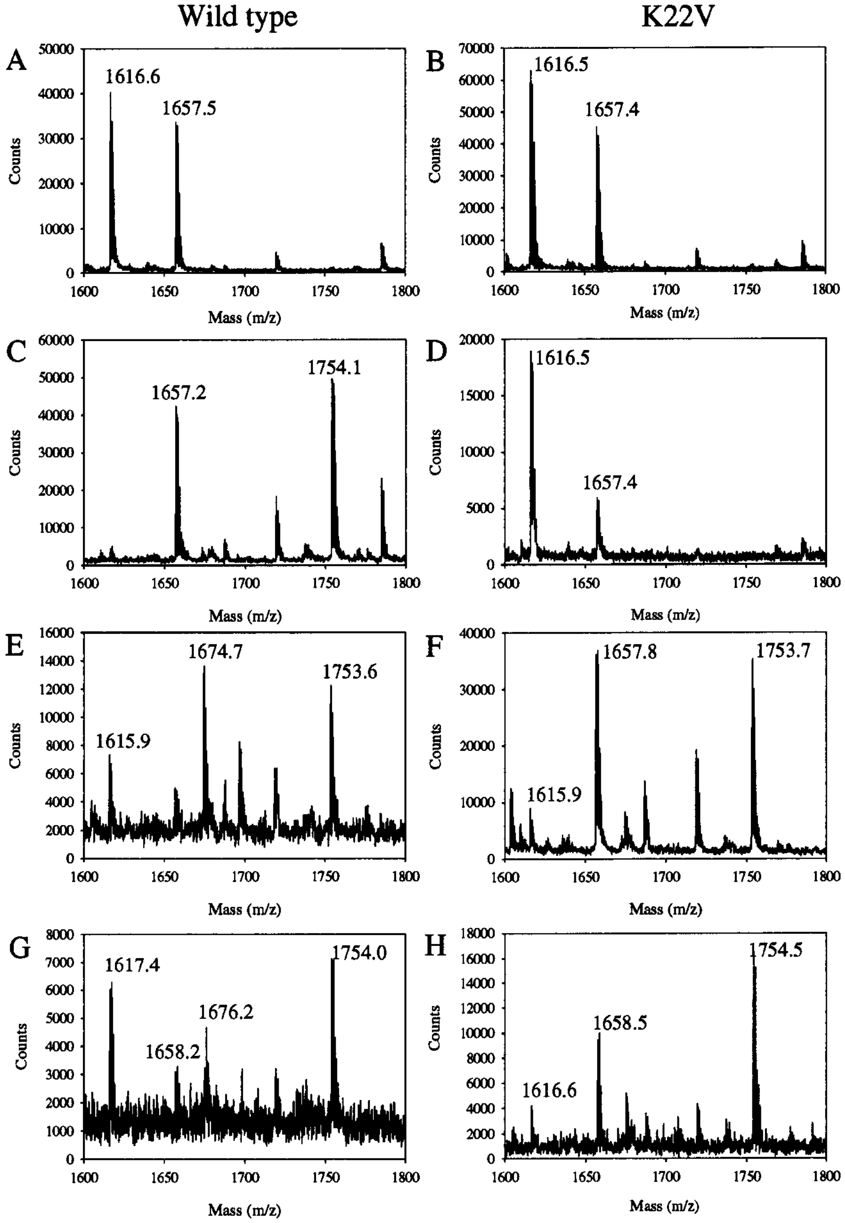

Figure 4.2: Comparison of the MALDI-TOF spectra obtained under the different incubation conditions. Spectra are only shown in the range 1600 to 1800 m/z. Wild type is shown on the left hand panels and the K22V mutant protein is shown on the right hand panels. Panels A and B: wild type and K22V MurA, respectively, incubated with neither UDPNAG or fosfomycin, panels C and D: wild type and K22V, respectively, incubated with 10 mM fosfomycin, panels E and F: wild type and K22V, respectively, incubated with 1 mM UDPNAG and 10 mM fosfomycin, panels G and H: wild type and K22V, respectively, incubated with 10 mM UDPNAG and 1 mM fosfomycin. The mass peak of 1616 m/z is converted to 1754 m/z on binding of fosfomycin and comprises the amino acids 104 to 120 of the MurA sequence. In panels E and G, a peak of 1674 m/z is observed while in the remaining panels a peak of 1657 m/z is observed. This peak is thought to comprise the amino acids 295 to 310.

The K22R mutant shows a profile similar to that of the wild type MurA in that the fosfomycin adduct can form under all experimental conditions used (figure 4.3). The K22E mutant on the other hand, can not form the fosfomycin adduct under any of the experimental conditions (figure 4.3). These results are explained by the charges that are attached to the side chains. The K22R mutant retains the positive charge that the lysine has and so the change to the enzyme should be minimal, the K22E mutant on the other hand, introduces a negative charge to the protein resulting in the repulsion of the negatively charged fosfomycin from the active site.

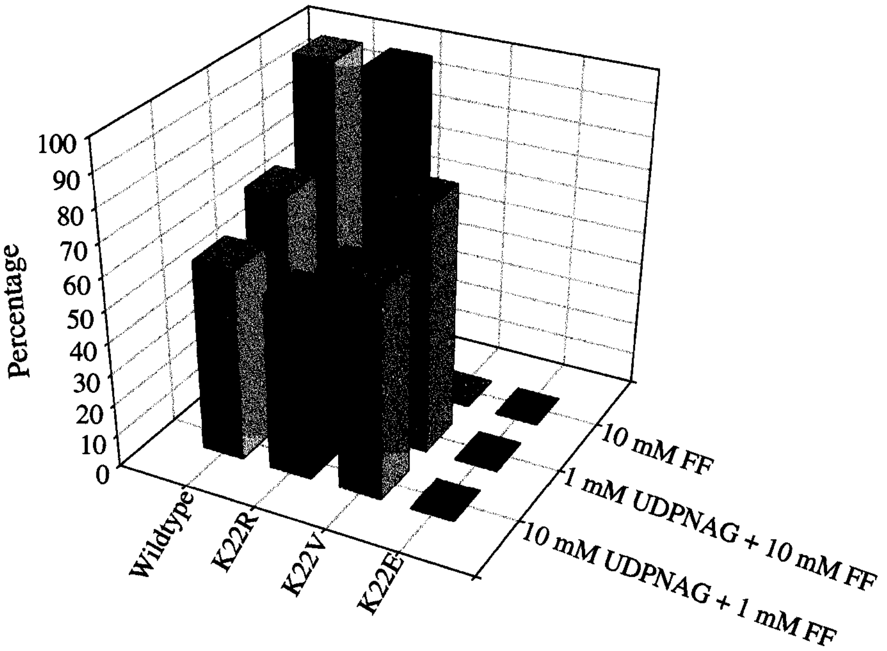

Figure 4.3:Formation of the covalent adduct for the wild type and K22 mutant proteins in the presence of 10 mM fosfomycin, 10 mM fosfomycin and 1 mM UDPNAG or 1 mM fosfomycin and 10 mM UDPNAG. The formation is shown as a percentage.

Interestingly, it was observed that the formation of the fosfomycin adduct is less than 100 % in the presence of UDPNAG (figure 4.3). On the other hand, formation of this adduct is 100 % in the absence of UDPNAG (figure 4.3). These results were consistently obtained in repeated experiments. As MALDI-TOF mass spectrometry is not a quantitative method these results can not be interpreted as suggesting that the presence of UDPNAG inhibits the formation of this adduct with fosfomycin.

4.3.3 Isothermal titration calorimetry of K22V MurA

By measuring the change in heat capacity of the *En. cloacae* MurA it was shown that a conformational change occurs upon the binding of UDPNAG to MurA (Samland et al. 2001b). To investigate the binding of UDPNAG to K22V at different temperatures and subsequently determine the heat capacity (ΔC_P), isothermal titration calorimetry (ITC) was employed. The binding of UDPNAG to K22V MurA was measured at 10, 15, 20, 25 and 30 °C. An example of such a titration is shown in figure 4.4. The top panel of this figure shows the raw calorimetric data. The peaks are negative indicating that the reaction occurs exothermically as with the wild type MurA (Samland et al. 2001b). The magnitude of the heat produced per injection was determined by integration of the area under the individual peaks. The area decreased in response to a reduced number of available binding sites. The bottom panel shows the amount of heat generated per injection plotted as a function of the molar ratio. From this, the change in enthalpy (ΔH), the change in entropy (ΔS) and the free energy (ΔG) of the reaction can be determined.

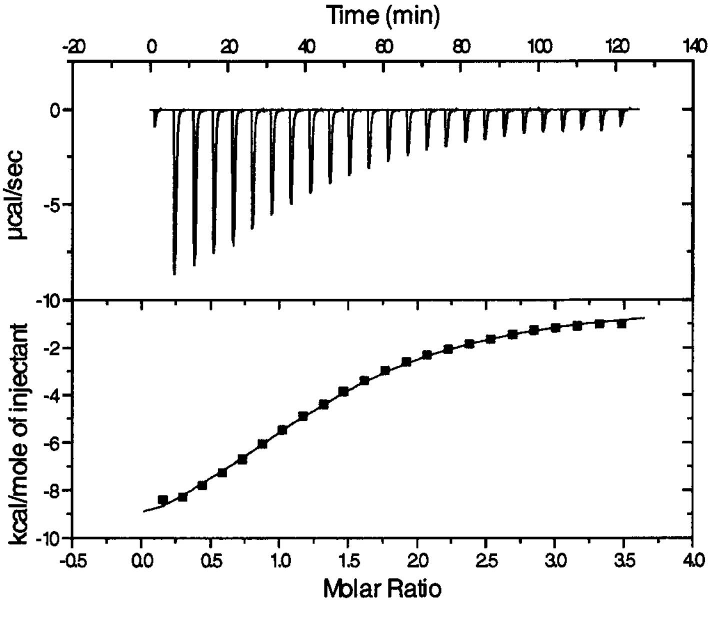

Figure 4.4: Titration data for K22V (200 to 220 µM) titrated with 5 mM UDPNAG at 25 °C. Top panel shows the raw data. Bottom panel shows the best-fit curve of the integrations. Produced using the program Microcal origin v. 2.9, which calculates the data in calories (cal).

These values were plotted against the temperature (K) (figure 4.5, table 4.1). From the graph, it is clear that the ΔG remains constant over the temperature range measured. The ΔH decreases as the temperature increases, i.e. the reaction becomes more favourable, whereas the TΔS increases as the temperature increases. This suggests that the ΔG is kept stable over the temperature range by altering the enthalpy and entropy effects, i.e. a large entropy-enthalpy compensation occurs. This was also shown to be the case for the wild type MurA (Samland et al. 2001b). The K_D of K22V MurA is also affected by temperature as shown in table 4.1. The K_D is increased as the temperature increases indicating that the binding of UDPNAG to K22V is tighter at lower temperatures.

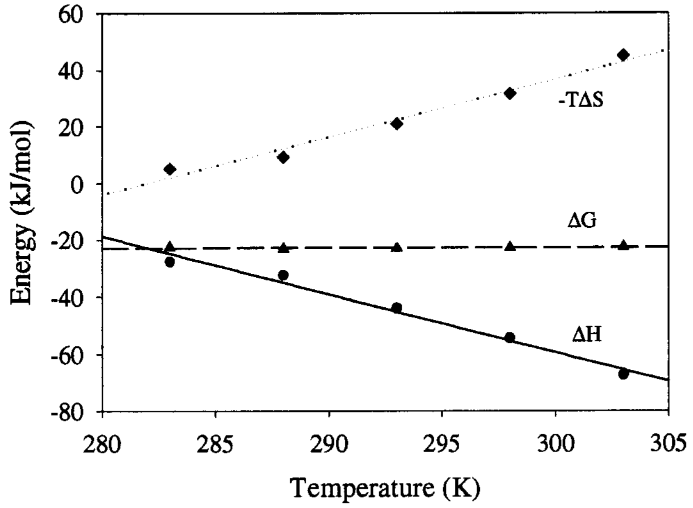

Figure 4.5: Temperature dependence of the binding of UDPNAG to K22V MurA on ΔH, ΔG and -TΔS values. The values are averages of duplicate experiments. Energy (kJ/mol) is plotted against temperature (K). K22V MurA (200 to 220 μM) was titrated with 5 mM UDPNAG.

The calculated values are shown in Table 4.1 in comparison with the ΔH values obtained in a similar experiment by Samland et al. (2001b).

The ΔH values obtained for wild type MurA and K22V MurA are very similar. From the slope of the ΔH line in figure 4.5, the ΔC_p (change in heat capacity) can be calculated. The ΔC_p for wild type MurA was determined to be -1.87 kJ mol^{-1} K^{-1} whereas the ΔC_p for K22V MurA was calculated to be -2.01 kJ mol^{-1} K^{-1} (Table 4.1). There is a difference between these of only 0.16 kJ mol^{-1} K^{-1} and this is not thought to be a significant difference. This difference may be due to the presence of the K22V residue, which may affect the accessible surface area. The lack of a difference between the ΔC_p for the wild type MurA and the K22V MurA indicates that the conformational change occurs even in the mutant. The ΔC_p calculated from the accessible surface areas in the open and closed conformations is -1.3 kJ mol^{-1} K^{-1}. This is significantly smaller than the experimentally determined heat capacities for this process in wild type and

K22V enzymes. This was thought to demonstrate that the change in buried surface area upon UDPNAG binding is not the only process responsible for the observed ΔC_p (Samland et al. 2001b).

	MurA + UDPNAG[a]	K22V MurA + UDPNAG			
T (°C)	ΔH	ΔH	ΔG	TΔS	K_D (μM)
10	nd	-27.66	-22.53	-5.13	68.5
15	-35.5	-32.41	-23.11	-9.31	64.3
20	-46.8	-43.98	-22.95	-21.03	80.5
25	-52.8	-54.41	-22.78	-31.63	96.5
30	-64.6	-67.51	-22.51	-45.00	131.5
ΔC_p	-1.87	-2.03			

Table 4.1: The effect of temperature on the thermodynamic parameters of K22V MurA. [a] values are taken from Samland et al. (2001b). Values are from duplicate experiments. ΔC_p was calculated from the slope of the regression of ΔH versus temperature. All values except ΔC_p and K_D are in kJ mol^{-1}. ΔC_p is in kJ mol^{-1} K^{-1} and K_D is in μM. The calculated ΔC_p from the structure is -1.3 kJ mol^{-1} K^{-1}. ΔG was calculated from $\Delta G = -RT \ln K_D$. The errors are estimated to be ± 1 % for ΔG, ± 3 % for ΔH, ± 9 % for ΔS and ± 15 % for ΔC_p.

5. Discussion

5.1 The naturally occurring variants of MurA

Although MurA from *Chlamydia trachomatis* and *Borrelia burgdorferi* could not be obtained as a purified preparation, due in part to problems encountered during cloning and the inability to express the protein in a bacterial expression system, MurA from *Mycobacterium tuberculosis* was obtained with ca. 98 % purity (figure 2.3.4). *Mt*MurA was expressed in two forms, a native and a C-terminally histidine-tagged form. However, only the native form was used for subsequent characterisation as the histidine-tagged *Mt*MurA appeared to be misfolded and therefore, was not amenable to purification. In order to determine whether or not this misfolding was common to other MurA proteins, the MurA from *Enterobacter cloacae* was also cloned as a C-terminal histidine-tagged protein. This protein was successfully purified with a yield of 83 mg per litre of cell culture and a purity of ca. 99% as judged by SDS-PAGE (figure 3.3). Although purification of the protein was possible, binding of the histidine-tag to the Ni-NTA agarose was still relatively weak and may reflect the partial inaccessibility of the histidine-tag. This effect is more pronounced for *Mt*MurA-His, rendering the histidine-tag completely unavailable for binding to the resin. The one-step purification of *Enc*MurA is accompanied by a 40 % reduction in enzyme activity (table 3.1). It is possible that the histidine-tag affects the binding of UDPNAG and/or PEP. If this were the case, the K_M values for UDPNAG and PEP in the *Enc*Mur-His enzyme would be expected to be higher than in the untagged *Enc*MurA enzyme. This loss of activity is one of the potential problems associated with the attachment of any tags, e.g. GST, His-tag, T7-tags, to enzymes. Hence, it is desirable to purify the protein in its native form, even though the purification procedure may be tedious, or one must alternatively cleave off the tag using proteases. A decrease in activity to the extent observed in this study is often construed as showing the same activity as the wild type (Halliwell et al. 2001). Expression of the histidine-tagged proteins as both active and inactive forms may occur in the same batch of purified protein resulting in misleading activity values (Halliwell et al. 2001). Other problems that have been associated with the use of histidine-tags include the interference of the tag in the assembly of enzyme complexes (Tang and Chitnis 2000) and the dimerization of histidine-tagged proteins (Wu and Filutowicz

1999). Hence, the use of the native protein is preferable to a tagged protein in order to obtain accurate kinetic data.

The purification of *Mt*MurA resulted in a low yield of protein (10 to 15 mg per 20 g wet cell paste). Unfortunately, this meant that we could not utilise techniques such as isothermal titration calorimetry (ITC) in order to measure K_D or K_M values. K_D values can be measured directly using ITC, whereas the determination of K_M values requires several measurements using different substrate concentrations. The main problem was that the majority of the protein remained in the insoluble fraction. Isolation of the insoluble protein was not attempted, as the protein may not have been able to return to the correctly folded state. Recently, a new expression system was established specifically to increase the soluble expression of insoluble proteins (Hoang et al. 1999). It utilises a low copy plasmid that contains all of the features of the pET vectors (Hoang et al. 1999). One could attempt to clone *Mt*MurA and express it in this vector in an attempt to increase the solubility and therefore, increase the yield of purified protein obtained. Additionally, the BIAcore system could be utilised as it only requires nmol amounts of protein and can be used to measure K_M or K_D values (Deinum et al. 2002). As the histidine-tagged *Mt*MurA is not suitable for this application, chemical coupling of the untagged enzyme to a sensor chip may be possible.

The following discussion will first focus on the kinetic comparison between *Mt*MurA and *Enc*MurA, followed by a comparison of *Mt*MurA and D117CMurA and finally a comparison of D117CMurA and *Enc*MurA.

The specific activity of *Mt*MurA is substantially reduced compared to that of *Enc*MurA, i.e. 2 x 10^4-fold lower than that of *Enc*MurA. Although there is only 40 % identity between the amino acid sequences of *Mt*MurA and *Enc*MurA, it is possible that the presence of the aspartate residue in *Mt*MurA may be an important factor in this reduced rate of catalysis. Another enzyme involved in peptidoglycan biosynthesis, alanine racemase, has also been characterised from *Mycobacterium tuberculosis* and was shown to have a 10-fold reduction in its specific activity compared to its counterpart in *E. coli* (Strych et al. 2001). It has been demonstrated that the growth rate of the organism is correlated with peptidoglycan turnover, i.e. synthesis and degradation (Cheung et al. 1983). This reduction in specific activity may therefore be related to the slow growth rate of mycobacteria, i.e. *Mycobacterium tuberculosis* divides once every 24 hours (Cole et al. 1998). Interestingly, other pathogens that contain the aspartate to cysteine mutation also have a long generation time, for example *Borrelia burgdorferi* divides once every six to twelve hours (Barbour and Hayes 1986). Perhaps the requirement for a high rate of peptidoglycan biosynthesis is diminished in these pathogenic bacteria. However, the presence of this aspartate residue in the MurA of *Mycobacterium smegmatis*, which divides once every three to four hours, suggests that there may be an alternative reason for the reduced rate of catalysis. Analysis of MurA from *Mycobacterium smegmatis* may therefore, provide further information with regard to this enzyme. Kim et al. (1996a) also saw a six-fold reduction in the catalytic activity, at pH 8.0, of the *E. coli* C115D mutant protein compared to that of the *E. coli* wild type protein. However, as the extent of this reduction is more pronounced for *Mt*MurA, it suggests the involvement of other factors.

The K_M values for both substrates were determined in *Mt*MurA to be 40 and 4.5 µM for UDPNAG and PEP, respectively (table 2.3.2). These are similar to the K_M values that have been determined for *Enc*MurA (70 and 7.5 µM for UDPNAG and PEP, respectively) (Samland 2001). The *Mycobacterium tuberculosis* alanine racemase also showed similar K_M values to those of its *E. coli* counterpart (Strych et al. 2001). For UDPNAG, K_M values of 53 µM (Krekel 1998) and K_D values of 51 and 59 µM (Samland et al. 1999, Schönbrunn et al. 1998) have also been determined for *Enc*MurA. As the K_M and K_D values are very similar, they agree with the proposed compulsory order mechanism. The range of values that have been measured for *E. coli* and *En. cloacae* MurA is very large, from 14 to 70 µM for UDPNAG and 0.4 µM to 1 mM for PEP (Marquardt et al. 1992, Kim et al. 1996a, Krekel 1998, Samland 2001), and may reflect differences in the methods used to determine these values (table 2.3.2). As the *Mt*MurA enzyme does not possess the cysteine that is required for the formation of the covalent intermediate, it was thought that the binding of PEP to the enzyme active site would be weaker resulting in a higher K_M value. This was observed in the *E. coli* C115D mutant enzyme, where the K_M of UDPNAG was unaffected by the mutation but the K_M of PEP was increased 100-fold (Kim et al. 1996a). However, this increase in the K_M of PEP is not observed for *Mt*MurA. It suggests that the enzyme has compensated by making other interactions using neighbouring amino acids in order to maintain substrate binding in a suitable range. In the active site of *Mt*MurA, the substrate PEP or the inhibitor fosfomycin are surrounded by invariant residues but on the other side of the active site there are variant residues that may lead to new and favourable interactions in order to maintain an efficiently low K_M for PEP (figure 5.1). The lower specific activity observed in *Mt*MurA and the similar K_M values result in a greatly reduced catalytic efficiency (expressed as k_{cat}/K_M) of *Mt*MurA compared to *Enc*MurA for both substrates, i.e. 1.32 x 10^4- and 1.38 x 10^4-fold for UDPNAG and PEP, respectively (table 2.3.2). The data suggests that the presence of the aspartate in *Mt*MurA or the *E. coli* C115D mutant protein is related to the reduction in catalytic activity of the enzyme. However, as the catalytic power of the *Mt*MurA is further reduced compared to *Enc*MurA, other factors may be involved.

The kinetic parameters of D117CMurA in comparison to *Mt*MurA show that the specific activity of D117CMurA is increased five-fold (table 2.3.2). The K_M values of D117CMurA for UDPNAG and PEP are 7- and 11-fold lower, respectively (table 2.3.2, figure 2.3.12, and figure 2.3.13), indicating that both substrates exhibit tighter binding to D117CMurA than to the *Mt*MurA enzyme. The presence of the cysteine residue in D117CMurA suggests that the *O*-phosphothioketal is formed and therefore, the K_M value for PEP may reflect the tighter binding of this substrate. However, the presence of the cysteine was not thought to have an effect on the binding of UDPNAG, yet the K_M value observed is 7-fold lower. In *E. coli* MurA, the cysteine itself does not react with UDPNAG (Skarzynski et al. 1996). Coupled with new and favourable interactions in the active site for UDPNAG, it is possible that the presence of the *O*-phosphothioketal may further contribute to UDPNAG binding resulting in an even lower K_M. The lowered K_M values observed rationalises the higher catalytic efficiency of D117CMurA compared to *Mt*MurA, i.e. 38- and 60-fold higher for UDPNAG and PEP, respectively (table 2.3.2). Interestingly, the *E. coli* C115D MurA mutant protein showed a 20-fold reduction in the catalytic efficiency for PEP and a two-fold increase in the catalytic efficiency of UDPNAG (Kim et al. 1996a). This suggests that it is not the invariant residues that contribute to this effect but other variant residues in and around the active site of *Mt*MurA.

A comparison of the kinetic parameters of D117CMurA with those of *Enc*MurA show that the specific activity of the D117CMurA is 4 x 10^3-fold lower than that of *Enc*MurA. The catalytic efficiency of the D117CMurA is also reduced compared to that of *Enc*MurA, i.e. 344- and 229-fold for UDPNAG and PEP, respectively (table 2.3.2). However, this reduction is less pronounced than that observed with *Mt*MurA as a result of the different K_M values. The results obtained by Kim et al. (1996a) for the *E. coli*

C115D mutant protein imply that the formation of the covalently bound enzyme intermediate is important for catalysis. Yet the presence of a cysteine residue and therefore, a covalently bound intermediate, is not sufficient for D117CMurA to attain full catalytic power.

Why is the catalytic activity of *Mt*MurA dramatically reduced, when the K_M values are the same as those of *Enc*MurA for both substrates? By examining the structure of *E. coli* MurA complexed with UDPNAG and fosfomycin and identifying the position of invariant residues, an explanation for the decreased catalytic activity and the similar K_M values can be proposed (figure 5.1) (Skarzynski et al. 1996).

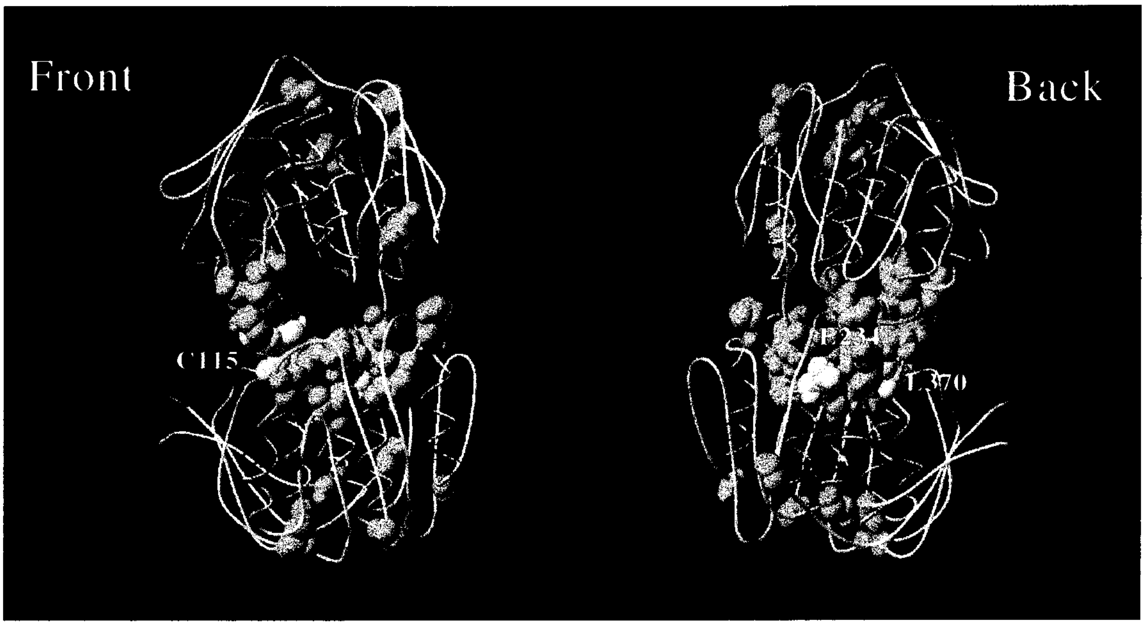

Figure 5.1: Distribution of invariant amino acid residues in MurA's. The structure shown is that of the *E. coli* MurA (PDB coordinates 1UAE) complexed with UDPNAG and the inhibitor fosfomycin. Alpha helices, beta-strands and loops are shown in red, yellow and gray respectively. UDPNAG and the covalent inhibitor fosfomycin are shown in blue and orange, respectively. Invariant amino acid residues are shown in green and those that differ only in mycobacteria (*M. chelonae*, *M. smegmatis* and *M. tuberculosis*) are shown in magenta (C115D, E234V, L370I; numbering of *E. coli* sequence).

The active site of MurA consists of well-conserved residues (represented by green spheres). As shown in figure 5.1, only five amino acids are invariant in each of the upper and lower domains (G14, L34, G133, N184, G202, G217, G270, G319, L360, and G410). The mycobacterial MurA's carry three amino acid changes that are C115D, E234V and L370I (figure 5.1). The exchange of the leucine in position 370 to an isoleucine is a minor exchange that would have little effect on the interactions within the protein. The overall catalytic power of the enzyme is not achieved by the mutation of the aspartate to the cysteine residue as shown by the five-fold increase in the specific activity of D117CMurA compared to *Mt*MurA (table 2.3.2). This suggests that there are non-conserved amino acid residues that are directly or indirectly involved in the reaction mechanism or in the maintenance of a favourable structure. It is conceivable that the glutamate 234 may play a role in the active site even though it is not directly located in the vicinity of the substrates (figure 5.1). In the closed structure of *E. coli* MurA, the carboxyl side chain of Glu234 interacts with the ε-amino group of Lys405 (Skarzynski et al. 1996). In this position, arginine or histidine residues are also found. This interaction may have a structural role and may also be important in the dynamic properties of the enzyme, i.e. conformational change. In *Mt*MurA, the Glu234 is replaced by a valine and the Lys405 is replaced by an asparagine, therefore an interaction is not feasible between these residues. Additionally, background interactions between variant amino acids may impede the dissociation of UDPNAG or PEP, or moreover the products, from the active site accounting for the difference in catalysis between *Mt*MurA and *En. cloacae* MurA. However, in this study it was not possible to measure the K_D values of UDPNAG and PEP due to the limited amount of protein that was obtained. Therefore, there is no conclusive evidence to suggest that the dissociation of substrates or products is slower in *Mt*MurA.

In addition to its role as a nucleophile that directly attacks the C2 of PEP to form the *O*-phosphothioketal, Cys115 was also proposed to act as a general acid. It is thought to protonate the C3 of PEP subsequent to the nucleophilic attack of the 3'-hydroxyl group of UDPNAG on the C2 of PEP (Kim et al. 1996a). This was based on the observation that the activity of the *E. coli* C115D mutant exceeds that of the wild type at lower pH values (Kim et al. 1996a). This reflects the pKa values (3.86) for the carboxyl side chain of aspartate, and therefore, at higher pHs the weakly nucleophilic aspartate becomes deprotonated and can no longer function as a general acid. In MurA, the pKa value for the thiol group of the cysteine residue has on the other hand been determined as 8.3, where greater than 50 % of the cysteines are protonated and therefore can not fulfill their role as a nucleophile in the active site. However, they can act as proton donors. Additionally, the rest of the cysteine residues are deprotonated and are able to act either as nucleophiles or bases (Krekel et al. 2000). This pKa of 8.3 is similar to the physiological pH indicating that the cysteine can easily alternate between a nucleophile and a general acid (Krekel et al. 2000). In this study, *Mt*MurA, which contains the aspartate residue, has a lower activity than the D117CMurA over the pH range measured (figure 2.3.14). *Mt*MurA demonstrates a broad pH optimum of around pH 5.5 to 8.5 and the pH optimum of the D117CMurA enzyme is slightly shifted to an alkaline pH (pH 7.0 to 9.0) (figure 2.3.14). This indicates that both of the enzymes have weak pH dependence and that the function of the aspartate as a general acid in *Mt*MurA has a diminished impact on catalysis. The pH profiles may also represent the unmasking of another residue that is involved in catalysis in *Mt*MurA. Both of these possibilities suggest that the rate-limiting step is different in *Mt*MurA compared to *E. coli* MurA.

Fosfomycin resistance has previously been observed in *Mycobacterium tuberculosis* MurA, however, no detailed biochemical study was carried out in order to determine the mechanistic basis of this resistance (De Smet et al. 1999). The *E. coli* C115D mutant enzyme was shown to bind fosfomycin in a competitive manner with a high K_i (Kim et al. 1996a). In this study, it was shown that fosfomycin binds to *Mt*MurA competitively with respect to PEP (figure 2.3.15). The K_i of fosfomycin inhibition in *Mt*MurA was determined to be in the range of 3.5 to 5.0 mM. Similar values were also determined for the *E. coli* C115D mutant enzyme (1.0 mM at pH 6.0 and 2.0 mM at pH 8.0) (Kim et al. 1996a). In *E. coli* MurA, the K_i of fosfomycin is 8.6 μM in the presence of UDPNAG and in its absence, the K_i is 1.1 mM (Samland 2001). The latter K_i value is similar to that determined in this study for *Mt*MurA, suggesting that in *Mt*MurA there is no formation of the covalent adduct due to the absence of the cysteine residue. Hence, it appears that the fosfomycin is capable of binding in the active site but it can not form a covalent adduct. This is consistent with previous results suggesting that fosfomycin binds in the active site before covalently binding to the cysteine residue (Marquardt et al. 1994). When the aspartate residue is converted to a cysteine residue in the *Mt*MurA enzyme, this confers fosfomycin sensitivity on the enzyme (figure 2.3.16). In the D117CMurA, it is assumed that the presence of the cysteine allows fosfomycin to form a covalent adduct. The data suggests that the *Mt*MurA may have sacrificed catalytic activity in return for fosfomycin resistance.

Other factors that may be involved in the resistance of *Mycobacterium tuberculosis* to fosfomycin include the impermeability of the cell wall. As described previously, *Mycobacterium tuberculosis* has a cell wall that is composed of over 60 % of lipids

(Jarlier and Nikaido 1994). This may be responsible for the slow growth rate of these organisms (Barry and Mdluli 1996) and their pathogenicity (Cole et al. 1998). The cell wall is a highly organised hydrophobic structure that is 1000 times less permeable to hydrophilic molecules than that of *E. coli* (Barry and Mdluli 1996). Although this acts as a formidable barrier to antibiotics, its presence is not sufficient to affect antibiotic resistance which requires a second factor such as mutations in the target proteins or inactivation of the target proteins (Jarlier and Nikaido 1994). To determine whether or not fosfomycin resistance is attributable to the impermeability of the cell wall alone, *Mt*MurA should be replaced with D117CMurA in *Mycobacterium tuberculosis.* If impermeability of the cell wall is a major factor then resistance should still occur. However, if the absence of a cysteine residue in MurA is the major factor in the determination of resistance, then *Mycobacterium tuberculosis* containing D117CMurA should be fosfomycin sensitive.

One of the interesting questions that arises from this study is how do these organisms attain the aspartate residue in place of the cysteine? Did this mutation evolve in response to fosfomycin selection pressure or did it arise from the clinical use of antibiotics? As the clinical use of fosfomycin is limited due to the high rate of resistance observed (Wong and Pompliano 1998), it is unlikely that the mutation arose as a result of the latter. Phylogenetic analysis of 37 MurA sequences indicates that all of the MurA's containing an aspartate residue in place of a cysteine residue have a single common ancestor as shown in figure 5.2. The close relationships shown in figure 5.2 for Actinomycetales, Chlamydiae and Spirochaetes have also been established by phylogenetic analysis of various other proteins (Brown et al. 2001). This implies that the driving force behind the exchange of aspartate to cysteine may have been the acquisition of fosfomycin resistance and therefore an increased fitness of the organism.

As most of the bacteria that have this naturally occurring variant of MurA are intracellular pathogens, the question arises as to how these organisms were first exposed to fosfomycin? The phylogenetic analysis provides some clues. All of the bacteria containing this variant of MurA are pathogenic except *Mycobacterium smegmatis, Streptomyces coelicolor* and *Streptomyces lividans. Mycobacterium smegmatis* is a non-pathogenic organism that is a saprophytic soil dweller (Barry and Mdluli 1996). *Mycobacterium chelonae* is also found in the soil. Therefore, it is possible that the ancestor of mycobacteria inhabited the soil. The producing organisms of fosfomycin are

Streptomyces species that are also found in the soil. Therefore, it is feasible that the mycobacteria were exposed to fosfomycin secreted by *Streptomyces* into the soil. This resulted in the development of a mechanism of resistance to fosfomycin in mycobacteria, i.e. the mutation of the cysteine residue in MurA to an aspartate residue. In figure 5.2, *Streptomyces* species group together with the Chlamydiae and the Spirochetes and it is possible that their ancestor was also a *Streptomyces*-like organism that contained the aspartate residue and this was maintained. This aspartate mutation may have been maintained, as there was no advantage of mutating it to a cysteine as shown by the results obtained in this study with the D117CMurA protein, i.e. the mutation of the aspartate to a cysteine only resulted in a five-fold increase in activity. Interestingly, *Streptomyces coelicolor* and *Streptomyces lividans* are located within the group of MurA's containing the aspartate (figure 5.2), yet they have MurA's that contain a cysteine residue. This suggests that there has been an original mutation from a cysteine residue to an aspartate residue, followed by a subsequent mutation to a cysteine residue. These two species are not known to produce fosfomycin and perhaps the internal mechanism that allows for the inactivation of fosfomycin by phosphorylation (Kobayashi et al. 2000) is absent. The acquisition of an aspartate residue in MurA may have been in order to provide resistance to fosfomycin. However, the advantage of these organisms mutating this aspartate residue to a cysteine is unclear. Alternatively, these *Streptomyces* species may have always had a cysteine residue and they are falsely represented in the phylogenetic analysis. In order to confirm this, an ancient species of *Streptomyces* would have to be identified and its sequence compared to those of other MurA's.

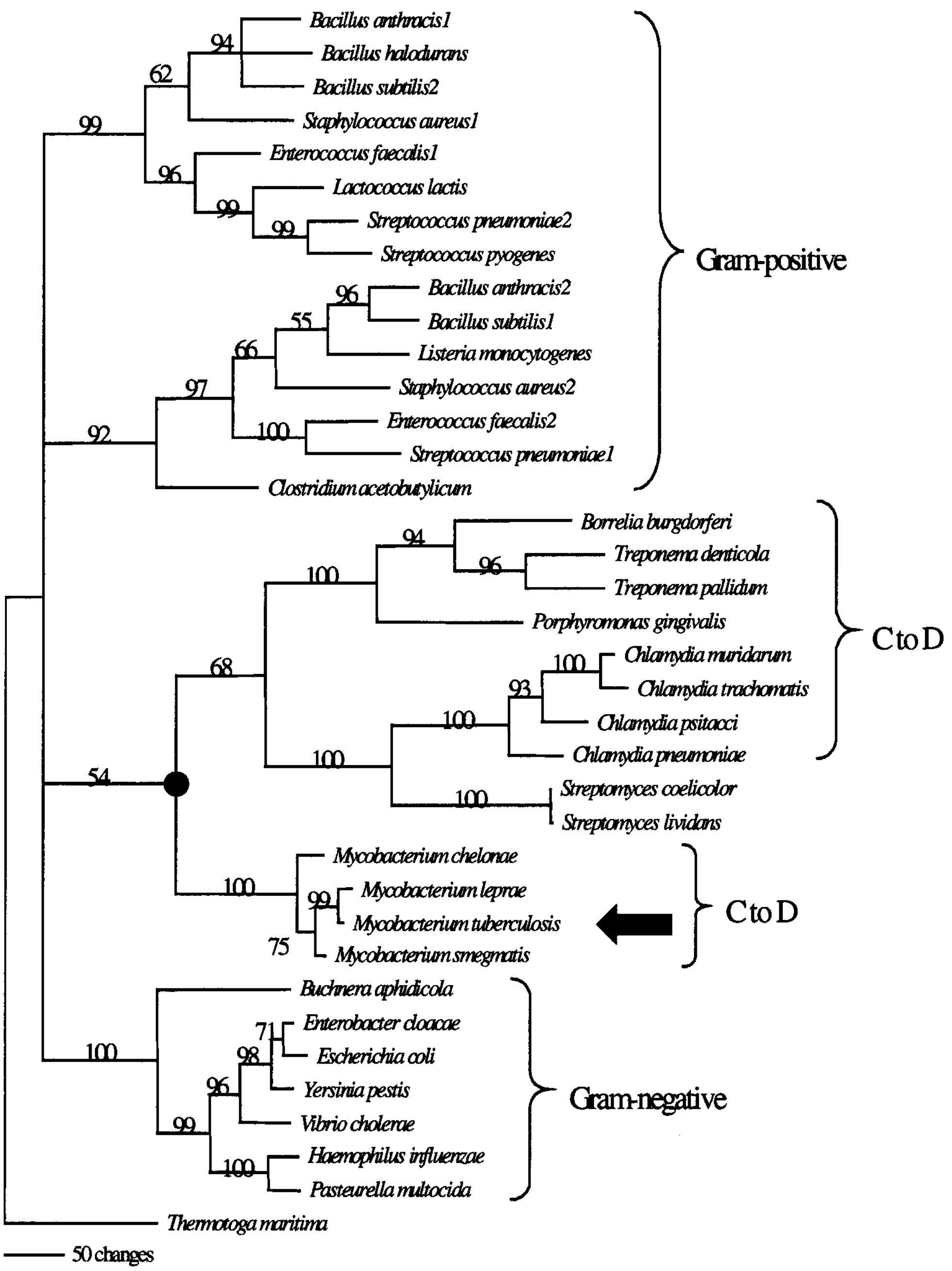
Bacillus anthracis1
94
Bacillus halodurans
62
Bacillus subtilis2
99
Staphylococcus aureus1
Enterococcus faecalis1
96
Lactococcus lactis
99
99
Streptococcus pneumoniae2
Streptococcus pyogenes
Gram-positive
96
Bacillus anthracis2
55
Bacillus subtilis1
66
Listeria monocytogenes
97
Staphylococcus aureus2
92
100
Enterococcus faecalis2
Streptococcus pneumoniae1
Clostridium acetobutylicum
Borrelia burgdorferi
94
Treponema denticola
96
100
Treponema pallidum
Porphyromonas gingivalis
CtoD
100
Chlamydia muridarum
68
93
Chlamydia trachomatis
100
Chlamydia psitacci
100
Chlamydia pneumoniae
54
100
Streptomyces coelicolor
Streptomyces lividans
Mycobacterium chelonae
100
99
Mycobacterium leprae
Mycobacterium tuberculosis
CtoD
75
Mycobacterium smegmatis
Buchnera aphidicola
71
Enterobacter cloacae
100
98
Escherichia coli
96
Yersinia pestis
Gram-negative
99
Vibrio cholerae
100
Haemophilus influenzae
Pasteurella multocida
Thermotoga maritima
50 changes

Figure 5.2: Reconstruction of the phylogenetic relationships among MurA. MurA sequences of 15 Gram positive, 7 Gram negative bacteria and 14 sequences of MurA's that exhibit the cysteine to aspartate exchange were used for alignment with ClustalX and analysed with PAUP* vs. 4beta using parsimony as criterion. The reliability of the emerging tree was evaluated by 1000 bootstrap runs and bootstrap values are shown at the branch points. The sequence of *Thermotoga maritima* MurA was used as an outgroup in order to root the tree with the remainder of the sequences forming the ingroup.

In this study, MurA from *Chlamydia trachomatis*, an aspartate containing MurA, has been cloned, expressed and partially purified. Further purification of the *Ct*MurA is necessary, as presently *Ct*MurA preparations are only ca. 10 to 15 % pure. Gel filtration and hydrophobic chromatography may be useful approaches. So far the activity has not been tested, as the protein sample may contain other enzymes or phosphorylated substrates that could give a false positive result. As was discussed in the introduction, *Ct*MurA and the rest of the peptidoglycan biosynthetic genes are present in the genome of *Chlamydia trachomatis* yet no peptidoglycan has been identified. The presence of a glycanless wall polymer has been suggested (Ghuysen and Goffin 1999). However, if the walls are glycanless, why would the organism contain the full complement of genes for peptidoglycan biosynthesis? Therefore, it will be interesting to see if the enzyme, which contains all of the conserved amino acids, is active. A perhaps more interesting question is whether or not the enzyme is expressed in *C. trachomatis*. One could raise an antibody against the *Ct*MurA enzyme expressed in an *E. coli* expression system and use this to probe *C. trachomatis* cultures at their various stages for expression of MurA. This would give a more precise answer to the current anomaly.

5.2 The conformational changes of MurA

Previous studies have demonstrated that the majority of the conformational change occurs as a result of UDPNAG binding (Schönbrunn et al. 1998, Krekel et al. 1999, Samland et al. 2001b). The amino acid, lysine at position 22 of the *E. coli* MurA sequence was thought to be involved in this conformational change (Samland et al. 1999).

The formation of the covalent adduct between fosfomycin and C115 is detectable using tryptic digestion and MALDI-TOF mass spectrometry analysis (Krekel et al. 1999). The C115 is located in the 1616 m/z peak and on the binding of fosfomycin this peak becomes 1754 m/z in accordance with the addition of 138 mass units which corresponds to fosfomycin (Krekel et al. 1999). This technique was utilised to investigate the formation of the covalent adduct in the K22 mutant proteins (Samland et al. 1999). Incubation of the K22 mutant proteins with fosfomycin in the presence and absence of UDPNAG gave some surprising results (figure 4.2, figure 4.3). The K22R mutant was able to form the covalent adduct under all of the conditions investigated as was the wild type (figure 4.3). This reflects the conservative exchange of the lysine to the arginine residue. Therefore the guanidium group of arginine is able to fulfill the function of the ε-amino group of lysine. On the other hand, the K22E mutant was unable to form the covalent adduct under any of the conditions tested (figure 4.3). This is not surprising based on the negatively charged side chain of the glutamate residue, which exerts a repulsive effect preventing the binding of fosfomycin in the active site. Interestingly, the exchange of the lysine to an uncharged valine retained the ability to form the covalent adduct, but only in the presence of UDPNAG (figure 4.2). This suggests that fosfomycin can only form a covalent adduct if the conformational change occurs upon binding of UDPNAG. The propensity of the K22V mutant protein to undergo the conformational change was further investigated using isothermal titration calorimetry. The heat capacity change of this process was determined to be identical to that observed for the *En. cloacae* MurA (table 4.1) (Samland et al. 2001b). This contradicts the earlier hypothesis that Lys22 is involved in the conformational switch, as these results demonstrate that the mode and action of the conformational change in K22V are the same as in the wild type.

The initial binding of fosfomycin in the active site of MurA requires the presence of a positively charged side chain at position 22 before subsequent formation of the covalent adduct. In the absence of this, UDPNAG is required to induce the conformational change resulting in more interactions that also favour fosfomycin binding. Without the conformational change, these interactions do not occur and fosfomycin is unable to bind. By examining the structure of the closed conformation in more detail, it can be seen that Lys22 interacts with the side chain of Asn23 and forms a salt bridge with the phosphonate group of fosfomycin (Skarzynski et al. 1996). Isothermal titration calorimetry studies also indicated that the binding of fosfomycin was affected in K22 mutant proteins (Samland et al. 1999). Lys22 is not involved in any interactions with UDPNAG (Skarzynski et al. 1996). This is reflected by the unaffected K_M observed for UDPNAG binding (Samland et al. 1999). As the K22V mutant can only bind fosfomycin in the presence of UDPNAG, the interactions that UDPNAG makes in the closed conformation may provide some insight with regard to this observation. In the closed conformation, the nitrogen of the acetyl group and the 2'-oxygen of the sugar ring of UDPNAG form hydrogen bonds with the phosphonate and the hydroxyl group of fosfomycin respectively (figure 5.3). These interactions can be regarded as a direct effect of UDPNAG that results in the binding of fosfomycin in the active site. As the diphosphate group of UDPNAG also forms a salt bridge with the guanidium nitrogen of Arg120 in this conformation, this may be an indirect effect of UDPNAG on the binding of fosfomycin (figure 5.3). Arg120 is located at the end of the loop structure and is thought to influence the position or conformation of the loop upon UDPNAG binding (Schönbrunn et al. 1996). As the bond between UDPNAG and Arg120 is not present in the open conformation of MurA, the binding of UDPNAG induces the conformational change bringing the loop, and therefore the Arg120 residue, into the active site. Arg120 then interacts with UDPNAG and also forms two hydrogen bonds between the side chain of Arg120 to the oxygens of the phosphonate group of fosfomycin (figure 5.3) (Skarzynski et al. 1996). These provide stronger interactions than those formed with UDPNAG (figure 5.3).

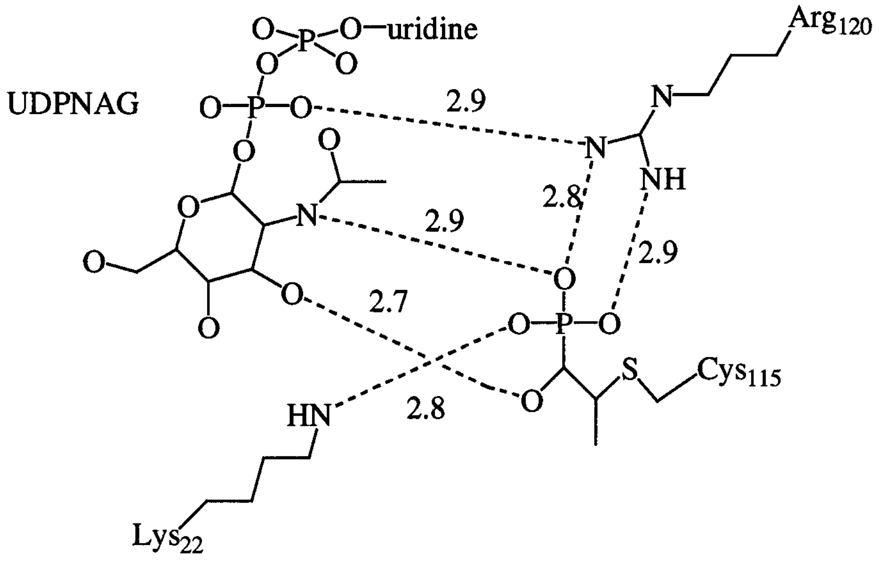

Figure 5.3: Interactions between UDPNAG, fosfomycin, K22 and R120. Distances of the H-bonds are indicated.

These interactions allow the inference of the following hypothesis for the covalent adduct formation observed in the K22V mutant. The binding of UDPNAG to K22V MurA induces the conformational change that brings Arg120 into the active site. In the absence of the positively charged side chain, fosfomycin can then be bound in the active site by the direct effect of UDPNAG but can also be held in position by the hydrogen bonds formed by Arg120. This then allows fosfomycin to react with Cys115 to form the covalent adduct. This invariant Arg120 residue may be important in the initial binding of fosfomycin and probably PEP. Site-directed mutagenesis of Arg120 in conjunction with Lys22, resulting in a double mutant, will confirm the role of this residue in MurA. In the double mutant, the lack of Arg120 would result in the inability of this mutant to form the fosfomycin covalent adduct in the presence of UDPNAG. This would confirm that Arg120 is important in the initial binding of fosfomycin to the active site. If the formation of the covalent adduct is still possible, then it would suggest that UDPNAG is important in the initial binding of fosfomycin to the active site and the binding observed by Arg120 is an indirect effect of UDPNAG binding.

However, this does not explain the 300-fold decrease in enzyme activity that is observed for K22V (Samland et al. 1999). The binding of PEP to the K22V mutant enzyme was unaffected as was the binding of UDPNAG (Samland et al. 1999). As the conformational change has been shown to occur in the K22V mutant upon binding of UDPNAG, why is the PEP unable to react with the 3'-hydroxyl group of the substrate? It is possible that steric and chemical constraints are imposed in the active site in order for the formation of product to occur. These are not necessary for fosfomycin binding. The stereochemical course of the reaction proceeds via an *anti*-addition, *syn*-elimination mechanism and requires the substrates to be correctly positioned by the neighbouring amino acid residues (Skarzynski et al. 1998). The shorter side-chain of the K22V mutant may influence the steric constraints of the substrates by preventing interactions between PEP and Arg120 from occurring. Therefore, the presence of the Lys22 residue is required in order to achieve the correct alignment of substrates required for catalysis.

It is still unclear as to which residues are therefore involved in initiating the conformational switch and this should also be investigated further. Site-directed mutagenesis of the Asn23 residue demonstrated that it has a role as a sensor of UDPNAG and in the stabilisation of the transition state (Samland et al. 2001a). In the presence of UDPNAG it interacts with Lys22, resulting in the breakage of the salt bridge between Lys22 and Asp49, and the 3'-oxygen of the pyranose ring of UDPNAG (Samland et al. 2001a). Asn23 is also part of an elaborate hydrogen-bonding network that includes Asp49 and Arg397, which have been proposed to be consecutive members of the chain of processes that lead to the closed conformation (Samland et al. 2001a). The structure of the closed conformation together with studies using ANS also indicates that Arg91 could be involved in the conformational change (Skarzynski et al. 1996, Schönbrunn et al. 2000b). Site-directed mutagenesis studies of these residues would further our understanding of this mechanism.

Additional information on the reaction mechanism may be gained from the following observation. In the spectra obtained from the analysis of MurA tryptic peptides, a peak of 1657 m/z was identified in the unliganded wild-type MurA. In the presence of UDPNAG, the peak 1657 m/z of wild type MurA disappears and the formation of a peak at 1674 m/z is observed (figure 4.3, panels E and G). Previous analysis of spectra identified this peak as comprising the fragment 295 to 310 and it was thought to be a result of some chymotrypsin activity that is present in the trypsin preparation (Samland et al. 2001a). The same phenomenon was also shown to occur with the K22R mutant in the presence of UDPNAG but not for the K22V or K22E mutants. The change in mass is consistent with the addition of a hydroxyl group onto an amino acid in this peptide. This fragment comprises the amino acid residue, Asp305, which has been shown to be the base involved in abstracting the proton from UDPNAG (Samland et al. 2001a). The identity of these peptides of 1657 and 1675 m/z, could be determined using tandem MS/MS sequencing and from this it may also be possible to identify the amino acid that is undergoing modification. If this is the case, it may provide further insight into the reaction mechanism. However, the question remains as to why this peak is not formed in the K22V mutant protein, which also binds UDPNAG?

To date, it is unknown which residues are responsible for the binding of PEP although there is evidence that the sites of PEP and fosfomycin binding are not identical but are overlapping (Skarzynski et al. 1998). Studies into this may also help to explain the lack of activity observed for the Lys22 mutant proteins.

As described in chapter one, the enzyme 5-enolpyruvylshikimate-3-phosphate synthase (EPSPS) catalyses the transfer of the enolpyruvyl moiety from PEP to shikimate-3-phosphate (S3P). EPSPS has been shown to have similar properties to MurA, with respect to its structure, mechanism and evolution. The overall structure of EPSPS is similar to MurA in both the open and closed conformations (Stallings et al. 1991, Schönbrunn et al. 2001). Fluorescence spectroscopy studies and tryptic digestion followed by MALDI-TOF mass spectrometry have suggested that a conformational change occurs on the binding of shikimate-3-phosphate (S3P) (Stallings et al. 1991, Krekel et al. 1999). The similarities between EPSPS and MurA allow us to draw comparisons regarding the conformational change and the reaction mechanism. Identification of residues thought to be involved in the conformational change of MurA can be spatially mapped in EPSPS (Schönbrunn et al. 2001). In MurA, Arg91, Asp231 and Asp369 are thought to ease the transition from open to closed conformations. These correspond to Arg100, Asp242 and Asp384 in EPSPS (Schönbrunn et al. 2001). Mutations in all three residues have dramatically reduced enzyme activity, perhaps by hindering domain closure (Shuttleworth et al. 1999). In MurA, the Asn23 residue was discussed to have a role in the stabilisation of the transition state (Samland et al. 2001a). In EPSPS, this residue is replaced by a serine indicating that the loss of stabilisation must be compensated for by other residues in the active site (Samland et al. 2001a). Additionally, the Lys22 residue in MurA is conserved in EPSPS as Lys22. Site-directed mutagenesis has indicated that Lys22 in EPSPS is involved in the binding of S3P, whereas in MurA, Lys22 is involved in fosfomycin and PEP binding (Samland et al. 1999, Shuttleworth et al. 1999). Additionally, the exchange of lysine for arginine in EPSPS results in decreased enzyme activity and therefore the positive charge is important for the binding of S3P but also the positioning of this charge in the active site is important (Shuttleworth et al. 1999). The positive charge of this residue is obviously important in both enzymes for the positioning of the substrates. Arg120 in MurA is also present in EPSPS (Arg124) and makes a salt bridge with the phosphonate group of the specific inhibitor glyphosate (Schönbrunn et al. 2001). However inhibitor binding by reinforcement of the initial binding site by the recruitment of secondary binding partners, i.e. Arg120, is not possible in EPSPS. This is due to the lack of a flexible loop structure, therefore, the same role presented in this study can not be envisioned for this residue in EPSPS (Stallings et al. 1991). This represents an important difference between these two enzymes. Further site-directed mutagenesis studies of Arg124 in EPSPS would provide further insight into the role of this residue in catalysis.

5.3 Outlook

The advent of resistance in bacteria to the available antibiotics, especially multi-drug resistance where bacteria are resistant to two or more antibiotics, demonstrates the urgent requirement for new effective antibiotics. Resistance to all antibiotics is inevitable over a period of months or years after the introduction and continuous use of the antibiotic. For example, penicillin resistance was observed two years after it was first introduced (Walsh 2000). Resistance rapidly spreads throughout bacterial populations as a result of the exchange of plasmids or transposons containing the resistance genes between species and genera (Wong and Pompliano 1998, Walsh 2000).

The importance of studying the MurA enzyme from bacteria that contain a cysteine or an aspartate at position 115 becomes more urgent in the face of fosfomycin resistance. Fosfomycin was first discovered as a secondary metabolite of *Streptomyces* sp. in 1969 (Hendlin et al. 1969). It is a broad-spectrum antibiotic that is naturally produced by several *Streptomyces* sp., e.g. *Streptomyces fradiae*, *Streptomyces wedmorensis*, and *Pseudomonas syringae* (Chopra and Ball 1982, Garcia et al. 1995, Hidaka et al. 1995). Fosfomycin acts synergistically with other antibiotics that inhibit peptidoglycan biosynthesis, e.g. β-lactams (Suarez and Mendoza 1991). It is commonly used Spain, France, Italy and Japan in the clinical treatment of urinary tract infections and is non-toxic to humans (Suarez and Mendoza 1991, Arca et al. 1997). Generally, its use is limited to acute cystitis due to the high rate of resistance that is observed (Wong and Pompliano 1998). Fosfomycin resistance was first observed in 1972 as a result of mutations in MurA (Venkateswaran and Wu 1972). Since then, other mechanisms of fosfomycin resistance have been observed. These include mutations in the uptake systems used to import fosfomycin into the bacterial cell, i.e. mutations in the L-α-glycerophosphate (Arca et al. 1988) or the hexose transport systems (Kahan et al. 1974). Resistance also occurs as a result of mutations in MurA, such as those observed in this study, or the overexpression of MurA in the bacterial cell (Horii et al. 1999). Gram negative bacteria also show the expression of a plasmid-encoded Mn^{2+} metalloglutathione transferase, FosA (Arca et al. 1990, 1997, Bernat et al. 1997). FosA catalyses the nucleophilic attack of glutathione on C1 of fosfomycin resulting in the opening of the epoxide ring and the subsequent inactivation of fosfomycin (figure 1.4) (Arca et al. 1997, Bernat et al. 1997). This mechanism of inactivation of fosfomycin is similar to that of MurA inactivation by fosfomycin, i.e. the attack of a thiol group on fosfomycin. Interestingly, Gram positive bacteria have a similar enzyme, FosB, that catalyses the nucleophilic attack of a thiol group on the C1 of fosfomycin, but not of glutathione as it is lacking in these bacteria (Cao et al. 2001). FosB is thought to have originated from the producing organisms (Suarez and Mendoza 1991) and is also thought to be an evolutionary precursor to FosA (Cao et al. 2001). These resistance mechanisms demonstrate the urgent need for the development of new compounds that inactivate MurA.

The study of MurA from *Mycobacterium tuberculosis* presented here, could lead to the design of new inhibitors that have a fosfomycin-like structure and are able to react with the aspartate residue in the active site. Such inhibitors could be used against all of the pathogenic bacteria that contain the naturally occurring variant of MurA. Recently three synthetic inhibitors against MurA were identified that inhibit Gram negative bacteria to the same extent as fosfomycin (Baum et al. 2001). These had the following structures, cyclic disulphide, a purine analog and a pyrazolopyrimidine. The disulphide inhibitor showed competitive inhibition but none of them formed a covalent adduct. Additionally, they showed weaker inhibition of Gram positive bacteria and there was a possible problem with the uptake of these inhibitors into the cell (Baum et al. 2001). However, they represent a scaffold from which new inhibitors can be developed. At the present time, there are no inhibitors that act against MurA as UDPNAG analogs.

Recently, an A_2 protein essential for host lysis was identified from the Qβ-virion. This was shown to act against the MurA enzyme and has potential as a possible inhibitor that may be used against all MurA containing organisms whether they contain an aspartate or a cysteine residue (Bernhardt et al. 2001). A mutation causing A_2 resistance was mapped to the exposed surface of MurA and determined to be the exchange of leucine to glutamate at position 138 of MurA (Bernhardt et al. 2001). The affinity of virion binding to MurA was in the 10 nM range, which is similar to that determined for fosfomycin binding. Leu138 is not a conserved residue in MurA and therefore the mode of action of A_2 is unknown. It is located on the surface of the protein near the active site of the enzyme and it is not involved in the conformational change. Perhaps the side chain of leucine is involved in the binding of A_2, testing the inhibition of this lytic protein against other MurA's containing other residues in position 138 may provide further insight into the inhibition mechanism of this protein. This may allow for the design of new inhibitors against MurA that are small proteins or peptides and inhibit non-conserved residues of MurA.

Some of the antibiotics known to inhibit steps in peptidoglycan biosynthesis are shown in figure 5.4. Cell wall biosynthesis is a good target for antibiotics as it is essential for survival and is only present in eubacteria (Wong and Pompliano 1998). Fosfomycin is so far the only antibiotic known to inhibit an enzyme in the early stages of peptidoglycan biosynthesis.

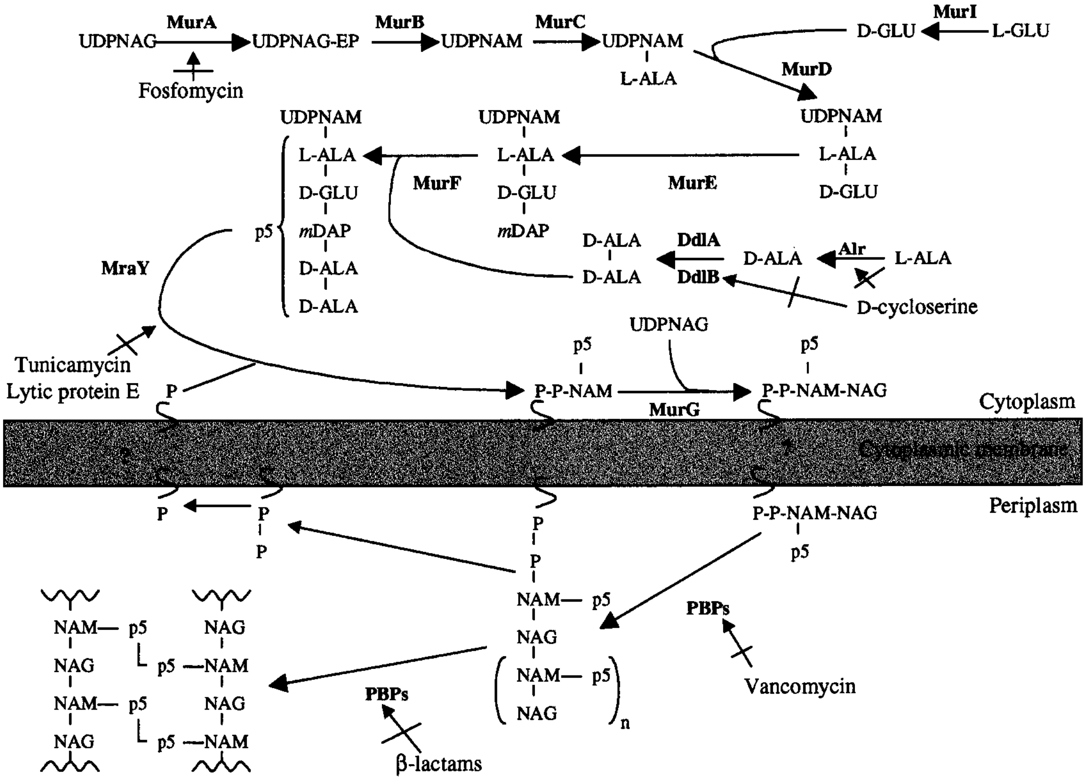
MurA
UDPNAG
UDPNAG-EP
Fosfomycin
MurB
UDPNAM
MurC
UDPNAM
L-ALA
D-GLU
MurI
L-GLU
MurD
UDPNAM
L-ALA
D-GLU
MurE
UDPNAM
L-ALA
D-GLU
mDAP
MurF
UDPNAM
L-ALA
D-GLU
mDAP
D-ALA
D-ALA
p5
D-ALA
D-ALA
DdlA
DdlB
D-ALA
Alr
L-ALA
D-cycloserine
MraY
Tunicamycin
Lytic protein E
P
UDPNAG
p5
P-P-NAM
MurG
p5
P-P-NAM-NAG
Cytoplasm
Cytoplasmic membrane
?
Periplasm
P
P
P
P
P
P-P-NAM-NAG
p5
NAM— p5
NAG
NAM— p5
NAG
n
PBPs
Vancomycin
PBPs
β-lactams
NAM— p5
NAG
NAM— p5
NAG
NAG
p5 —NAM
NAG
p5 —NAM

Figure 5.4: The actions of antibiotics on the inhibition of peptidoglycan biosynthesis. UDP: uridine diphosphate. NAG: *N*-acetylglucosamine. NAG-EP: *N*-acetylenolpyruvylglucosamine. L-ALA: L-alanine. D-ALA: D-alanine. D-GLU: D-glutamate. *m*DAP: *meso*-diaminopimelic acid. P-P: undecaprenyl pyrophosphate carrier. ?: unidentified flippase. PBPs: Penicillin binding proteins. The enzymes catalysing the various stages are depicted in bold type above or below the arrows. The crossed arrows indicate inhibition by the respective antibiotic.

Other antibiotics include β-lactams, vancomycin, D-cycloserine and tunicamycin. Only a few of these will be discussed in further detail. β-lactams target transpeptidation by acylating serine residues of PBPs leaving the wall weak and susceptible to lysis. Over 60 % of all antibiotics are β-lactams (Lee et al. 2001). Resistance to β-lactams involves the β-lactamases that attack the lactam ring structure and thus inactivate the antibiotic. Vancomycin is a member of the glycopeptide class of antibiotics and acts by binding the peptide substrate, D-ALA-D-ALA, via five hydrogen bonds and preventing transglycosylation (Bugg and Walsh 1992). An interesting resistance mechanism has been developed by bacteria that involves the synthesis of a D-ALA-D-lactate peptide that is incorporated into the cell wall (Bugg and Walsh 1992, Walsh 2000). These peptide antibiotics provide great potential for future antibiotics as they could be designed against other peptide substrates, such as the L-ALA-D-GLU present in peptidoglycan. These type of inhibitors are desirable as vancomycin resistance was first observed many years after it was first introduced (Wong and Pompliano 1998). Other potential drug targets are the specific amino acid ligases that are used to extend the pentapeptide chain, however as there are so many different amino acids that are added in different organisms, any drugs of this type would be of limited clinical use. The MurB enzyme has been extensively characterised and so a rational approach to drug design could be utilised in the design of inhibitors against this enzyme. Interestingly, a lytic protein, E, from the DNA phage ϕX174 has been shown to inhibit the enzyme, MraY. This is a similar example to that observed with the lytic protein A_2 described above (Bernhardt et al. 2001). This demonstrates the potential use of using small lytic bacteriophage proteins as inhibitors of enzymes involved in this pathway.

Ideally antibiotics need to be developed that are active against existing bacteria but also forestall the emergence of new resistance mechanisms. Potential strategies in the development of new antibiotics could involve the targeting of resistance mechanisms. For example, clavulonate binds to β-lactamases that degrade β-lactams. Also new classes of antibiotics could be developed especially with the advent of genome sequencing. In the meantime, a useful approach would be to extend the lifetime of current antibiotics by their selective and rotational use in the treatment of infections. However, any antibiotics that are designed will always have a limited use due to the propensity of bacteria to find new mechanisms with which to increase their survival rate.

6. Bibliography

Amann, E. and Brosius, J. (1985). *"ATG vectors' for regulated high-level expression of cloned genes in* Escherichia coli. Gene **40**: 183-90.

Arca, P., Rico, M., Brana, A. F., Villar, C. J., Hardisson, C. and Suarez, J. E. (1988). *Formation of an adduct between fosfomycin and glutathione: a new mechanism of antibiotic resistance in bacteria.* Antimicrob Agents Chemother **32**: 1552-6.

Arca, P., Hardisson, C. and Suarez, J. E. (1990). *Purification of a glutathione S-transferase that mediates fosfomycin resistance in bacteria.* Antimicrob Agents Chemother **34**: 844-8.

Arca, P., Reguera, G. and Hardisson, C. (1997). *Plasmid-encoded fosfomycin resistance in bacteria isolated from the urinary tract in a multicentre survey.* J Antimicrob Chemother **40**: 393-9.

Ausubel, F. M. (1987). *Current protocols in molecular biology.* Brooklyn, N. Y.

Barbour, A. G., Amano, K., Hackstadt, T., Perry, L. and Caldwell, H. D. (1982). Chlamydia trachomatis *has penicillin-binding proteins but not detectable muramic acid.* J Bacteriol **151**: 420-8.

Barbour, A. G. and Hayes, S. F. (1986). *Biology of* Borrelia *species.* Microbiol Rev **50**: 381-400.

Barry, C. E., 3rd and Mdluli, K. (1996). *Drug sensitivity and environmental adaptation of mycobacterial cell wall components.* Trends Microbiol **4**: 275-81.

Baum, E. Z., Montenegro, D. A., Licata, L., Turchi, I., Webb, G. C., Foleno, B. D. and Bush, K. (2001). *Identification and characterization of new inhibitors of the* Escherichia coli *MurA enzyme.* Antimicrob Agents Chemother **45**: 3182-8.

Bernat, B. A., Laughlin, L. T. and Armstrong, R. N. (1997). *Fosfomycin resistance protein (FosA) is a manganese metalloglutathione transferase related to glyoxalase I and the extradiol dioxygenases.* Biochemistry **36**: 3050-5.

Bernhardt, T. G., Wang, I. N., Struck, D. K. and Young, R. (2001). *A protein antibiotic in the phage Qbeta virion: diversity in lysis targets.* Science **292**: 2326-9.

Bouhss, A., Josseaume, N., Allanic, D., Crouvoisier, M., Gutmann, L., Mainardi, J. L., Mengin-Lecreulx, D., van Heijenoort, J. and Arthur, M. (2001). *Identification of the UDP-MurNAc-pentapeptide:L-alanine ligase for synthesis of branched peptidoglycan precursors in* Enterococcus faecalis. J Bacteriol **183**: 5122-7.

Brock, T. D. and Madigan, M. T. (1997). *Biology of microorganisms.* 8th Ed. Upper Saddle River, NJ, Prentice Hall.

Brown, E. D., Marquardt. J. L., Lee, J. P., Walsh, C. T. and Anderson, K. S. (1994). *Detection and characterization of a phospholactoyl-enzyme adduct in the reaction catalyzed by UDP-*N*-acetylglucosamine enolpyruvoyl transferase, MurZ.* Biochemistry **33**: 10638-45.

Brown, J. R., Douady, C. J., Italia, M. J., Marshall, W. E. and Stanhope, M. J. (2001). *Universal trees based on large combined protein sequence data sets.* Nat Genet **28**: 281-5.

Bugg, T. D. and Walsh, C. T. (1992). *Intracellular steps of bacterial cell wall peptidoglycan biosynthesis: enzymology, antibiotics, and antibiotic resistance.* Nat Prod Rep **9**: 199-215.

Cao, M., Bernat, B. A., Wang, Z., Armstrong, R. N. and Helmann, J. D. (2001). *FosB, a cysteine-dependent fosfomycin resistance protein under the control of sigma(W), an extracytoplasmic-function sigma factor in* Bacillus subtilis. J Bacteriol **183**: 2380-3.

Cassidy, P. J. and Kahan, F. M. (1973). *A stable enzyme-phosphoenolpyruvate intermediate in the synthesis of uridine-5'-diphospho-*N*-acetyl-2-amino-2-deoxyglucose 3-*O*-enolpyruvyl ether.* Biochemistry **12**: 1364-74.

Chatterjee, D. (1997). *The mycobacterial cell wall: structure, biosynthesis and sites of drug action.* Curr Opin Chem Biol **1**: 579-88.

Cheung, H. Y., Vitkovic, L. and Freese, E. (1983). *Rates of peptidoglycan turnover and cell growth of* Bacillus subtilis *are correlated.* J Bacteriol **156**: 1099-106.

Chopra, I. and Ball, P. (1982). *Transport of antibiotics into bacteria.* Adv Microb Physiol **23**: 183-240.

Chopra, I., Storey, C., Falla, T. J. and Pearce, J. H. (1998). *Antibiotics, peptidoglycan synthesis and genomics: the chlamydial anomaly revisited.* Microbiology **144**: 2673-8.

Cole, S. T., Brosch, R., Parkhill, J., Garnier, T., Churcher, C., Harris, D., Gordon, S. V., Eiglmeier, K., Gas, S., Barry, C. E., 3rd, Tekaia, F., Badcock, K., Basham, D., Brown, D., Chillingworth, T., Connor, R., Davies, R., Devlin, K., Feltwell, T., Gentles, S., Hamlin, N., Holroyd, S., Hornsby, T., Jagels, K., Barrell, B. G. and et al. (1998). *Deciphering the biology of* Mycobacterium tuberculosis *from the complete genome sequence.* Nature **393**: 537-44.

De Smet, K. A., Kempsell, K. E., Gallagher, A., Duncan, K. and Young, D. B. (1999). *Alteration of a single amino acid residue reverses fosfomycin resistance of recombinant MurA from* Mycobacterium tuberculosis. Microbiology **145**: 3177-84.

Deinum, J., Gustavsson, L., Gyzander, E., Kullman-Magnusson, M., Edstrom, A., Karlsson, R. (2002). *A thermodynamic characterization of the binding of thrombin inhibitors to human thrombin, combining biosensor technology, stopped-flow spectrophotometry, and microcalorimetry.* Anal Biochem **300**: 152-62.

Dixon, M. (1952). *The determination of enzyme inhibitor constants.* Biochem J **55**: 170-171.

Dmitriev, B. A., Ehlers, S., Rietschel, E. T. and Brennan, P. J. (2000). *Molecular mechanics of the mycobacterial cell wall: from horizontal layers to vertical scaffolds.* Int J Med Microbiol **290**: 251-8.

Du, W., Brown, J. R., Sylvester, D. R., Huang, J., Chalker, A. F., So, C. Y., Holmes, D. J., Payne, D. J. and Wallis, N. G. (2000). *Two active forms of UDP-*N-*acetylglucosamine enolpyruvyl transferase in gram-positive bacteria.* J Bacteriol **182**: 4146-52.

Dye, C., Scheele, S., Dolin, P., Pathania, V. and Raviglione, M. C. (1999). *Consensus statement. Global burden of tuberculosis: estimated incidence, prevalence, and mortality by country. WHO Global Surveillance and Monitoring Project.* JAMA **282**: 677-86.

Eschenburg, S. and Schönbrunn, E. (2000). *Comparative X-ray analysis of the un-liganded fosfomycin-target murA.* Proteins **40**: 290-8.

Essers, L. and Schoop, H. J. (1978). *Evidence for the incorporation of molecular oxygen, a pathway in biosynthesis of* N*-glycolylmuramic acid in* Mycobacterium phlei. Biochim Biophys Acta **544**: 180-4.

Frere, J. M., Dubus, A., Galleni, M., Matagne, A. and Amicosante, G. (1999). *Mechanistic diversity of beta-lactamases.* Biochem Soc Trans **27**: 58-63.

Garcia, P., Arca, P. and Evaristo Suarez, J. (1995). *Product of fosC, a gene from* Pseudomonas syringae, *mediates fosfomycin resistance by using ATP as cosubstrate.* Antimicrob Agents Chemother **39**: 1569-73.

Gateau, O., Bordet, C. and Michel, G. (1976). *Study of the formation of* N-*glycolylmuramic acid from* Nocardia asteroides. Biochim Biophys Acta **421**: 395-405.

Ghuysen, J. M. and Goffin, C. (1999). *Lack of cell wall peptidoglycan versus penicillin sensitivity: new insights into the chlamydial anomaly.* Antimicrob Agents Chemother **43**: 2339-44.

Ghuysen, J. M. and Hackenbeck, R. (1994). *Bacterial cell wall.* Amsterdam; New York, Elsevier.

Halliwell, C. M., Morgan, G., Ou, C. P. and Cass, A. E. (2001). *Introduction of a (poly)histidine tag in L-lactate dehydrogenase produces a mixture of active and inactive molecules.* Anal Biochem **295**: 257-61.

Hatch, T. P. (1996). *Disulfide cross-linked envelope proteins: the functional equivalent of peptidoglycan in chlamydiae?* J Bacteriol **178**: 1-5.

Hendlin, D., Stapley, E. O., Jackson, M., Wallick, H., Miller, A. K., Wolf, F. J., Miller, T. W., Chaiet, L., Kahan, F. M., Foltz, E. L., Woodruff, H. B., Mata, J. M., Hernandez, S. and Mochales, S. (1969). *Phosphonomycin, a new antibiotic produced by strains of* streptomyces. Science **166**: 122-3.

Hidaka, T., Goda, M., Kuzuyama, T., Takei, N., Hidaka, M. and Seto, H. (1995). *Cloning and nucleotide sequence of fosfomycin biosynthetic genes of* Streptomyces wedmorensis. Mol Gen Genet **249**: 274-80.

Hoang, T. T., Ma, Y., Stern, R. J., McNeil, M. R. and Schweizer, H. P. (1999). *Construction and use of low-copy number T7 expression vectors for purification of problem proteins: purification of* Mycobacterium tuberculosis *RmlD and* Pseudomonas aeruginosa *LasI and RhlI proteins, and functional analysis of purified RhlI.* Gene **237**: 361-71.

Holmes, D. S. and Quigley, M. (1981). *A rapid boiling method for the preparation of bacterial plasmids.* Anal Biochem **114**: 193-7.

Holtje, J. V. and Heidrich, C. (2001). *Enzymology of elongation and constriction of the murein sacculus of* Escherichia coli. Biochimie **83**: 103-8.

Horii, T., Kimura, T., Sato, K., Shibayama, K. and Ohta, M. (1999). *Emergence of fosfomycin-resistant isolates of Shiga-like toxin-producing* Escherichia coli *O26.* Antimicrob Agents Chemother **43**: 789-93.

Jarlier, V. and Nikaido, H. (1994). *Mycobacterial cell wall: structure and role in natural resistance to antibiotics.* FEMS Microbiol Lett **123**: 11-8.

Kahan, F. M., Kahan, J. S., Cassidy, P. J. and Kropp, H. (1974). *The mechanism of action of fosfomycin (phosphonomycin).* Ann N Y Acad Sci **235**: 364-86.

Kim, D. H., Lees, W., Haley, T. M. and Walsh, C. T. (1995). *Kinetic characterization of the inactivation of UDP-GlcNAc enolpyruvyl transferase by (Z)-3-fluorophosphoenolpyruvate: Evidence for two oxocarbenium ion intermediates in enolpyruvyl transfer catalysis.* J Am Chem Soc **117**: 1494-1502.

Kim, D. H., Lees, W. J., Kempsell, K. E., Lane, W. S., Duncan, K. and Walsh, C. T. (1996a). *Characterization of a Cys115 to Asp substitution in the* Escherichia coli *cell wall biosynthetic enzyme UDP-GlcNAc enolpyruvyl transferase (MurA) that confers resistance to inactivation by the antibiotic fosfomycin.* Biochemistry **35**: 4923-8.

Kim, D.H., Tucker-Kellog, G., Lees, W. J. and Walsh, C. T. (1996b). *Analysis of fluoromethyl group chirality establishes a common stereochemical course for the enolpyruvyl transfers catalyzed by EPSP synthase and UDP-GlcNAc enolpyruvyl transferase.* Biochemistry. **35**: 5435-40.

Kobayashi, S., Kuzuyama, T. and Seto, H. (2000). *Characterization of the fomA and fomB gene products from* Streptomyces wedmorensis, *which confer fosfomycin resistance on* Escherichia coli. Antimicrob Agents Chemother **44**: 647-50.

Krekel, F. (1998). *Strukturelle und kinetische Eigenschaften der UDP-*N-*Acetylglucosaminenolpyruvyltransferase aus* Enterobacter cloacae. Doctoral dissertation. Eidgenössiche Technische Hochschule Zürich.

Krekel, F., Oecking, C., Amrhein, N. and Macheroux, P. (1999). *Substrate and inhibitor-induced conformational changes in the structurally related enzymes UDP-*N*-acetylglucosamine enolpyruvyl transferase (MurA) and 5-enolpyruvylshikimate 3-phosphate synthase (EPSPS).* Biochemistry **38**: 8864-78.

Krekel, F., Samland, A. K., Macheroux, P., Amrhein, N. and Evans, J. N. (2000). *Determination of the pKa value of C115 in MurA (UDP-*N*-acetylglucosamine enolpyruvyltransferase) from* Enterobacter cloacae. Biochemistry **39**: 12671-7.

Laemmli, U. K. (1970). *Cleavage of structural proteins during the assembly of the head of bacteriophage T4.* Nature **227**: 680-5.

Lanzetta, P. A., Alvarez, L. J., Reinach, P. S. and Candia, O. A. (1979). *An improved assay for nanomole amounts of inorganic phosphate.* Anal Biochem **100**: 95-7.

Lauer, B., Sussmuth, R., Kaiser, D., Jung, G. and Bormann, C. (2000). *A putative enolpyruvyl transferase gene involved in nikkomycin biosynthesis.* J Antibiot (Tokyo) **53**: 385-92.

Lees, W. J. and Walsh, C. T. (1995). *Analysis of the enol ether transfer catalyzed by UDP-GlcNAc enolpyruvyltransferase using (E)- and (Z)-isomers of phosphoenolbutyrate: Stereochemical, partitioning and isotope effect studies.* J Am Chem Soc **117**: 7329-7337.

Lee, W., McDonough, M. A., Kotra, L., Li, Z. H., Silvaggi, N. R., Takeda, Y., Kelly, J. A. and Mobashery, S. (2001). *A 1.2-A snapshot of the final step of bacterial cell wall biosynthesis.* Proc Natl Acad Sci USA **98**: 1427-31.

Lewis, J., Johnson, K. A. and Anderson, K. S. (1999). *The catalytic mechanism of EPSP synthase revisited.* Biochemistry **38**: 7372-9.

Marquardt, J. L., Siegele, D. A., Kolter, R. and Walsh, C. T. (1992). *Cloning and sequencing of* Escherichia coli *murZ and purification of its product, a UDP-*N-*acetylglucosamine enolpyruvyl transferase.* J Bacteriol **174**: 5748-52.

Marquardt, J. L., Benson, E. D., Walsh, C. T. and Anderson, K. S. (1993). *Isolation and structural elucidation of a tetrahedral intermediate in the UDP-*N-*acetylglucosamine enolpyruvyl transferase enzymatic pathway.* J Am Chem Soc **115**: 10398-10399.

Marquardt, J. L., Brown, E. D., Lane, W. S., Haley, T. M., Ichikawa, Y., Wong, C. H. and Walsh, C. T. (1994). *Kinetics, stoichiometry, and identification of the reactive thiolate in the inactivation of UDP-GlcNAc enolpyruvoyl transferase by the antibiotic fosfomycin.* Biochemistry **33**: 10646-51.

Mengin-Lecreulx, D., Siegel, E. and van Heijenoort, J. (1989). *Variations in UDP-*N-*acetylglucosamine and UDP-*N-*acetylmuramyl-pentapeptide pools in* Escherichia coli *after inhibition of protein synthesis.* J Bacteriol **171**: 3282-7.

Nanninga, N. (1998). *Morphogenesis of* Escherichia coli. Microbiol Mol Biol Rev **62**: 110-29.

Park, J. T. (2001). *Identification of a dedicated recycling pathway for anhydro-*N-*acetylmuramic acid and* N-*acetylglucosamine derived from* Escherichia coli *cell wall murein.* J Bacteriol **183**: 3842-7.

Ramilo, C., Appleyard, R. J., Wanke, C., Krekel, F., Amrhein, N. and Evans, J. N. (1994). *Detection of the covalent intermediate of UDP-*N-*acetylglucosamine enolpyruvyl transferase by solution-state and time-resolved solid-state NMR spectroscopy.* Biochemistry **33**: 15071-9.

Rosenfeld, J., Capdevielle, J., Guillemot, J. C. and Ferrara, P. (1992). *In-gel digestion of proteins for internal sequence analysis after one- or two-dimensional gel electrophoresis.* Anal Biochem **203**: 173-9.

Sambrook, J., Fritsch, E. F. and Maniatis, T. (1989). *Molecular cloning: a laboratory manual.* Cold Spring Harbor, N.Y., Cold Spring Harbor Laboratory.

Samland, A. K. (2001). *Thermodynamic and mutational analysis of substrate and fosfomycin binding to UDP-*N-*acetylglucosamine enolpyruvyl transferase from* Enterobacter cloacae. Doctoral Dissertation. Eidgenössiche Technische Hochschule Zürich.

Samland, A. K., Amrhein, N. and Macheroux, P. (1999). *Lysine 22 in UDP-*N-*acetylglucosamine enolpyruvyl transferase from* Enterobacter cloacae *is crucial for enzymatic activity and the formation of covalent adducts with the substrate phosphoenolpyruvate and the antibiotic fosfomycin.* Biochemistry **38**: 13162-9.

Samland, A. K., Etezady-Esfarjani, T., Amrhein, N. and Macheroux, P. (2001a). *Asparagine 23 and aspartate 305 are essential residues in the active site of UDP-*N-*acetylglucosamine enolpyruvyl transferase from* Enterobacter cloacae. Biochemistry **40**: 1550-9.

Samland, A. K., Jelesarov, I., Kuhn, R., Amrhein, N. and Macheroux, P. (2001b). *Thermodynamic characterization of ligand-induced conformational changes in UDP-*N-*acetylglucosamine enolpyruvyl transferase.* Biochemistry **40**: 9950-6.

Sanger, F., Nicklen, S. and Coulson, A. R. (1977). *DNA sequencing with chain-terminating inhibitors.* Proc Natl Acad Sci USA **74**: 5463-7.

Schönbrunn, E., Sack, S., Eschenburg, S., Perrakis, A., Krekel, F., Amrhein, N. and Mandelkow, E. (1996). *Crystal structure of UDP-*N-*acetylglucosamine enolpyruvyltransferase, the target of the antibiotic fosfomycin.* Structure **4**: 1065-75.

Schönbrunn, E., Svergun, D. I., Amrhein, N. and Koch, M. H. (1998). *Studies on the conformational changes in the bacterial cell wall biosynthetic enzyme UDP-*N*-acetylglucosamine enolpyruvyltransferase (MurA).* Eur J Biochem **253**: 406-12.

Schönbrunn, E., Eschenburg, S., Krekel, F., Luger, K. and Amrhein, N. (2000a). *Role of the loop containing residue 115 in the induced-fit mechanism of the bacterial cell wall biosynthetic enzyme MurA.* Biochemistry **39**: 2164-73.

Schönbrunn, E., Eschenburg, S., Luger, K., Kabsch, W. and Amrhein, N. (2000b). *Structural basis for the interaction of the fluorescence probe 8-anilino-1-naphthalene sulfonate (ANS) with the antibiotic target MurA.* Proc Natl Acad Sci USA **97**: 6345-9.

Schönbrunn, E., Eschenburg, S., Shuttleworth, W. A., Schloss, J. V., Amrhein, N., Evans, J. N. and Kabsch, W. (2001). *Interaction of the herbicide glyphosate with its target enzyme 5-enolpyruvylshikimate 3-phosphate synthase in atomic detail.* Proc Natl Acad Sci USA **98**: 1376-80.

Shuttleworth, W. A., Pohl, M. E., Helms, G. L., Jakeman, D. L. and Evans, J. N. (1999). *Site-directed mutagenesis of putative active site residues of 5-enolpyruvylshikimate-3-phosphate synthase.* Biochemistry **38**: 296-302.

Skarzynski, T., Mistry, A., Wonacott, A., Hutchinson, S. E., Kelly, V. A. and Duncan, K. (1996). *Structure of UDP-*N*-acetylglucosamine enolpyruvyl transferase, an enzyme essential for the synthesis of bacterial peptidoglycan, complexed with substrate UDP-*N*-acetylglucosamine and the drug fosfomycin.* Structure **4**: 1465-74.

Skarzynski, T., Kim, D. H., Lees, W. J., Walsh, C. T. and Duncan, K. (1998). *Stereochemical course of enzymatic enolpyruvyl transfer and catalytic conformation of the active site revealed by the crystal structure of the fluorinated analogue of the reaction tetrahedral intermediate bound to the active site of the C115A mutant of MurA.* Biochemistry **37**: 2572-7.

Stallings, W. C., Abdel-Meguid, S. S., Lim, L. W., Shieh, H. S., Dayringer, H. E., Leimgruber, N. K., Stegeman, R. A., Anderson, K. S., Sikorski, J. A., Padgette, S. R. and Kishore, G. M. (1991). *Structure and topological symmetry of the glyphosate target 5-enolpyruvylshikimate-3-phosphate synthase: a distinctive protein fold.* Proc Natl Acad Sci USA **88**: 5046-50.

Steinrücken, H. C. and Amrhein, N. (1984). *5-Enolpyruvylshikimate-3-phosphate synthase of* Klebsiella pneumoniae *2. Inhibition by glyphosate [*N-*(phosphonomethyl)glycine].* Eur J Biochem **143**: 351-7.

Stephens, R. S., Kalman, S., Lammel, C., Fan, J., Marathe, R., Aravind, L., Mitchell, W., Olinger, L., Tatusov, R. L., Zhao, Q., Koonin, E. V. and Davis, R. W. (1998). *Genome sequence of an obligate intracellular pathogen of humans:* Chlamydia trachomatis. Science **282**: 754-9.

Storey, C. and Chopra, I. (2001). *Affinities of beta-lactams for penicillin binding proteins of* Chlamydia trachomatis *and their antichlamydial activities.* Antimicrob Agents Chemother **45**: 303-5.

Strych, U., Penland, R. L., Jimenez, M., Krause, K. L. and Benedik, M. J. (2001). *Characterization of the alanine racemases from two mycobacteria.* FEMS Microbiol Lett **196**: 93-8.

Suarez, J. E. and Mendoza, M. C. (1991). *Plasmid-encoded fosfomycin resistance.* Antimicrob Agents Chemother **35**: 791-5.

Tang, H. and Chitnis, P. R. (2000). *Addition of C-terminal histidyl tags to PsaL and PsaK1 proteins of cyanobacterial photosystem I.* Indian J Biochem Biophys **37**: 433-40.

van Heijenoort, J. (2001). *Formation of the glycan chains in the synthesis of bacterial peptidoglycan.* Glycobiology **11**: 25R-36R.

Venkateswaran, P. S. and. Wu., H. C. (1972). *Isolation and characterization of a phosphonomycin-resistant mutant of* Escherichia coli *K-12.* J Bacteriol **110**: 935-44.

Walsh, C. T. (2000). *Molecular mechanisms that confer antibacterial drug resistance.* Nature **406**: 775-81.

Wanke, C., Falchetto, R. and Amrhein, N. (1992). *The UDP-*N-*acetylglucosamine 1-carboxyvinyl-transferase of* Enterobacter cloacae. *Molecular cloning, sequencing of the gene and overexpression of the enzyme.* FEBS Lett **301**: 271-6.

Wanke, C. and Amrhein, N. (1993). *Evidence that the reaction of the UDP-*N-*acetylglucosamine 1-carboxyvinyltransferase proceeds through the* O-*phosphothioketal of pyruvic acid bound to Cys115 of the enzyme.* Eur J Biochem **218**: 861-70.

Wong, K. K. and Pompliano, D. L. (1998). *Peptidoglycan biosynthesis. Unexploited antibacterial targets within a familiar pathway.* Adv Exp Med Biol **456**: 197-217.

Wu, J. and Filutowicz, M. (1999). *Hexahistidine (His6)-tag dependent protein dimerization: a cautionary tale.* Acta Biochim Pol **46**: 591-9.

Wyss, C. (1989). *Dependence of proliferation of* Bacteroides forsythus *on exogenous* N-*acetylmuramic acid.* Infect Immun **57**: 1757-9.

Zemell, R. I. and Anwar, R. A. (1975). *Mechanism of pyruvate-uridine diphospho*-N-*acetylglucosamine transferase. Evidence for an enzyme-enolpyruvate intermediate.* J Biol Chem **250**: 4959-64.

7. Publications

1. Characterization of a naturally occurring variant of UDP-*N*-acetylglucosamine enolpyruvyl transferase from *Mycobacterium tuberculosis.*
   Alison M. Thomas, Nikolaus Amrhein and Peter Macheroux.
   Submitted

2. The charge of the amino acid side chain in position 22 is critical for fosfomycin binding to UDP-*N*-acetylglucosamine enolpyruvyl transferase.
   Alison M. Thomas, Nikolaus Amrhein and Peter Macheroux.
   Manuscript in preparation.

8. Acknowledgements

Firstly, I would like to thank Prof. Dr. N. Amrhein for providing me with the opportunity to work in his group and on these particular projects. I would also like to thank him for his support and interest in these projects.

I would also like to thank Dr. P. Macheroux for his support and encouragement throughout these projects. Also for his enthusiasm and constructive criticism.

In particular, I would like to thank Dr. Teresa Fitzpatrick, Dr. Karina Kitzing, Dr. Anne Samland and Cristian Ginj for their support and suggestions when things were not going to plan. Together with the rest of the D38ers they created a relaxed and enjoyable working atmosphere.

Special thanks also go to Peter and Karina for their help in writing the Zusammenfassung.

Additional thanks go to Dr Roger Kuhn for his help with all of the computing problems that arose, Dr. Ilian Jelesarov and Prof. H. Bosshard at the University of Zurich for the use of their microcalorimeter and Dr. R. Brunisholz at the Institute of Molecular Biology and Biophysics, ETH-Hönggerberg for the N-terminal sequencing.

Last but not least, I would like to thank my family and Salim for their love and support during the last few years.

9. Curriculum vitae

Personal Data

Name: Alison Margaret Thomas

Date and Place of Birth: 10th September 1976 in Edinburgh, Scotland.

Nationality: British

Civil Status: Single

Education

1981-1988: Primary school in Edinburgh, Scotland.

1988-1994: Secondary school in Edinburgh, Scotland.

1994-1998: Bachelor of Science (Hons) Medical Biochemistry, University of Glasgow, Scotland.

1998-2002: Doctoral student at the Eidgenössische Technische Hochschule Zürich in the Institute of Plant Science (Prof. Dr. N. Amrhein, PD Dr. P. Macheroux).